Identification of key mechanisms in the cytotoxic effect of two novel anti-cancer compounds on breast cancer cells

by

Timothy Paul Wood

submitted in fulfilment of the requirements for the degree

Magister Scientiae in Human Genetics

In the

Faculty of Health Sciences

University of Pretoria

Pretoria

July 2012

Supervisor: Professor E. Jansen van Rensburg

Dedication:

To Maryna, Olga and Vera

Acknowledgements:

I would like to thank Professor Lizette van Rensburg for her guidance and the insight she has given me into the world of science.

Declaration of work and plagiarism:

I, Timothy Paul Wood, hereby declare that the work presented in this document is my own, with the exception of IC_{50} studies and the DNA binding assay performed by Mrs M. DelaRey. Literature utilised for this thesis is referenced from the source; if not possible a secondary reference is provided.

_____   _____

Signature   Date

CONTENTS

LIST OF TABLES

LIST OF FIGURES

LIST OF ABBREVIATIONS

5-FU	5-fluoroucil
ABC	ATP binding cassette
ADME	Adsorbsion, distribution, metabolism and excretion
ANT	Adenine nucleotide translocase
APC	Antigen presenting cells
ATP	Adenosine triphosphate
CAD	Caspase activated DNase
CDK	Cyclin dependant kinase
cDNA	Complimentary DNA
Ct	Crossing threshold
DMSO	Dimethyl sulfoxide
DNA	Deoxyribonucleic acid
DISC	Death inducing signalling complex
DSB	Double strand break
ENT	Equilibrative nucleoside transporter
FA	Fanconi anaemia
Fc	Ferrocene
FNA	Fine needle aspirates
GOI	Gene of interest
HDAC	Histone deacetylase
HKG	House keeping gene
HTS	High throughput screening
IC_{50}	Cellular inhibitory concentration that affects 50% of a population
INK	Inositol kinase
IPA	Ingenuity Pathway Analysis
MDR	Multidrug resistance
MPT	Mitochondrial permeability transition
MPTP	Mitochondrial permeability transition pore
MTT	3-(4,5-dimethylthiazol-2-yl)-2,5-diphenyltetrazolium bromide
MTX	Methotrexate
NAD	β-nicotinamide adenine dinucleotide
NBF	Nucleotide-binding folds
NCI	National Cancer Institute
OMIM	Online Mendelian inheritance in man
PBS	Phosphate buffered saline
PCR	Polymerase chain reaction
PI	Propidium iodide
PI(3)K	Phosphatidylinositol-3-OH kinase
PBS	Phosphate buffered saline
PRC	Pre-replicative complex

PS	Phosphatidyl serine
QSAR	Quantitative structure-activity relationship
Rb	Retinoblastoma protein
REST	Relative Expression Software Tool
RNA	Ribonucleic acid
ROS	Reactive oxygen species
RPA	Replication protein A
Rpm	Revolutions per minute
Rh-fc	Rhodium-ferrocene
RFC	Reduced folate carrier
RSR	RAD17-containing complex
RT-PCR	Real-time/Reverse-transcriptase polymerase chain reaction
RTK	Receptor tyrosine kinases

PREFACE

Throughout the ages disease has had a striking impact on the history of mankind. With every era, a specific disease would stand out in the pages of history, such as the bubonic plague in the Renaissance. However, with the advent of effective anti-microbials, ailments that were once fatal are now completely curable (Pitot, 2002). Although these plagues affected many lives, they never persisted for any long period of time. One, however, has had true historical staying power. Cancer has hung like a spectre over mankind, since the earliest recorded times. Multicellularity, by its very nature, lends itself to be affected by cancer. Records, such as the Ebers papyrus, bear testament to attempts by the ancient Egyptians to treat cancer (Ebbell, 1936).

Unlike most illnesses, the fundamental cause of cancer is not always due to an infectious agent, but because of aberrations in the cell's own machinery. Pathogens such as human papilloma virus may induce cancer, but the actual pathological state of cancer is due to malfunctions within the cell's regulatory mechanisms. Cancer is a multifactorial disease that finds its origins in not only exterior influences, but inherent, heritable predispositions within the organism itself. This sets cancer apart not only pathologically, but also adds layers of complexity regarding its treatment.

In their seminal paper, Hanahan and Weinberg (2000) summarise the six basic "hallmarks of cancer". These properties come about as a result of mutation and heritability, ultimately leading to increased fitness and survival. Cancerous cells are insensitive to antigrowth signals and are also self sufficient with respect to growth signalling. A characteristic conferring increased survival is the cell's ability to evade apoptosis. This aspect adds an extra dimension of complexity when considering treatment. In addition to avoiding cell-death the cancerous cell has an "unlimited" propensity for growth and replication. To sustain this, the cancerous tissue in most cases has an increased ability to promote and perpetuate angiogenesis. Finally, cancer exhibits the property of tissue invasion and metastasis in which neoplastic cells spread through

the body and proliferate. These six hallmarks of cancer should always be kept in mind not only when studying the disease but also when developing novel treatment methods.

When considering the treatment of cancer one must develop a method to selectively destroy aberrant cells while sparing unaffected cells. An ideal anticancer agent will therefore selectively destroy cancerous cells and not harm normal healthy cells. In addition to this challenge, the concepts of drug resistant cancers as well as cancers that have acquired resistance should be borne in mind.

This is clearly a complex disease and to date no universal treatment has been developed. With that said however, certain drugs such as the organometallics, of which cisplatin is a member, have been widely shown to have therapeutic value. Cisplatin binds to DNA, interfering with normal transcription and DNA replication mechanisms, ultimately leading to cell death. Unfortunately, due to its non-specific action it is associated with a number of severe side effects such as nephrotoxicity. Additionally the concept of acquired resistance is prevalent when this drug is utilised for the treatment of cancer (Fuertes *et al.*, 2003).

In this vein, the research group of J Swarts (University of the Free State), in collaboration with the CANSA Research Consortium for the Development of Novel Anti-cancer Drugs, have sought to develop novel therapeutic measures to overcome inherent and acquired drug resistance in cancer. This has lead to the synthesis and testing of a number of novel organometallic agents. Among these are the Rhodium complexes which show promise as anti-neoplastic agents while displaying limited, or no, nephrotoxicity (Craciunescu *et al.*, 1991; Fiamiani *et al.*, 1990; Kopf-Maier, 1994).

For these reasons, in this research we consider and study the properties of two novel organometallic drugs, which may have therapeutic value in the treatment of cancer. Due to the structure of the drugs and the basic properties of organometallic therapeutics, it was postulated in this research that Ferrocene and Rhodium-ferrocene bind to and damage DNA. The drugs'

cytotoxicity and possible therapeutic properties are therefore a direct result of the cell's inability to replicate due to genomic damage. The quintessential essence of the drugs' therapeutic value, therefore, is the cancerous cells' inability to effectively repair DNA damage; thereby leading to selective therapy for cancer.

Here we set out to prove, from a cellular to a molecular level, the drugs' influence on cancerous as well as normal cells *in vitro.* The *in vitro* model is based on a cancerous breast epithelial cell line and a "normal" immortalised breast epithelial line, grown in a monolayer at controlled conditions. Cells are treated with fixed drug concentrations and at each step, the interaction of the drugs with DNA, in a specific experimental setting will be analysed.

Firstly, to prove the drugs interact with DNA a restriction enzyme inhibition assay is performed. This allows for the identification of the specific DNA sequence the drugs bind to. The macromolecular (cellular) effects were then analysed using flow cytometry, with reference to cell cycle and cell death effects. The influence of the bound drug on DNA synthesis during mitosis may be determined, and the subsequent effect on the cell's passage through the various cell cycle stages. DNA damage also influences the cell death machinery and the apoptotic process requires relatively intact gene expression mechanisms. One would therefore postulate that if a cell's DNA was severely damaged, and gene expression was compromised, the cell death mechanism would more than likely be a form of necrosis or apo-necrosis.

Finally these data guided us to determine the changes in gene expression induced by the two drugs. By analysing gene expression changes in cell cycle genes one would gain insight into the specific mechanism of cellular inhibition. DNA-damage related genes are also indicative of the type of damage exerted by an exogenous stimulus. The differences in gene expression between cancerous and normal cells would give an indication of the specific toxicity of the drugs on genotypically dissimilar cells. Gene expression changes in toxicity related genes would also provide insight into the drugs' mechanism of action. Through determining Ferrocene and

Rhodium-ferrocene's toxicities and mechanism of action we may be able to optimise their therapeutic value through chemical modification and lead optimisation practices.

Further long term objectives of this research include the establishment of a chemogenomic drug development infrastructure at the University of Pretoria. Through the combination of classical cell biology and novel methods in molecular biology we seek to establish a robust framework for the investigation of promising therapeutic compounds.

CHAPTER 1: INTRODUCTION

Few diseases have been as ever present throughout human history as cancer. It is the leading cause of death world-wide, accounting for more than seven million deaths each year (World Health Organisation Fact Sheet No. 297, 2008). Given the international burden of disease as well as the resulting associated morbidity, research to find effective treatments continue on a large scale.

In order to develop and understand the mechanism of action of a drug, and for that matter cancer, one first has to consider the various regulatory aspects of the cell. These include, amongst others, the molecular elements of cell cycle regulation, metabolism and cell death. In the following sections cell division and cell death, in the context of cancer, are discussed. The "Hallmarks of Cancer" proposed by Hanahan and Weinberg (2000 and 2010), will be utilized as a lodestar throughout the following sections and the research as a whole. When describing the cell cycle, cell death or therapy, with reference to cancer, these hallmarks should always be borne in mind. The "hallmarks" are biological processes and capabilities that have been acquired as a result of the development of cancerous tissue. From this perspective, the cancer cell is able to: sustain proliferative signaling, evade growth suppressors, overcome cell death mechanisms, facilitate replicative immortality, induce angiogenesis (to supply nutrients) and spread through the organism by metastasis (Hanahan and Weinberg, 2000). A further two hallmarks have been added recently which encompass the reprogramming of energy metabolism and the cancerous cell's ability to circumvent immune destruction (Hanahan and Weinberg, 2010).

1.0 Cell Cycle Regulation and Cancer

Cancer can be seen to arise as the result of aberrations in the various regulatory elements that control cellular proliferation (Luo *et al.,* 2009). Mutations that produce oncogenes with dominant gain of function, and, tumour suppressor genes with recessive loss of function have

been found to contribute to the development of the cancerous phenotype. Over the past number of years, cancer research has illustrated that this disease is associated with dynamic changes in the genome (Hanahan and Weinberg 2000 and 2010).

Cell division, or the "cell cycle", is the process by which cells replicate. This universal process is responsible for the growth and development of all living organisms (Csikasz-Nagy *et al.*, 2006). The main component of the process is the replication and division of the cell's DNA compliment; known as the S phase of the cell cycle. This is then followed by cellular division, the M phase. A gap exists before the S phase, which is designated as the G1 phase, in which cells prepare for DNA synthesis. There is also a gap before division known as the G2 phase (Nurse, 2000).

The transition between the cell phases occur in an extremely defined manner and is controlled by a number of different genes and proteins (gene and protein abbreviations mentioned in the following text are listed in Appendix 1). Cyclin-dependant kinases (CDKs), a family of serine/threonine kinases that act in conjunction with a number of cyclins, are key regulatory elements at each phase of the cell cycle. The various cyclins and CDKs activated at a particular stage of the cell cycle are summarised in Table 1.1.

Table 1.1: A summary of cyclin-CDK complexes at the various points in the cell cycle.

CDK	Cyclin	Cell Cycle Phase Activity
CDK4	Cyclin D1, D2, D3	G1 phase
CDK6	Cyclin D1, D2, D3	G1 phase
CDK2	Cyclin E	G1/S phase transition
CDK2	Cyclin A	S phase
CDK1	Cyclin A	G2/M phase
CDK1	Cyclin B	Mitosis
CDK7	Cyclin H	CDK activating kinase, all phases

The mechanisms controlling the progression through the G1 phase of the cell cycle are largely dependent on cell type. There are however some criteria that are universal for most cells, such as the activation of the CDKs. These protein kinases need to bind cyclins to become active (Morgan, 1997; Massague, 2004; Murray, 2004). The various CDKs, bound to their respective cyclins, are responsible for amongst others regulation of: transcription, differentiation and

nutrient uptake. They also form key "switches" throughout the cell cycle. The timing and degree of CDK activation is controlled by the phosphorylation and protein interaction of the CDK-cyclin complexes (Massague, 2004). The expression levels of the various cyclins, during the stages of the cell cycle, is pictured in Figure 1.1.
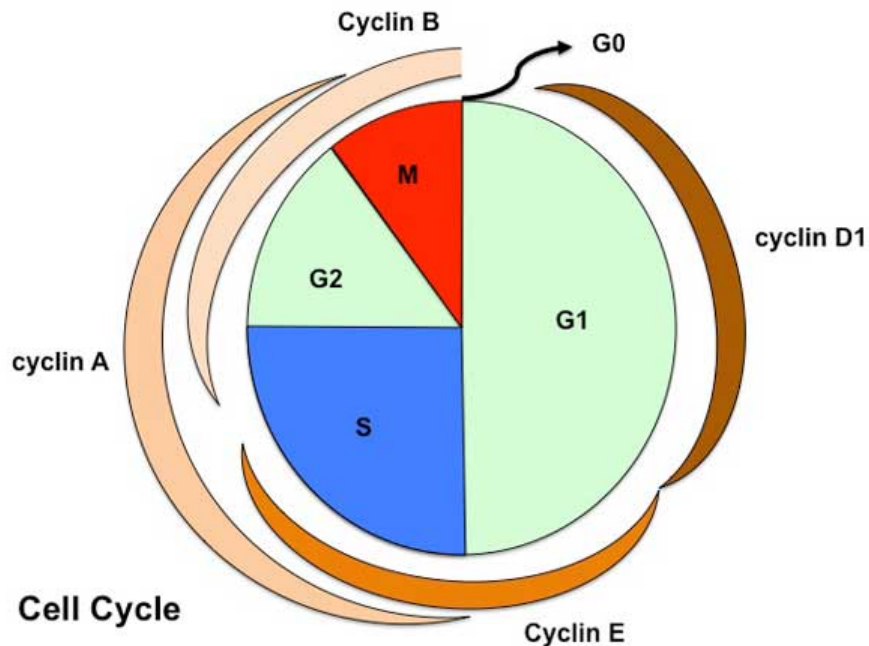
Figure 1.1: Changes in cyclin expression levels at various phases of the cell cycle (from: http://php.med.unsw.edu.au/cellbiology/index.php?title=File:Cell_cycle1.jpg).

Cdk1, which associates with cyclins A and B, is active at the transition between the G2 and M phases. The entry and exit from mitosis is mediated by the level of cyclins A and B respectively. They accumulate during the cell cycle and are degraded at the start of anaphase. With the decrease in Cdk1 activity after M phase the replication origins on the chromosomes can be loaded with a pre-replicative complex (PRC) in preparation for S phase. At this point the G1 CDKs initiate DNA replication. Cdk2, which associates with E-type cyclins (E1 and E2) and cyclin A, is activated and the PRC recruits DNA helicases, polymerases and primases. These cause the unwinding and replication of the DNA (Kelly and Brown, 2000; Prasanth *et al.*, 2004; Massague,

2004). A simplified schematic of the interactions of the cyclin complexes in the various stages of the cell cycle is depicted in Figure 1.2 (Vermeulen *et al.*, 2003).
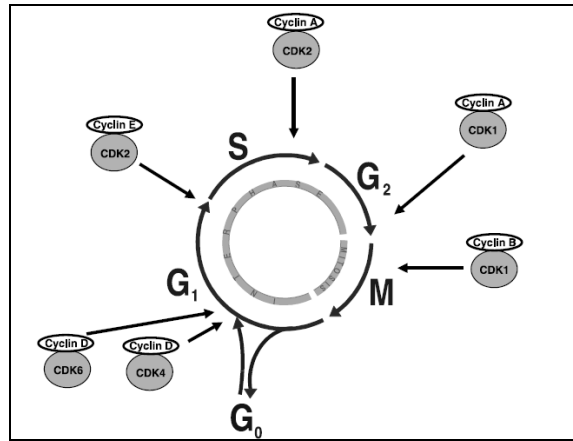
Figure 1.2: The stages of the cell cycle indicating the activity of regulatory cyclin/CDK complexes (Vermeulen *et al.*, 2003).

In embryonic cells the level of cyclin E is constantly high. This allows for rapid Cdk2 activity and a quick progression between M and S phase. In most other cells there are mechanisms in place to inactivate Cdk2 and thus create a gap (G1) between mitosis and DNA replication. This gap gives the cell an opportunity for repair and growth, and aberrations at this point are common in carcinogenesis (Massague, 2004).

1.1.1 Cyclin Dependant Kinase Inhibition Mechanisms (Rb)

The expression of cyclin E is dependant on E2F transcription factors, which in resting cells, are normally found bound to retinoblastoma protein (Rb) or to family members p107 and p130 (Lipinski and Jacks, 1999; Massague, 2004). Retinoblastoma (a childhood malignancy) is often considered a model for loss of tumour suppressor function, where Rb serves as a key regulator (Ho and Dowdy, 2002; Weinberg, 1995). Hypophosphorylated Rb (active form) binds to the E2F transcription factor which prevents the expression of the E2F target genes (Ho and Dowdy, 2002). Unphosphorylated Rb however, does not associate with E2F in the G0 phase. It has been suggested that cyclin D hypophosphorylates Rb in early G1, which activates its E2F inhibitory activity (Ezhevsky *et al.*, 2001; Ho and Dowdy, 2002).

When the cells are prompted to divide (mitogenic stimuli), the levels of cyclin D increase as a result and associate with Cdk4 and Cdk6. This complex then goes on to hyperphosphorylate Rb (a tumour suppressor gene), which inactivates it (Massague 2004). When Rb is hyperphosphorylated, in late G1, it dissociates from E2F thus allowing for E2F-dependant transcription (Ezhevsky *et al.*, 2001; Ho and Dowdy, 2002). CyclinD/Cdk4 complexes may therefore have a role in promoting the gap between mitosis and S phase to allow cellular metabolism. This is contrary to the supposition that it functions solely to promote the transition into S phase (Datar *et al.*, 2000; Ho and Dowdy, 2000; Meyer *et al.*, 2000). Besides controlling the levels of cyclin E, E2F transcription factors are also responsible for the transcription of the various accessories required for DNA transcription. It can therefore be seen that cyclin D, Cdk4 and Cdk6 are proto-oncogenes. They are over expressed in many neoplastic cell types whereas Cdk2 rarely is (Ho and Dowdy, 2002). Cyclin D over expression can be found in 50% of breast cancers (Massague, 2004). Here we should take note, in the context of the "six hallmarks of cancer" (Hanahan and Weinberg, 2010), that dysregulation of the genes mentioned earlier would promote the potential for unlimited growth, leading to cancer.

1.1.2 Externally Activated Proliferation

CDKs and inhibitory molecules, which control the transition between G and S phase, have been found to be under the influence of externally activated signaling pathways. Two of the most well researched of these are the Ras and PI(3)K (phosphatidylinositol-3-OH kinase) pathways (Vivanco and Sawyers, 2002). Many of the mitogenic factors activate these pathways by acting on receptor tyrosine kinases (RTKs) or G-protein-coupled receptors. The Ras and PI(3)K pathways are activated by the interaction of Ras and PI(3)K with receptor tyrosine kinases and their phosphorylated substrates, which are localised to the cell membrane (Pawson, 2004; Massague, 2004; Schlessinger and Lemon, 2003). The RTKs achieve this by creating phosphotyrosine sites to engage Ras, PI(3)K and various effectors. Once the Ras family members (H-Ras, K-Ras and N-Ras) have been recruited to the membrane they undergo GTP loading and hydrolysis by the guanine-nucleotide-exchange factor SOS and the GTPase-activating proteins (p120 and neurofibromin) respectively. When Ras is bound to GTP it interacts with a group of

effectors. One of these, the Ras-MEK-ERK kinase cascade, plays an integral part in CDK activation. ERK phosphorylates and stabilises the transcription factor c-Myc which in turn induces the expression of cyclin D and suppresses the expression of the CDK inhibitors. This point serves to illustrate the interconnectedness of this pathway with some of the key players of the cell cycle. One could also extrapolate the possible progression of carcinogenesis from the Ras pathway (Massaugue, 2004).

Mutations that activate Ras are frequently found in carcinomas, those that activate B-Raf are found in most melanomas and PI(3)K and Akt activating mutations can also be found in carcinomas. As a result of the importance of the Ras pathway in carcinogenesis, the associated receptors, ligands and the pathway have become important therapeutic targets. In addition to its interaction with FOXO, which prevents Bim expression, and cyclin D, Akt also phosphorylates and inhibits Bad. Akt activity can also be mediated by the kinase IKK. This kinase activates the transcription factor NF-kB, which induces the expression of BclXL. This serves to preserve mitochondrial integrity as well as that of the inhibitors of apoptosis proteins in order to inhibit caspases. In addition to Akt's inhibition of FOXO, IKK phosphorylates FOXO, which marks it for nuclear exit and destruction (Hu *et al.*, 2004; Massague, 2004). The activities of Akt and IKK all promote cellular survival, which is an important point of consideration concerning carcinogenesis. The role Ras plays in cellular survival is to interact with ERK and the effect of this varies according to tissue type. The ERK-activated kinase, p90rsk, phosphorylates and inhibits Bad in neurons, whereas in fibroblasts ERK inhibits PAR-4, a transcriptional repressor of *Bcl2* (Barradas *et al.*, 1999; Bonni *et al.*, 1999; Massague, 2004).

After considering the normal aspects of cell cycling as well as their relationships within the cancer paradigm, it is pertinent to reflect on the mechanisms by which this machinery may become perturbed. One of the most important causes of genomic instability and genetic dysregulation is DNA damage.

1.2 The Cellular Response to DNA Damage

The human genome is constantly exposed to agents that threaten its integrity. These agents can damage the bases directly or the DNA strand itself. Due to this constant threat, living organisms have evolved mechanisms to deal with both external and metabolic sources of DNA damage. These mechanisms allow the cell to detect and respond to DNA damage. Various repair mechanisms exist, each one dealing with a specific type of DNA damage. There are four types of pathways that are activated by DNA damage, these are: DNA repair, DNA damage checkpoints, transcriptional response and apoptosis (Sancar *et al.,* 2004).

A number of different types of DNA damage exist which arise from environmental stresses such as ionizing radiation, genotoxic chemicals (e.g. chemotherapeutics), or even as a result of normal metabolism (e.g. reactive oxygen species). DNA damage may take the form of either or a combination of: altered bases, abasic sites, single strand breaks, intrastrand crosslinks, interstrand crosslinks, bulky adducts, base mismatches, insertions, deletions or double strand breaks. A schematic of the different types of DNA damage, the resulting lesions and the possible repair processes is pictured in Figure 1.3.
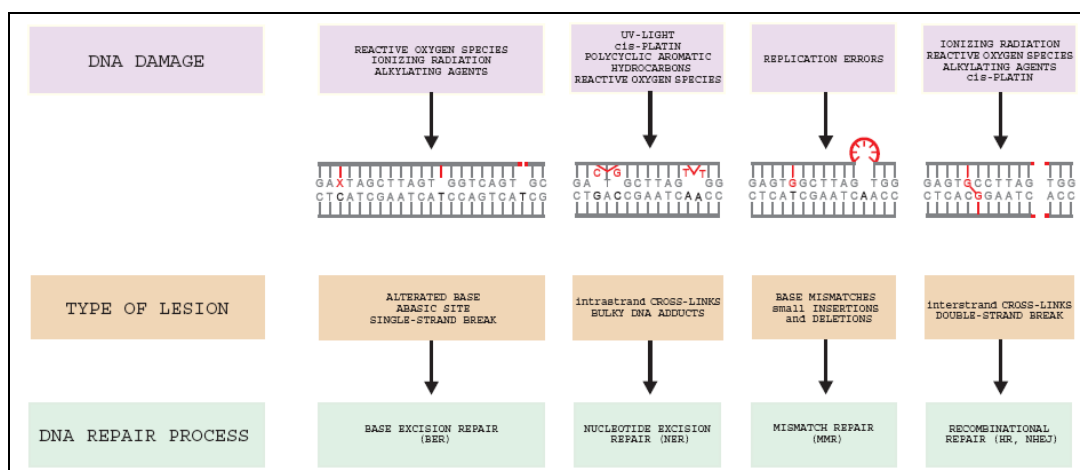
Figure 1.3: A schematic of common DNA damaging agents, lesion types and the resulting repair processes (Houtgraaf *et al.*, 2006).

It is well known that one of the causes of cancer is DNA damage. Susceptibility to cancer has been found to be associated with mutations in genes involved in DNA damage responses (Kastan and Bartek, 2004). In addition to causing cancer, DNA damage is also one of the preferred modes of cancer treatment. This is because tumour cells tend to have imperfect mechanisms of DNA repair, which makes them more susceptible to DNA damaging agents (Borst and Rottenberg, 2004). The DNA damage caused by the therapy is, unfortunately, the cause of many of the side-effects associated with chemotherapy. Therefore, an understanding of all the aspects relating to the cellular response to DNA damage is critical in the treatment and study of cancer.

The cell-cycle has various checkpoints, which have the function of arresting the cell to ensure the completion of an earlier process, such as DNA replication, before the completion of mitosis. These checkpoints may also be activated if the cellular DNA is compromised and repair mechanisms are initiated. This ensures the faithful replication of the genome prior to mitosis (Kastan and Bartek, 2004). The cell cycle checkpoints are controlled by proteins and processes that fall into the class of either sensors, transducers, mediators or effectors. A simplified view of this process is shown in Figure 1.4, in which representatives of each class are displayed in the context of the cell cycle.
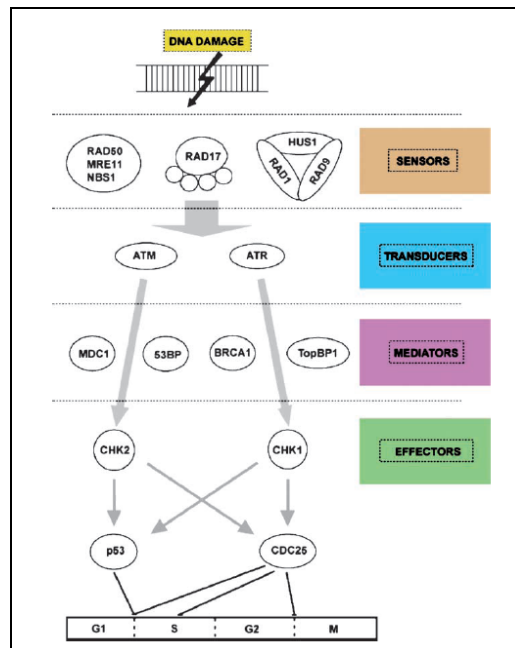
Figure 1.4: A schematic representation of the DNA damage-induced checkpoints in the context of the different phases of the cell cycle. The process is divided by the specific activity of the proteins involved (Houtgraaf *et al.*, 2006).

Nuclear proteins sense DNA damage and facilitate the attachment of repair proteins to the site of damage. Through signal transduction and the phosphorylation of targets such as p53, replication is arrested in either G1/S, in S phase or G2/M (Houtgraaf *et al.*, 2006).

1.2.1 ATM and ATR Activation in the G1 Checkpoint

To avoid unnecessary damage, the cell-cycle should be arrested as fast as possible after exposure to stress. The mechanisms that cause the arrest should however not negatively influence the cell in the absence of stress.

ATM (ataxia telangiectasia mutated) and ATR (ataxia telangiectasia mutated and Rad3 related) are (350 and 301 kilodaltons respectively) protein kinases and have to phosphorylate a variety of substrates in order to perform their function (Katan and Lim, 2000; Kastan and Bartek, 2004). Cells, patients and mice that lack functional ATM are still viable, which suggests that ATM is not crucial for normal cell function (Kastan and Bartek, 2004; Shiloh and Kastan, 2001). In unstressed cells, ATM activity is low, and is present in the form of a homodimer. The kinase

domain is physically blocked by binding to the protein surrounding serine 1981. In the case of a DNA double stranded break, the conformation of ATM changes, which causes it to phosphorylate serine 1981. This in turn leads to the dissociation of the homodimer (Bakkenist and Kastan, 2003; Kastan and Bartek, 2004). Once ATM is in the monomeric form it can phosphorylate its substrates, which include: p53, NBS1 (Nijmegan breakage syndrome 1), BRCA1 (breast cancer 1) and SMC1 (structural maintenance of chromosome 1). Thus to summarise ATM activation: it autophosphorylates and dissociates from the homodimer form in response to structural changes in the chromatin and it is recruited to its substrates, some of which localise to the DNA damage site (Kastan and Bartek, 2004).

ATR exists in association with ATRIP (ATR-interacting protein) and its function is largely controlled by cellular localisation. Therefore it is always ready within the cell to phosphorylate its substrates (Cortez *et al.*, 2001; Kastan and Bartek, 2004; Zou *et al.*, 2003). The current model suggests that ATR is localised to sites of replication fork arrest as a result of the binding of ATRIP with RPA (replication protein A) (Kastan and Bartek, 2004; Zou *et al.*, 2003). RPA is a single stranded DNA binding protein that is associated with DNA replication. Therefore, if an event occurs that leads to a long stretch of ssDNA, such as a replication fork arrest, RPA would bind to the strand. The accumulation of RPA would then lead to the binding of ATRIP. When the ATR-ATRIP complex is associated with the DNA, ATR is able to phosphorylate its substrates, which include RAD17 and CHK1. To phosphorylate CHK1, ATR must attach to the ssDNA in conjunction with other proteins, such as: the RAD17-containing complex, RSR, which facilitates the loading of the RAD9-RAD1-HUS1 (9-1-1) sliding clamp onto chromatin and the claspin protein (Kastan and Bartek, 2004).

ATR is most likely required for the progression of the cell through the cell cycle, since cells and animals lacking ATR are not viable (Brown and Baltimore, 2003; Kastan and Bartek, 2004; Zou *et al.*, 2002). ATR has been found to respond to other types of stress, such as hypoxia and DNA replication inhibitors (Kastan and Bartek, 2004; Zou *et al.*, 2003). An example of these replication inhibitors would be chemotherapeutic agents that target DNA and form bulky

adducts. This serves to further illustrate ATR's integral role in DNA replication as well as its importance in cancer progression and therapy (Kastan and Bartek, 2004).

1.2.2 The Effects of ATM and ATR Signaling

To initialise a global cellular response, ATM and ATR (proximal checkpoint kinases) interact with two other classes of proteins. These are the checkpoint mediators and the transducer kinases, CHK1 and CHK2. How the checkpoint mediators' function has still not been adequately elucidated, yet it is believed that they interact with ATM and ATR by mediating their substrate interaction; in order to form the necessary protein complexes at the DNA damage sites at the right time (Kastan and Bartek, 2004). Three of the checkpoint mediators, of ATM, are currently known and they appear to localise to DNA damage sites or replication blockages independently of ATM and ATR. Because of this, it is believed that they could be involved in identifying sites of DNA damage (Goldberg *et al.*, 2003; Kastan and Bartek, 2004). The ATM mediators are: MDC1 (mediator of DNA damage checkpoint 1), 53BP1 (p53 binding protein 1) and BRCA1 (Kastan and Bartek, 2004; Sancar *et al.*, 2004). It has been discovered that any cells lacking these proteins are more sensitive to DNA damaging agents and have ineffective cell-cycle checkpoints, which plays a major role in carcinogenesis (Kastan and Bartek, 2004).

If a single mutated allele of either *BRCA1* or *BRCA2* is inherited, the incidence of breast or ovarian cancer in women is greatly enhanced. The *BRCA* gene products have distinct roles in the DNA damage pathways and are integral to the cell cycle checkpoints (Kastan and Bartek, 2004). BRCA1 has also been found to inhibit the oestrogen receptor, which indicates its importance in breast cancer prevention (Macleod, 2000).

Once the cell passes through the Rb/E2F restriction point, it is committed to DNA replication and cell division. It is possible however for the ATM/ATR-CHK1/CHK2 checkpoints to halt the cell anywhere in G1, S or G2 phases in response to genotoxic stress. This is vital for the maintenance of genomic integrity, for the prevention of cancer. The levels of ATR and CHK1 are quite low in the early G1, but their activities become more important and pronounced closer to the G1/S

transition. The expression of ATM and CHK2, on the other hand, are relatively constant throughout the cell-cycle (Kastan and Bartek, 2004).

p53 is phosphorylated by ATM/ATR in its amino-terminal transactivation domain (mostly serine 15). Amino acids in the same domain are also targeted by CHK1/CHK2 (Houtgraaf *et al.*, 2006; Kastan and Lim, 2000; Kastan and Bartek, 2004). Besides this, after DNA damage ATM/ATR target MDM2, a ubiquitin ligase that normally binds p53. CHK1 and CHK2 have also been found to behave in a similar fashion towards MDM2. These interactions with p53 and MDM2 serve the purpose of stabilising p53, as well as to increase the protein's concentration and activity. The transcriptional target of p53 is p21CIP1/WAF1, which is an inhibitor of the cyclin dependant kinases. This acts by silencing the activity of cyclin E/Cdk2, which causes G1 arrest. The cell is therefore unable to initiate DNA synthesis, and the Rb/E2F restriction point is still active in its inhibition, which leads to arrest in the G1 phase. Therefore, through their action, this checkpoint targets two of the major tumour suppressor pathways controlled by p53 and Rb, which are commonly deregulated in cancer (Kastan and Bartek, 2004). A simplified schematic of the G1 checkpoint is pictured in Figure 1.5.
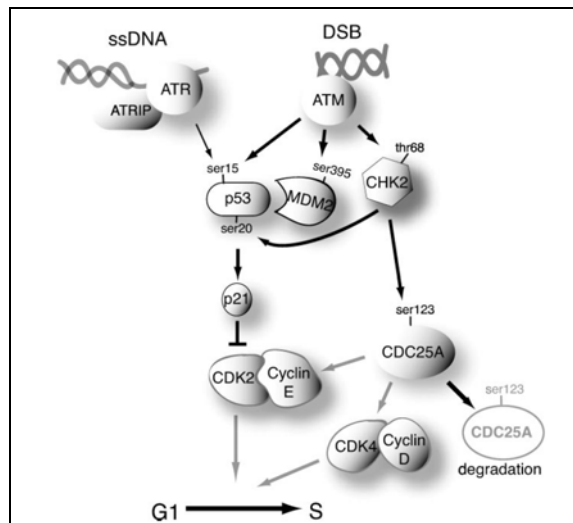
Figure 1.5: The G1 checkpoint which primarily blocks Cdk2-cyclin E activity. p53 is stabilised and Cdc25A is degraded to maintain Cdk2 inhibitory phosphorylation (Nyberg *et al.*, 2002).*

*Grey arrows indicate functionality lost through checkpoint initiation and labelled amino acids on proteins indicate phosphorylation sites.

The expression of ATR and CHK1 increases in late G1. In addition to this, cyclin A and E, and CDC25A activity is induced. CDC25A, a phosphatase that activates the E/A/Cdk2 complex, is phosphorylated by ATR/CHK1 in order to maintain optimal levels of CDC25A during proliferation. It has been found to be up-regulated in certain tumour cell lines, which is indicative of its role in proliferation (Wegner *et al.* 2000). When the cell is exposed to genotoxic stress however, the enhanced activity of ATM/ATR leads to the down regulation of CDC25A. This in turn leads to the inhibition of the cyclin E(A)/CDK2 complexes. The inhibition of CDK2 prevents the loading of CDC45 onto the chromatin. This protein plays a role in the recruitment of DNA polymerase α into the pre-replication complexes (Kastan and Bartek, 2004). CDC25A is hyperphosphorylated by CHK1 and CHK2, which stimulates its ubiquitin mediated proteolysis. It has been found that the protein is targeted by β-TrCP for degradation by the Skp1/Cul1/F-box protein complex (Busino *et al.* 2003).

The checkpoint kinases phosphorylate both p53 and CDC25A in the stress response, yet the influence of the CDC25A degradation cascade on the cell cycle is more rapid than that of p53. This is because, unlike p53, the CDC25A checkpoint does not rely on the transcription and accumulation of new proteins. The CDC25A checkpoint can therefore act independently of p53 and delay the G1/S transition for a few hours. At this point, if the stress persists, p53 can prolong the arrest (Kastan and Bartek, 2004).

1.2.3 The G2/M Checkpoint

This checkpoint exists to prevent the cell's transition into mitosis if DNA damage is present. Cyclin B/CDK1 promotes mitosis, but is inhibited by ATM/ATR, CHK1/CHK2 or p38 kinase activity. The inhibition or degradation of the CDC25 proteins, which activate CDK1, is another mechanism of CDK1 inhibition. It has been found that cancer cells deficient in the G1/S checkpoints tend to accumulate in G2 after DNA damage, which indicates that the mechanisms independent of p53 are enough to maintain the G2 arrest. With this in mind, research to hinder the G2 arrest is underway, in order to sensitize cancer cells to DNA damaging agents (Kastan and Bartek, 2004).

In the G2/M checkpoint Cdc2 is targeted to maintain its inhibitory phosphorylation state to prevent transition to M phase. In doing so a number of pathways that promote mitosis are affected. Activation of ATR, as a result of DNA damage, leads to CHK1 phosphorylation, which negatively regulates Cdc25C through phosphorylation at Ser216. This phosphorylation results in the creation of a binding site for 14-3-3 proteins which decreases Cdc25C catalytic action. CHK1 may also be activated by BRCA1 to promote G2/M arrest. ATM is activated in G2 by DNA damage; leading to CHK2 activation (Nyberg *et al.*, 2002). The mammalian G2/M checkpoint is schematically represented in Figure 1.6.
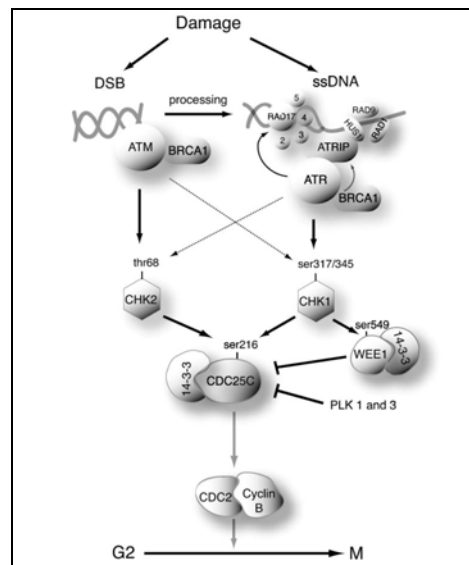
Figure 1.6: The G2/M DNA damage checkpoint which serves to block the function of Cdc2-cyclin B activity (Nyberg *et al.*, 2002).

*Grey arrows indicate functionality lost through checkpoint initiation and labelled amino acids on proteins indicate phosphorylation sites.

From the preceding text it is clear that the DNA damage response exists as a number of complex and interacting pathways with a number of levels of redundancy. Ultimately this damage may be repaired, or, under normal circumstances would lead to programmed cell death. This may be in the form of either necrosis or apoptosis.

1.3 The Cellular Response to Stress: Apoptosis and Necrosis

Cell death is an essential and tightly regulated process that is required for normal development, as well as avoiding aberrant growth as a result of stress. Three major types of cell death have been identified: apoptosis, autophagy and necrosis.

1.3.1 Apoptosis

In response to aberrant cell growth, which cannot be repaired, the cell initiates its own death, through a variety of mechanisms. Cell death may happen via apoptosis, which is a highly ordered process whereby the cell is dismantled into vesicles, which are then engulfed by phagocytes, thus preventing the release of the cell's components into the system (Nelson and White, 2004).

Apoptosis is controlled by a variety of tumour suppressor genes and oncogenes. In addition to the much lamented p53; PTEN, APC and PML have been shown to have tumour suppressor activity by inducing apoptosis. Loss of the various tumour suppressors have been found to result in reduced apoptosis and increased tumour growth (Macleod, 2000). Figure 1.7 is a simplified schematic of the apoptotic and associated regulatory pathways.
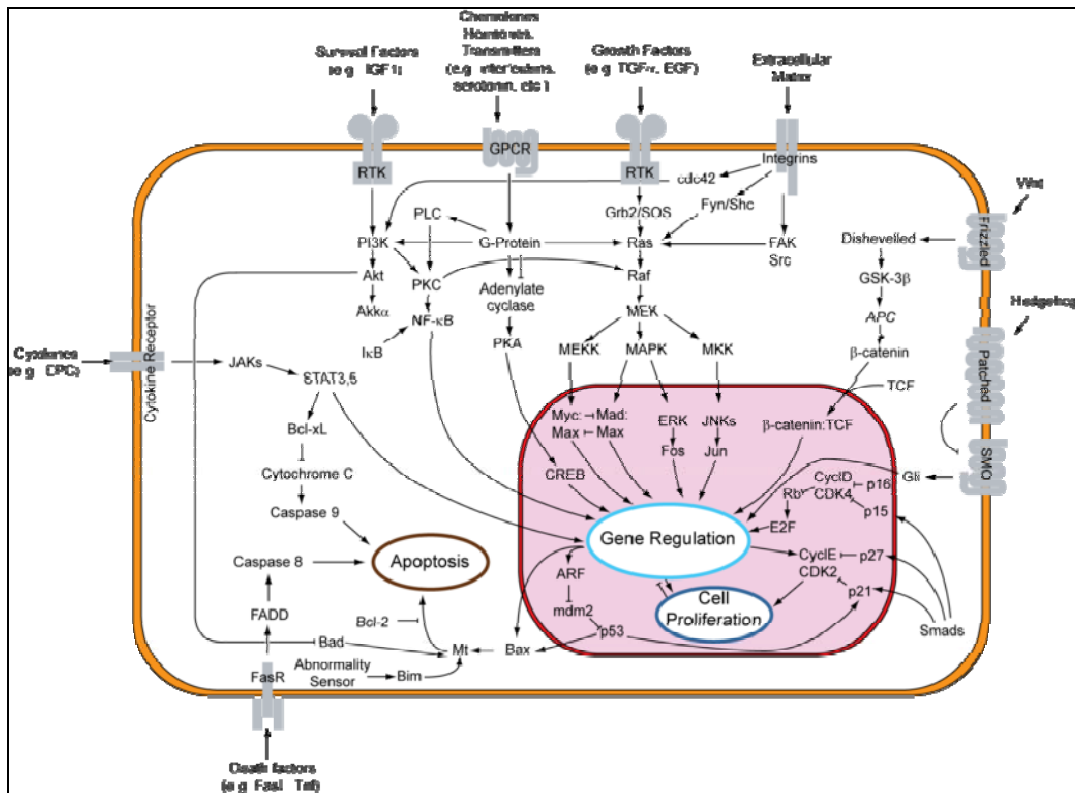
Figure 1.7: The extrinsic and intrinsic signal transduction pathways associated with apoptosis in the mammalian cell (Wikipaedia).

Although cell proliferation and death seem in direct opposition to each other, they are in fact linked. Two general programmes exist that control apoptosis, and many of the proliferative molecules are involved in them. The intrinsic pathway responds to survival factors, cellular stress and injury, and the general focus of this pathway is the mitochondrion. The inter-membrane space of the mitochondria contains molecules that trigger apoptosis once the membrane is permeabilised. The permeability of the membrane is determined by the balance between the anti-apoptotic Bcl2/BclXL and the pro-apoptotic Bax/Bak proteins. These proteins are positively or negatively regulated by a variety of BH3 proteins. Once the effect of the pro-apoptotic Bax/Bak proteins becomes dominant, pro-apoptotic factors such as cytochrome c are released. Cytochrome c acts with Apaf-1 to activate caspase 9, a cysteine protease that activates the proteolytic cascade involving caspase 3 and caspase 7. The caspases' function is to degrade proteins that are essential for cell survival (Lowe *et al.,* 2004).

The extrinsic death pathway is put in to play by the ligation of death receptors on the cellular surface. Fas/CD95, TNFR (tumour necrosis factor receptor) and DF-5 are examples of these receptors, and with FasL, TNFα and TRAIL as their respective ligands. Once the ligands have bound to the receptors, they form the death inducing signaling complex (DISC), which in turn activates caspase 8. This caspase can induce the caspase cascade, which results in apoptosis, in some tissues. In other tissues however, the mitochondrial pathway is recruited by caspase 8 and Bid (a BH3 related protein) (Lowe *et al.,* 2004).

p53 Signaling and Apoptosis

p53, a transcription factor, is a tumour suppressor that is activated in response to DNA damage or oncogenic stress. It mediates cell cycle arrest by its activity as a transcription factor and the gene expression it regulates. It may also have a non-transcriptional role by directly interacting with certain proteins in the cell. Besides being activated by the DNA damage-response proteins, p53 activity is also initiated by many other oncogenes such as Myc, E1A and E2F. This type of oncogene-dependant activation is mediated by the tumour suppressor ARF. This protein is not always required however for the DNA damage response, which serves to highlight the intricacies of these pathways (Lowe *et al.*, 2004). The two major results of p53 activity are cell cycle arrest and apoptosis, which are achieved by the expression of genes that function to execute this (Gottlieb and Oren, 1998). p53 is mutated in 50% of human cancers which indicates the integral role this tumour suppressor plays in preventing tumour formation, as well as the high selective pressure placed on it during carcinogenesis (Hollstein *et al.*, 1991).

The apoptotic machinery can also be set into motion by various oncogenes. For instance, Myc sensitizes cells to death receptor signalling. In addition to this oncogenes have also been found to influence members of the Bcl2 family. Myc, for instance, represses the expression of *bcl2* and *bclXL*, whereas E1A and E2F suppress *mcl-1.* Myc and E2F also trigger BH3-only killer (e.g. Bim) protein expression and in addition to this E2F is also able to induce many of the downstream components of apoptosis, such as the caspases (Lowe *et al.,* 2004).

Results of Apoptotic Signaling

Once the cell has initiated apoptosis and has entered the death phase, the body has to deal with the cellular remnants. Various genes are expressed within the apoptotic cell to induce inter-cellular signalling. These signals enable recognition of the cell and facilitates engulfment by the macrophage. The signalling may take various forms, including: alterations in the composition of the cell surface phospholipids, conformational changes in existing molecules, changes in surface glycoproteins, changes in membrane charge, or, serum proteins and other molecules from other cells may attach to the membrane. Phosphatidylserine (PS) is one of the better known molecules involved in membrane signalling. PS is usually on the inner section of the membrane, but after apoptosis it is exposed on the outer membrane. This allows for annexin V staining, which interacts with PS, as a method of detecting apoptotic cells (Ravichandran, 2003). These changes in membrane composition and cellular signalling may provide valuable indicators for the study of cancerous cells in culture.

1.3.2 Necrosis as a Mechanism of Cell Death

Necrosis describes the form of cell death characterised by the swelling and rupture of the cell. This usually happens as a result of severe physical damage and results in the release of the intracellular contents into the surrounding microenvironment. An inflammatory response occurs due to this release and this may be beneficial as it activates immunity and wound healing, in response to a pathogen or tumour. Some believe however that the release of the cellular components may be toxic to the surrounding cells and lead to a greater incidence of mutations (Nelson and White, 2004).

It has been a long held belief that necrosis is an uncontrolled process that only occurs as the result of severe stress. Some researchers however, suggest that necrosis forms part of an organism's normal developmental program and thus a certain level of control should exist. This can be seen in the cellular renewal found in the intestinal tract, where both apoptosis and necrosis play a role (Proskuryakov and Konoplyannikov, 2003). This would suggest that various aspect of necrosis, such as gene expression, may be quantifiable.

Necrosis can occur as an alternative to apoptosis if the apoptotic pathways are blocked. Various researchers suggest that necrosis may serve as an alternative target for cancer therapy, as opposed to apoptosis. This is because several of the key apoptotic components are inactivated in cancer cells, leading to apoptotic insensitivity and therefore excluding apoptosis as a therapeutic target (Nelson and White, 2004; Proskuryakov and Konoplyannikov, 2003; Zong *et al.,* 2004). With the identification of apoptotic genes, the general impression was that apoptosis is a well planned form of cell death and necrosis is an uncontrolled event. But, it turns out that a wide spectrum of suicide programmes exist within the cell, with apoptosis and necrosis existing as the polar extremes (Proskuryakov and Konoplyannikov, 2003).

Necrotic Induction

Necrosis may be initiated by, amongst others, cytokines released by surrounding tissue as a result of inflammation or infection. Pancreatic β-cells, in the cellular model of diabetes, die by apoptosis and necrosis when exposed to IL-1β, TNF-α or IFN-γ. Necrosis may also be induced by the TNF receptor family (TNF, FAS and TRAIL), that usually induce apoptosis (Proskuryakov and Konoplyannikov, 2003).

The stress activated kinases (JNK and MAP) usually associated with inducing apoptosis, have been found to play a role in necrosis. JNK activation has been found in heat-shock induced necrosis of osteoblasts as well as in ceramide induced necrosis in prostate carcinoma (Proskuryakov and Konoplyannikov, 2003; Engedal and Saatcioglu, 2001). Inhibition of other stress related proteins, such as p38, has also been found to decrease the necrotic response (Ma *et al.*, 1999). A high level of inter-relatedness is suspected between apoptosis and necrosis *in vivo*. Caspase activation is usually associated with apoptosis alone, but may also induce necrosis by promoting ionic overload in the cell (Nicotera and Melino, 2004).

Besides shared function in stress response proteins, necrosis also responds to a variety of anti-apoptotic proteins. AKT kinase and MAP kinase ERK, which prevent apoptosis, have also been

found to have a role in preventing necrosis. It has been shown that over expression of *Akt*, in certain tissues, prevents necrosis (Mochizuki *et al.*, 2002).

The Mitochondrial Role in Necrosis

Besides playing an integral role in apoptosis, certain mitochondrial activities influence necrosis as well. The mitochondria serve as a source of ATP for ATP-dependant programmes, such as apoptosis. If the ATP levels drop below a certain point, the cell fate may switch from apoptosis to necrosis. It has also been found that mitochondrial inhibitors also lead to necrosis (Proskuryakov and Konoplyannikov, 2003).

The mitochondrial respiratory chain generates reactive oxygen species (ROS), which may trigger necrosis. The ROS oxidise key molecules, leading to the release of executor proteases, lipases and nucleases from the mitochondria. In response to this, the cell uses caspase dependent autophagy to rid itself of the aberrant mitochondria. If the caspases are inhibited, the entire cell may undergo necrosis (Fiers *et al.,* 1999).

Mitochondria may also be a source of pro-necrotic factors. Under certain circumstances (high Ca^{2+} or oxidative stress) the mitochondria undergo mitochondrial permeability transition (MPT) which is characterised by certain changes, such as: inner membrane de-energization, swelling and permeablisation. MPT is usually irreversible and leads to mitochondrial death ("mitoptosis") and may eventually cause necrosis. MPT and this form of necrosis originate from the opening of a pore known as the mitochondrial permeability transition pore (MPTP), which is located on the mitochondrial membrane. An increase in Ca^{2+} and oxygen free radicals, initiate the pore opening which leads to MPT. The pore is believed to be made up of three components: adenine nucleotide translocase (ANT), which is found on the inner membrane and usually transports ATP out of the mitochondria, the voltage dependent anion transporter, found in the outer membrane, and, cyclophillin D which is found inside the mitochondria. Cyclophillin D is a small soluble protein that is named for its binding of the immunosuppressant drug cyclosporin A. This drug prevents cyclophillin D binding to ANT, which inhibits the MPTP activity. It is believed that

cyclophillin D facilitates a calcium triggered change in ANT which leads to opening of the pore and the release of ATP. The depletion of ATP in this fashion is believed to lead to necrosis, whereas the closed pore would allow for ATP retention and the progression of apoptosis (Halestrap, 2005).

At this point it is important to note that the MPTP does not have a significant role in apoptosis. Apoptosis is triggered by the release of proteins from the inter-membrane space of the mitochondrion. Proteins, such as cytochrome c, then initiate the apoptotic cascade. The belief that the opening of the MPTP leads to mitochondrial rupture and cytochrome c release is unlikely, since this would be to the detriment of ATP production. This is not to say that the MPTP plays absolutely no role in apoptosis. Transient MPTP opening may be sufficient to release cytochrome c for apoptotic initiation (Halestrap, 2005).

Necrosis: Immunity and Therapeutic Purposes

The signals the immune system receives from necrotic cells are mediated by: Hsp70 (heat-shock protein), calreticuline, oligonucleosomes and carbohydrates. When these substances are released into the extracellular space, they activate antigen presenting cells (APC). Hsp70 is also able to induce the production of pro-inflammatory cytokines by activating CD14 receptors in monocytes. It has been shown that necrotic cells stimulate the APC and T-cell response more efficiently than apoptotic cells. This may be an adaptive mechanism to quickly eliminate a pathogen. With the insensitivity of certain tumours to apoptosis in mind, necrosis may serve as an effective method of cancer therapy. Some treatments that are currently used, besides causing apoptosis, also induce necrosis. These include: gamma irradiation, photodynamic therapy, docetaxel and phenritinide (Proskuryakov and Konoplyannikov, 2003).

Since PARP activation results in depletion of cellular ATP and eventually necrosis, normal cells that can maintain non-glucose-dependent oxidative phosphorylation are less sensitive than those who cannot, as is the case in many cancer cells. This would indicate that necrotic inducers would be more effective against cancer cells than normal tissue (Zong, *et al.*, 2004)

CHAPTER 2: CHEMOTHERAPY AND DRUG DEVELOPMENT

2.1 Introduction

The ancient Egyptians describe malignant diseases and their treatments in documents such as the Ebers papyrus (Ebbel, 1936; Tu, 2010). But, chemotherapy as we know it began in the 1940's with the publication of research describing the anti-tumour effect of estrogens in prostate cancer. In the same period nitrogen mustard, a by-product of World War One, was found to have therapeutic value in the treatment of cancer. This alkylating agent was determined to have chemotherapeutic properties and in principle is still used today. A wide spectrum of chemotherapeutic drugs were developed between 1945 and 1965, such as actinomycin D, the vinca alkaloids, 5-fluorocil, progesterones and cyclophosphamide. Cisplatin was found to be effective against ovarian and testicular cancer in the early 1970's and interestingly derivatives of this drug are still used today (Young, 1996; DeVita and Chu, 2008).

Insight into the growth characteristics of normal and tumour cells have lead to many chemotherapeutic tenets. Tissue can be divided into three categories: renewing, expanding and static. The static tissue-types, which are well differentiated, do not proliferate actively during adult life, and rarely divide. Tissues of this type, such as striated muscle and nerve tissue, do not respond well to drugs that work on rapidly proliferating cells. The expanding tissue type does not proliferate actively, but maintains the ability to do so due to stress or injury. Liver tissue is an example of this tissue type. The third type of normal tissue, the renewing tissue-type, is constantly dividing. Bone marrow and gastrointestinal mucosa are examples of this tissue. By understanding these three categories of tissue, the toxicity of compounds directed at proliferating cells may be explained. Renewing tissues are usually the most affected by chemotherapy, whereas static and expanding tissues are injured to a lesser degree (Young, 1996).

Therefore, within the framework of tissue growth dynamics the challenge exists to develop less toxic forms of chemotherapy.

2.2 Chemotherapeutic Agents

Chemotherapeutic drugs are classed according to their cellular target and the cellular phase which they affect. Agents that are not specific to a particular phase, e.g. alkylating agents, show a linear dose-response curve, whereas phase-specific drugs have a plateau with regards to killing ability (Pazdur, *et al.*, 2005). These are important considerations for therapeutic efficacy.

2.2.1 Alkylating Agents

Alkylating agents form covalent bonds with amino, carboxyl, sulfhyryl and phosphate groups in biologically important molecules, which results in impaired cellular function. The most important alkylation targets are DNA (e.g. the nitrogen at position 7 of guanine), RNA and proteins. These agents are not phase specific, but do depend on cell proliferation for their activity. Resistance to this drug type can be caused by a number of factors such as glutathione conjugation or enhanced DNA repair. The alkylating agents are classified according to their chemical structures and covalent bonding mechanisms. Included in this group are the nitrogen mustards, nitrosoureas and the platinum complexes (Pazdur, *et al.*, 2005; Eckhardt, 2002). Nitrogen mustards are highly reactive in aqueous solution and the active alkylating moiety is the ethylene imonium ion which binds to DNA. These compounds are powerful vesicants and can cause tissue necrosis, pulmonary fibrosis, hemorrhagic cystitis, and, affect the hematopoietic system (Pazdur, *et al.*, 2005).

The Nitrosoureas are characterised by their high lipid solubility and chemical instability. These compounds spontaneously decompose into two reactive intermediates: isocyanate and chloroethyl diazohydroxide. Due to their lipophilicity, the nitrosoureas are able to pass across lipid membranes and therefore penetrate the blood brain barrier. As a result of this, these agents are used to treat brain tumours (Pazdur *et al.*, 2005).

An example of platinum drugs, as mentioned earlier, is cisplatin, which produces intrastrand and interstrand DNA crosslinks. DNA adducts are formed as a result, which in turn inhibits DNA, RNA and protein synthesis. Carboplatin has the same diamine platinum structure as cisplatin, but it is

bonded to an organic carboxylate group which alters the compound's toxicity profile. Oxaliplatin possesses a di-amino-cyclohexane ring, bound to the platinum molecule, which distinguishes it from the other platinum compounds. This addition interferes with the resistance mechanisms to this class of drugs (Pazdur *et al.*, 2005; Eckhardt, 2002).

2.2.2 Anti-metabolites

These drugs are analogues of naturally occurring metabolites involved in DNA and RNA synthesis. The antimetabolites can be divided into substituted ureas, purine analogues, pyrimidine analogues, adenosine analogues or folate analogues. Their mechanism of action is based on either competing with metabolites for the catalytic or regulatory site of an enzyme, or, by incorporating themselves into DNA or RNA, instead of their natural counterparts. Because of this, these compounds are only active when the cells are in S-phase and have negligible effect on G_0-phase cells. Therefore, these drugs are most effective against tumours with a high growth fraction (Pazdur *et al.*, 2005; Parker, 2010).

2.2.3 Natural Products

Many chemotherapeutic agents have been isolated from natural sources such as plants, fungi and bacteria. These compounds are either semi-synthetic or are synthetically based on the parent compound. These drugs include the anti-tumour antibiotics, anthracyclines, epipodophyllotoxins, vinca alkaloids, taxanes and the campothecins. The mode of action of these drugs vary greatly from the generation of free radicals to intercalating action (Pazdur *et al.*, 2005).

2.3 Drug Resistance

Drug resistance is multifactorial, and is one of the most confounding factors of chemotherapy. Resistance to one or a number of chemotherapeutic agents may be intrinsic, acquired or induced. Intrinsic resistance describes instances when a tumour does not respond to the first dose of a specific therapy. Acquired or induced resistance describes tumours that no longer respond to therapies they were initially sensitive to. Acquired resistance may be to a specific

agent, e.g. methotrexate resistance as a result of increased dehydrofolate reductase production, or pleitropic (resistance to a number of agents). Many cellular mechanisms exist that determine drug resistance such as drug transport, ineffective drug activation, altered hormone receptor concentration or affinity, altered DNA repair, altered gene expression, changed target proteins, defective drug metabolism and altered intracellular nucleotide pools (Young,1996). Many of these mechanisms can lead to multidrug resistance in which the cell becomes resistant to a number of compounds in addition to the one it was originally exposed to (Sparreboom *et al.*, 2003; Baguley, 2010).

Drug resistance or sensitivity can also be seen from the point of view of cancer development. Some cancers can be intrinsically sensitive, such as childhood cancers, leukaemias and lymphomas in adults, or, intrinsically resistant, as is the case with many adult epithelial tumours. Intrinsic chemosensitivity can be related to the cancer's origin. Sensitive tumours arise quickly, and have no recognizable pre-malignant states. In contrast, cancers that arise after prolonged pre-malignant states have had the time to develop a more complex karyotype and are less genetically stable. This is found in most adult epithelial cancers (lung, colon etc.) and tends to lead to a more resistant phenotype. This phenotype is the result of the inactivation of tumour suppressor genes in the apoptotic pathway and the activation of dominant acting genes (Kruh, 2003).

A common characteristic of cancer is drug resistance, which can arise as a result of cancer's genomic plasticity and somatic mutations. In the course of therapy, normal tissues, such as bone marrow and the mucosa are often depleted. This is because resistance does not develop in normal tissue due to the fact that the mutation rate is to low to confer resistance. By exploring the mechanisms of drug resistance, researchers will be able to develop better treatments for cancer patients. Much of the knowledge we have today was gleaned from creating and studying resistant cell lines (Kruh, 2003). The mechanisms of resistance are divided into categories and can be explored on an individual basis.

2.3.1 Transportation and Drug Resistance

Membrane transporters and channels, known collectively as the transportome, control the influx and efflux of ions, nutrients and drugs. Two of the key factors that determine a cell's sensitivity, is the ability of a compound to enter the cell and whether or not it is pumped out of the cell.

The ATP-binding cassette (ABC) genes represent the largest family of transmembrane proteins that bind ATP and use the energy to transport molecules across the membrane (Borst *et al.*, 2000; Sparreboom *et al.*, 2003). It is well recognized that the ABC transporter family plays a major role in detoxification and protection against xenobiotic substances. It has been found, by sequencing, that certain allelic variants affect the activity of the genes *in vivo* (Fromm, 2002), and, these types of polymorphisms could affect the way a patient responds to a specific treatment.

The best characterised mechanism of multidrug resistance is caused by *MDR1* (also known as ABCB1) and its product, the P170 glycoprotein. Resistance by this mechanism is usually associated with insensitivity to drugs such as the vinca alkaloids, actinomycin D, doxorubicin and paclitaxel. The mechanism of this type of resistance is based on increasing drug efflux causing a lower intracellular concentration (Young, 1996). The ABC pumps are mostly unidirectional, and in eukaryotes they move compounds from the cytoplasm to the outside of the cell or to an intracellular compartment. The ABC transporters either exist as full transporters, containing two transmembrane domains and two nucleotide-binding folds (NBF), or as half transporters. To form a functional transporter, the half transporters must form either homodimers or heterodimers. The ABC gene type is wide-spread among eukaryotes and they are conserved between species. Many of the mammalian ABC's have been categorised by the Human Gene Organization (Cotton and Horaitis, 2002; Sparreboom *et al.*, 2003).

Multi-drug resistance has been linked to P-glycoprotein (P-gp) over-expression and this has lead to the development of P-gp inhibitors. Third generation cyclosporin-based inhibitors such as

tariquidar and zosuquidar, have undergone clinical trials in conjunction with chemotherapy. This is to determine if P-gp inhibition can enhance or prolong drug sensitivity (Longley and Johnston, 2005).

2.3.2 Drug Targets and Resistance

The target of a specific drug may change or decrease, leading to ineffective interaction. An example taken from gynaecologic cancers is altered hormone receptor concentration or altered binding which is associated to resistance to steroid hormone therapy (Young, 1996).

Taxanes (paclitaxel and docetaxel) and vinca alkaloids suppress microtubule polymerisation and dynamics, which results in mitotic inhibition. The cells are arrested in the metaphase-anaphase boundary and eventually die by apoptosis (Longley and Johnston, 2005). Changes in the microtubule dynamics and the level of tubulin isotypes have been associated with paclitaxel and vinca alkaloid resistance (Burkhart *et al.*, 2001; Longley and Johnston, 2005). In addition to this, specific β-tubulin mutations have been found to alter paclitaxel sensitivity (Giannakakou *et al.*, 1997; Cheung *et al.*, 2010).

The ability of a cancerous cell to repair DNA, can determine its resistance to chemotherapeutic drugs that damage DNA directly (e.g. platinum compounds) or indirectly (e.g. 5-FU or topoisomerase inhibitors). The cell can either repair the resulting damage or enter apoptosis, which has a dramatic effect on drug efficacy (Longley and Johnston, 2005).

An increasing amount of evidence suggests that apoptosis and cell growth are directly linked; therefore, if drug mediated cell death occurs via apoptosis, even with intense selective pressure, cells rarely eliminate all the apoptotic machinery (Kruh, 2003). With this said, a number of cancers have mutated forms of p53 which has been found to confer resistance to apoptosis (Longley and Johnston, 2005). In other instances however, p53 mutation has conferred sensitivity to drugs such as cisplatin due to the reduced time for DNA repair because of the loss of p53 function (Fan *et al.*, 1995).

Zembutsu *et al.* (2002) compared chemosensitivity to gene expression using genome wide arrays for 85 tumour xenografts. This *in vivo* study screened nine commonly used cancer agents and found a number of biologically relevant associations. It was found that increased *topoisomerase IIα* expression is related to doxorubicin resistance. They found a negative correlation between *aldehyde dehydrogenase 1* and camptothecin sensitivity as well as between *thymidylate synthetase* and 5-FU sensitivity. In addition to this they found that reduced expression of the G2M regulators, such as *cyclin B1* and *BUB 1β,* is related to chemoresistance. This is significant since a number of anti-cancer drugs induce a G2M arrest.

Given the existence of extrinsic and intrinsic resistance to therapy, as well as the slow pace of development using animal models and classical pharmacology, there is a great need to identify novel therapeutics faster and at a lower cost. With advances in molecular biology drug candidates may be screened and identified faster than ever before. Failed compounds may be excluded before reaching clinical trials and the mechanism of action of promising compounds may be elucidated prior to animal studies.

2.4 High Throughput Drug Discovery: Chemogenomics and Pharmacogenomics

Chemogenomics describes the focused study of target gene families that are identified by the interaction of a single member of the family with a small molecular probe (e.g. a drug). These methods integrate target as well as drug discovery by using active compounds as probes; and have been applied in a variety of areas. This methodology promises great advances in cancer research, not only for the development of new chemotherapy drugs but also in gaining a greater understanding of cancer's characteristics (Bredel and Jacoby, 2004; Wuster and Babu, 2008; Marechal, 2008).

Chemistry has been one of the major role-players in the development of chemogenomics, which can be seen to have branched off of the fields of chemical genetics and genomics. Chemogenomics can be seen as the study of all potential drugs to be used against all possible

targets as opposed to chemical genetics which takes a more specific target and compound approach (Gagna *et al.*, 2004; Marechal, 2008). Typically, chemical genetics uses defined probes to dissect various aspects of biology (Carson *et al.*, 2001). Chemogenomics therefore allows for high throughput experimentation to determine either a drug target or drug efficacy depending on the experimental design.

In reverse chemogenomics target gene sequences are cloned and expressed as target proteins in a high throughput system. A compound library is then used in a target-based fashion. This allows for the identification of compounds that have a desired function (e.g. inhibit mitosis in a tumour cell). In general, cell free methods are used since in an *in vitro* system multiple interactions take place, which requires a higher level of characterization. Forward chemogenomics on the other hand, relies on a biological system in the form of single cells. In this instance the molecular basis of a desired phenotype is not known. Compounds are thus identified as useful on the basis of a conditional phenotypic effect in a biological system, as opposed to just one target protein. This type of phenotypic screening leads to the identification of a conditional phenotype (loss or gain of function) as well as the target protein or pathway. Compounds identified by reverse chemogenomics can also be validated by forward chemogenomics, which would allow for greater characterisation of their affect (Bredel and Jacoby, 2004). Many studies have shown the importance of combining these two approaches. It has been found that targets identified for certain compounds by phenotypic screening can be used subsequently in high throughput screening to develop more powerful drug analogues.

As an example of this, forward and reverse chemogenomics led to the identification of histone deacetylase (HDAC), and following this, HDAC inhibitors such as depsipeptide, sodium phenylbutyrate, CI-994 and suberoylanilide hydroxamic acid. These compounds have already entered the clinical phase for the treatment of a variety of cancers. There is vast potential in the chemogenomic field, but presently two major problems exist: identifying the plethora of pathological changes, and thus possible targets, in the tumour cell, and, identifying therapeutics that are able to address as many targets as possible (Bredel and Jacoby, 2004).

2.4.1 Predictive Chemogenomics

In predictive chemogenomics the primary aim is to determine the response to a specific treatment and secondly to discover novel therapeutic molecules. A specific cell type is treated with various drugs and the genomic response, as well as the pharmacological action is determined. This can be done by microarray analysis and growth inhibition assays respectively. By integrating the data from a variety of drug or cell types, relationships between genes and drugs or drug classes can be determined.

Predictive chemogenomics is similar to pharmacogenomics, but chemogenomics deals with the target-ligand interaction of thousands of drugs, whereas pharmacogenomics deals with one molecule at a time (Bredel and Jacoby, 2004). Pharmacogenomics, as a discipline, also seeks to determine the genetic reasons for the differences in drug response between individuals (Lee *et al.,* 2005).

2.4.2 Chemogenomics in Practice: Cancer Research

These strategies can be applied to a diverse array of research fields, ranging from studies in inflammatory and hormone disease to cancer research. The wide applicability of chemogenomics can be summarised into three main uses. It can firstly be used to identify new drug targets and possible insight into their biological function may be gained. Secondly, through the use of chemogenomics, new chemical candidates can be discovered for specific targets and phenotypes of interest. Lastly, chemogenomics can illustrate the mechanism of drug action as well as finding genetic markers for drug susceptibility (Bredel and Jacoby, 2004).

An important hurdle chemogenomics faces is the fact that before novel drugs can be linked to specific genes, the role of the proteins they encode have to be described (Bredel and Jacoby, 2004). The National Cancer Institute (NCI) announced in 1996 the inception of the Cancer Genome Anatomy Project which aims to describe the molecular characteristics of normal, pre-cancerous and malignant cells. This project has been very productive to date and has greatly

enabled chemogenomic methods by providing relevant molecular information (Weinstein and Buolamwini, 2000).

One of the most ambitious chemogenomic projects, analyzing gene expression, protein expression and growth profiles, has been undertaken by the National Cancer institute (NCI), who have been experimenting on sixty human cell lines known as the NCI60. The NCI60 is used for the screening of the NCI's chemical libraries. These libraries consist of in excess of 140 000 compounds, and from experimentation a fingerprint is created for these compounds. Possible candidates are then selected and evaluated for therapeutic effect (Weinstein and Buolamwini, 2000; Shoemaker *et al.* 2002; Bredel and Jacoby, 2004).

The NCI test the compounds from its libraries for the ability to inhibit cellular growth in the 60 cell lines. The reasoning behind this is: if a compound shows inhibitory activity in a cell line *in vitro* it may also act on the corresponding tumours in humans. The data obtained for a compound would be in the form of a specific inhibitory concentration (IC_{50} or GI50) which would inhibit 50% of the cell culture's growth. This is done by exposing the cells to a defined range of chemical concentrations (Boyd and Paull, 1995; Weinstein and Buolamwini, 2000). This data was then analysed and used to predict the activity and mechanism of action of the drugs that followed. A candidate compound's activity is then screened using chemogenomic, proteomic and a variety of other techniques to fully characterise the drug's activity.

Once a compound is identified as having potential, further high throughput assays are carried out. In a cell-based scenario, at the NCI, drug effects (phenotype) are characterised utilising a variety of assays set up for high throughput screening. The ability of a drug to induce apoptosis is monitored using commercially available reagents that are based on the fluorescence of rhodamine, which serves as an indicator of caspase activity and hence apoptosis (Monks *et al.*, 1991; Shoemaker *et al.*, 2002).

The aim of high throughput screening is to identify novel compounds that have an effect on a specific molecule or pathway. This method is not expected to produce candidates that can be streamed directly to therapeutic development, but rather to identify molecules that show promise. Analogues of these active compounds can then be developed or selected from a library and screened in a similar fashion, to improve on a desired activity. This method allows for the rapid optimisation of promising compounds (Shoemaker *et al.*, 2002).

Various other pharmacological characteristics (adsorbsion, distribution, metabolism and excretion [ADME]) of new compounds have to be determined before they can be considered for therapeutic use. The standard method is to simulate an *in vivo* situation by making use of animal models.

2.4.3 Molecular Techniques in Drug Development

With the advent of high throughput molecular techniques such as the microarray, the effect of a drug can be determined on the genomic scale. In other words, the effects of various chemicals on a biological system can be determined. At this point it is easy to draw the distinction between chemogenomics and classical pharmacology. The difference lies in how the effect of a compound is measured. Pharmacology relies on physiological readouts (blood pressure, swelling etc.) while chemogenomics utilises genomic tools to measure mRNA levels or protein phosphorylation. The reductionist approach to drug discovery, which focuses on one target at a time, is fast being replaced by the chemogenomic approach. This allows the researcher to determine all the possible interactions and effects a drug might have in a specific system (Browne *et al.*, 2002).

Differential expression analysis is based on comparing gene expression levels before and after a certain treatment, within or between different cell types. One of the most common practices, especially in cancer research, is to treat cells with a compound already known to halt the cell cycle, and then to observe which genes change expression levels (Walker, 2001). Drug discovery

programmes such as the NCI identify cell cycle inhibitors and cytotoxic compounds *en mass*, in their cytotoxicity screens.

Determining the effect a specific compound has on gene expression is an important facet of drug discovery and development. Expression analysis provides proof of the molecular action of the drug as well as providing data relating to its efficacy. Profiling in response to treatment may also identify pharmacodynamic markers (Clarke *et al.*, 2004). Analysing the expression profile of human tumours is generally considered complex and difficult to interpret. This is because of fragmented treatment history as well as a variety of uncontrollable variables. The NCI thus embarked on the analysis of the NCI 60's gene expression profiles. By that point in time the NCI 60 were pharmacologically well characterised, having been exposed to in excess of 70 000 different compounds (Scherf *et al.*, 2000).

Scherf and co-workers (2000) compared information gained from the treatment of the NCI 60 using a variety of compounds, with the gene expression profiles of the cell lines. This study utilises the expression of mock-treated cells, and the focus is on drug sensitivity rather than the molecular consequences of therapy. This study can be related to clinical tumours, for the discovery of sensitivity markers and the prediction of therapeutic sensitivity. Through a better understanding of molecular pharmacology, one is able to select a therapy on the basis of the molecular characteristics of a patient's tumour. Various drawbacks exist with this kind of approach, such as the fact that the study is correlative and not causal, as well as the fact that cell culture is not a true representation of the tumour microenvironment. None the less, much insight stands to be gained from this type of study. The gene expression data obtained proved to be coherent, as most of the cell lines clustered themselves according to tissue origin. When the cells were clustered according to drug activity pattern, the cells did not cluster according to tissue type. The reason for this is that a single gene can have a large impact on the activities of many drugs, but plays a small role when cells are clustered according to expression. An example of this would be the impact *ABCB1* has on drugs it can transport out of the cell. Since at least one cell line from each tissue type expresses *ABCB1* at significant levels, the grouping by tissue

type on the basis of drug response is confounded. Thus expression levels of a specific tissue type, in general, may not correlate well with a single cell line's drug sensitivity. A more specific approach to investigating expression on a single gene level may be required. Besides this, all relevant information may not be obtained from expression studies alone; protein analysis is required for more clarity.

The transcriptional profiling of various tumours and their respective cell lines may prove to be a useful tool in oncology, drug design and drug development. By characterising the genes in tumours, the tumours may be separated into subsets with a specific transcriptional profile. These subsets may utilise specific pathways and the molecular aspects of these pathways could serve as potential drug targets, and hence, provide therapies for the specific tumour subset. Another aspect of this type of study is the molecular characterisation of a drug's action. This would provide information regarding the specific pathways involved as well as to facilitate the generation of drug analogues (Sauseville and Holbeck, 2004).

This type of data has contributed immensely to the study of novel compounds. It was found that diethyldithiocarbamate, an inhibitor of NFκB, correlates with the expression of the type-2 interleukin (IL)-1 receptor and a sphingomyelinase. Activation of the IL-1 receptor leads to signalling through phospholipase C which serves to modulate sphingomyelinase and the degradation of IκB (activates NFκB signalling). Therefore, if one was unaware of the function of diethyldithiocarbamate, insight into its function could be gained from expression studies (Kim *et al.*, 2000; Sauseville and Holbeck, 2004).

A variety of studies that describe the transcriptional response to DNA-damaging drugs or irradiation have been concluded to date. Zhou *et al.* (2002) measured the effect that two concentrations of camptothecin have on HCT116 colon carcinoma cells' expression levels (the cells were synchronised in S phase). A reversible G2 arrest was observed with the lower drug concentration whereas a permanent G2 arrest was seen for the higher concentration. Similarly, different gene expression patterns were observed for the two concentrations. The DNA damage

inducible genes (also associated with apoptosis and the cell cycle) were only expressed as a result of a high drug dose. This serves to highlight the results of varying DNA insults; either temporary or permanent G2 arrest. Cells that have been treated with cytotoxic agents, such as DNA damaging agents, may undergo apoptosis or growth arrest. The cell's fate is determined by the extent of the damage as well as its genomic make-up. The resulting permanent cellular arrest shares various features with cellular senescence (Clarke *et al.*, 2004).

MCF-7 breast and H630 colon cells were treated with 5-FU, raltitrexed and oxaliplatin, which resulted in the induction of *p53* expression. Following 5-FU treatment, a variety of genes showed increased expression. These included the *fas-receptor*, genes involved in signal transduction, cell cycle regulation, and polyamine metabolism as well as a variety of others. p53 was inactivated by the expression of the E6 viral protein and it was found that the induction of a number of genes decreased, yet some were unaffected (Maxwell *et al.*, 2003).

When screening the gene expression response to a number of compounds, microarray technology may not be feasible. An alternative is to select genes from an initial microarray for use in a multiplex RT-PCR approach. Johnson and co-workers developed a similar approach for six genes known to be over expressed in prostate cancer. This assay measured the expression of a homeodomain transcription factor *HOXB-13*, *hPSE/PDEF* an ETS transcription factor family member, *survivin*, *INA D* a PDZ-domain protein and a novel gene *BLX-33*. In addition to this they measured 5 genes involved in stress or DNA damage as well as two housekeeping control genes. More than 9000 compounds were tested in pools of ten and a variety of promising compounds and activities were identified (Johnson *et al.*, 2002).

By profiling the transcription of various cell lines and those treated with a specific compound, one is able to mine a wealth of information regarding the test compound. Insight into the compounds' mechanism of action could be gained, as well as information regarding the particular metabolic effect it would have. This could potentially make researchers less reliant on animal models.

2.4.4 Expression Analysis and Drug Sensitivity and Resistance

Intrinsic or acquired resistance to chemotherapy is a serious problem in oncology. By determining the molecular mechanisms that cause resistance, researchers may be able to alleviate this problem (Clarke *et al.*, 2004).

The NCI 60 database of gene expression was analysed using a statistical method known as partial least squares modeling. This identified correlation with sensitivity to 171 drugs with known and unknown mechanisms of action. The responsiveness to topoisomerase inhibitors, RNA/DNA antimetabolites, alkylating agents but not antimitotic agents was found to be influenced by six gene products. *Methylenetetrahydrofolate dehydrogenase-2*, whose product is involved in formylmethionyl-tRNA synthesis in the mitochondria, as well as *SP2*, which codes for a splicing protein in the mitochondrion, were found to be associated with sensitivity to DNA/RNA antimetabolites. This indicates that mitochondrial transcription is a possible target for DNA/RNA antimetabolites (Musumarra *et al.*, 2001; Clarke *et al.*, 2004).

Using the NCI60 cell panel probed with oligonucleotide arrays, Huang and co-workers (2004) identified many drug/transporter relationships which highlight the prominent role membrane transport plays in chemosensitivity. Expression levels were correlated with 119 known drugs, which resulted in the identification of known and unknown drug/transporter interactions. It was found that cells with higher expression of the equilibrative nucleoside transporter (ENT, SLC29A1) are more sensitive to nucleoside analogues, also, that the expression of three ABC efflux transporters (*ABCB1*, *ABCC3* and *ABCB5*) correlated negatively with a number of drugs, which suggests a mechanism of resistance. The expression of *ABCB1* was decreased by RNA interference, which subsequently leads to an increase in drug sensitivity for those specific cells. The level of ion exchangers, ion channels, and subunits of proton and sodium pumps correlated with drug potency. From this study, the researchers suggest that measuring transportome gene expression levels may be useful in predicting the response to anticancer agents.

The mechanisms of resistance may be determined *in vitro* by continuously exposing cells to a specific drug until a resistant clone develops. This clone can then be compared to the original cell line by using microarray analysis. Reinhold and colleagues (2003) studied acquired resistance to camptothecin, a topoisomerase 1 inhibitor. They found that the expression of 181 genes was significantly altered (1.5 fold) when the resistant cell line was compared to the original cell line. Amongst these, genes such as those involved in NF-κB signalling and apoptosis were found to be significantly involved.

2.4.5 Transcriptome Analysis and Pre-clinical Toxicology

The transcriptome represents the sum total of transcribed genes. Transcriptome analysis describes the transcription rate of any given gene and has the potential to radically improve the drug safety assessment process by identifying toxic liabilities earlier. These methods may be used to understand mechanisms of toxicity, predict toxicity, for the development of surrogate models and screens, and, for the development of toxicity biomarkers (Searfoss *et al.*, 2005).

The assessment of a candidate drug's toxicity is a vital part of the drug development process. Traditionally this has largely been carried out in animal models. As the drug candidate moves towards clinical trials, rodent and large animal tests are carried out. These involve the clinical observation of the animals and examination of their organs and bodily fluids. This process is not only labour intensive and expensive, but may also fail to identify long-term toxicity. This method is largely a descriptive process, with little underlying mechanistic understanding. By utilising high throughput technologies researchers would need less drug, fewer animal models and would be able to predict compound liabilities more efficiently. These techniques fall under the discipline of toxicogenomics, which can be seen as a branch of chemogenomics. Gene expression data is considered more sensitive and informative than previous methodologies, with the endpoint goals being the increase of safety and the reduction of development time and costs. By analysing the transcriptome, researchers can determine the mechanisms of toxicity of a drug. Toxicological studies on off-target as well as on-target hits would provide valuable information for lead optimisation and the prediction of toxicity. Drug induced changes in mRNA

levels cause changes in the proteins they encode, which allows researchers to understand how the cell is being affected by the treatment. Since the liver is a common target of toxicity, a variety of studies have used transcriptome analysis to characterise hepatotoxicity (Searfoss *et al.*, 2005).

Drug-induced hepatotoxicity is of major therapeutic importance since it leads to significant levels of morbidity and mortality, which are major considerations in drug development. The mechanisms of drug induced liver damage are not well known and this prompted Reilly *et al.* (2001) to investigate the effect acetaminophen has on gene expression in mouse livers. They used oligonucleotide microarrays to characterise more than 11 000 genes and expressed sequence tags (ESTs). They found significant changes in expression, such as a two-fold increase in genes relating to the cell cycle and growth arrest, stress-induced proteins, the transcription factor LRG-21, suppressor of cytokine signalling (SOCS)-2-protein and plasminogen activator inhibitor-1. Many of these genes' expression products were only present after treatment, which suggests a possible role in propagating or preventing liver injury.

The greatest contribution transcriptome analysis could give to toxicology would be in the field of predictive toxicology. The vast majority of research in this aspect of toxicology is grounded in the formation and study of databases (expression, physiology etc.). Data can be mined and correlated to research to predict the activity of a compound, much in the same way as chemogenomic data mining (Searfoss *et al.*, 2005).

2.4.6 Proteomics in Drug Development

The human proteome is believed to consist of between 100 000 and several million different protein molecules. Therefore the chemogenomic ligand or target spectrum should cover more than 100 000 molecules. These should represent individual proteins, their splice variants and any post-translational modification (Klebl, 2004).

The term chemoproteomics has emerged to describe protein structure and function using chemistry. This aspect of research has usually fallen under the chemogenomics umbrella, but, by drawing distinctions such as these one is able to determine relationships between proteins, nucleic acids and drugs (Gagna *et al.*, 2004).

The vast majority of drug targets are proteins; therefore it is reasonable to assume that, concerning pharmacological studies, proteomic profiling would be more informative than gene expression data. Proteomic profiling should give more direct answers to biological and pharmacological questions. In the past, two-dimentional polyacrylamide gel electrophoresis has been used for protein quantification, but has proved problematic as far as global protein data is concerned. Microarrays have also been utilised for proteomic studies. Generally, this technology is based on the robotic spotting of anti-bodies or ligands on glass slides, to capture sample proteins (Nishizuka *et al.*, 2003).

Reverse-phase protein lysate microarrays are based on inverting the principle of the classic protein microarray. Samples, that are to be measured, are robotically spotted and using an antibody the concentration of a particular protein in a spot can be determined (Paweletz *et al.*, 2001). This method, as opposed to the other methods (Marron and Jayawickreme, 2003), can only measure one protein per slide, but has the advantage that all of the cell lysates can be assayed simultaneously, and compared. This proves to be advantageous since more often than not assays are concerned with the variability of a single protein across different samples, as opposed to comparing samples across different proteins (Nishizuka *et al.*, 2003).

This technology was limited by the amount of spots one could generate per slide. That is until Nishizuka and colleagues (2003) developed their method. They spotted ten two-fold serial dilutions for every cell lysate as well as including controls, leading to 648 spots per array. The lysates were obtained from the NCI 60, which are already well characterised. The researchers found, using cluster maps, highly interpretable patterns of protein expression. Their preliminary results yielded two promising markers for distinguishing colon from ovarian adenocarcinomas.

When they compared their data to the existing gene expression data for the NCI 60, they found interesting relationships. It was determined that cell structure-related protein concentrations showed a high level of correlation with mRNA levels, whereas non-structure related proteins did not.

The protein kinases were considered to be un-druggable proteins until the release of Gleevec the first designer drug, which inhibits the Bcr-Abl kinase. This has opened many doors for possible research into protein families as drug targets. This is fortuitous since focusing on a single protein, as a target, is extremely unpractical. Thus, using a protein family, such as the kinases, as a target may accelerate the development of effective drugs. The members of the kinase family all share a common feature, their catalytic centre (known as the kinase domain). The kinases transfer the γ-phosphate of their co-substrate ATP onto a protein, peptide or lipid substrate and it has been found that the kinase's ATP binding site is an ideal target for the binding of chemical ligands (Klebl, 2004).

2.5 Bioinformatics

With the advent of high throughput methodologies in drug development and testing, vast amounts of data are being generated. This prompts the need for systems that can efficiently handle and analyse large quantities of data. Various aspects of bioinformatics can be found to play a role in drug development. There are a variety of applications in use, such as those used for processing data generated by experimentation, thereby using bioinformatics as an endpoint to find answers, or, as a starting point to identify (and even create) compounds for experimentation.

Chemoinformatics (a subsection of bioinformatics) describes the creation, design, organisation, management, analysis, retrieval, visualisation, dissemination and use of chemical data. It can also be defined as the use of chemical information for the advancement and acceleration of drug development (Gagna *et al.*, 2004).

Computational screening can be used when the target structure is unknown, using known activity data. A pharmacophore model, which contains the positioning of key features such as hydrogen bonding and hydrophobic groups, can be used as a template to select compounds. Or, if the target structure is known, candidate compound can be selected virtually or from a library (Jorgensen, 2004).

If the target structure is known (e.g. through X-ray crystallography), the most common screening approach used would be molecular docking (Shoichet *et al.*, 2002). Potential ligands are created virtually, positioned in the binding site and then scored for potential activity. The most promising compounds can then be purchased or synthesised and tested experimentally. An interesting example of virtual screening can be found in the identification of DNA gryrase inhibitors after high through-put screening failed to do so. Alternatively inhibitors can be created "from scratch" to work on a specific binding site. One is able to use docking programmes in conjunction with structure generators, but it is more practical to use specialised programmes which are able to build ligands in binding sites (Jorgensen, 2004).

Corwin Hansch was one of the first people to quantify the relationship between a compound's physiochemical properties and its biological activity. This research laid the groundwork for quantitative structure-activity relationships (QSARs), which has been used widely in drug discovery. The aim of QSAR is to identify relationships between various aspects of molecular structure and the compounds toxicological, pharmacodynamic and pharmacokinetic properties. Early QSAR models examine the compound's structure and did not take ligand/target interactions into account. Furthermore, they only seem efficient to predict activity of a compound if it is similar to that of the training set. This limits the model's ability to predict truly novel activities. With this said, newer QSAR models are being used increasingly to predict ADME parameters (Greener, 2005).

With the improvement of bioinformatics technology, it has become possible to identify potential therapeutic compounds without experimentation. Ray *et al.* (2005) used a cluster of

computers to identify possible candidates, from a library of compounds, for the treatment of amyotrophic lateral sclerosis. This disease is characterised by the instability of a mutant protein dimmer (SOD1). Using an 18-node "Beowulf" Linux cluster, the researchers identified a number of promising compounds. 15 of these were found to stabilise the mutant SOD1 and may therefore have therapeutic activity. It is apparent that this approach is also extremely relevant for anti-cancer drug research.

With these concepts, and those of inherent and acquired drug resistance in mind, the research group of J C Swarts (University of the Free State) in collaboration with the CANSA Research Consortium for the Development of Novel Anti-cancer Drugs sought to develop effective therapies for cancer based on organometallic drugs. Among the organometallics, compounds containing Ferrocene and Rhodium complexes have been found to show promise as anticancer agents, with lower (than classical organometallics) levels of nephrotoxicity. Of the many isomers and variants created in this work, two candidates Ferrocene [ferrocenoyltrichloroacetone] and Rhodium-ferrocene [(1.5 cyclooctadiene)(1-ferrocenyl-4,4,4-trichloro-1,3-butanedionate] have been selected for further study. This decision was based on *in vitro* toxicology data for these and other similar compounds. These compounds have been tested for anticancer activity against a number of cell lines (human cervix, colon and large-cell lung cancer cell lines as well as a cisplatin resistant large-cell lung cancer cell line) by the research group of Prof. CE Medlen (Department of Pharmacology, University of Pretoria). These compounds, especially those containing Rhodium complexes were found to effectively destroy cancer cells at relatively low concentrations. The compounds were found to perform better than cisplatin in all of the cell lines and especially in the resistant cell line. In order to develop these drugs further, data regarding their mechanism of action is required.

The work presented here seeks to encompass advancements made in molecular biology and predictive toxicology for the preclinical development of these drugs. By gaining insight into possible mechanisms of action, we stand to gain much information that would aid the further development of these compounds as therapies for cancer.

2.6 Aims

The specific aim of this research is to identify the cellular targets of two novel anticancer agents, Ferrocene [ferrocenoyltrichloroacetone] and Rhodium-ferrocene [(1.5 cyclooctadiene)(1-ferrocenyl-4,4,4-trichloro-1,3-butanedionate], and in so doing, determine the mechanism of action of these drugs.

Specific objectives are:
1. To determine the effect of the drugs on the cell cycle.
2. To determine the mechanism of cell death.
3. To provide information that can contribute to the further development/optimization of these drugs for clinical use.

Long term aims of this research include the establishment of a chemogenomic drug development infrastructure at the University of Pretoria. By combining classical cell biology and novel methods in molecular biology we seek to establish a robust framework and methodology for the investigation of promising therapeutic compounds. To this end we hope glean a greater amount of pre-clinical and pre-animal trial information from a specific drug candidate, prior to and in aid of further development.

CHAPTER 3: MATERIALS AND METHODS

3.1 Anti-Cancer Compounds

Ferrocene [ferrocenoyltrichloroacetone] and Rhodium-ferrocene [(1.5 cyclooctadiene)(1-ferrocenyl-4,4,4-trichloro-1,3-butanedionate] were obtained from JC Swarts (University of the Free State). Figure 3.1 depicts the chemical structures of these drugs. In these experiments, the variant with a methyl trichloride side-chain was used (R=CCl_3).

Both drugs were dissolved in dimethylsufoxide (DMSO) and filter sterilised. Stock solutions containing drug, DMSO (<1% v/v) and culture medium were stored at -70°C until use. These were then further diluted, using the appropriate culture medium, to specific working concentrations. All experimentation was performed at $5xIC_{50}$ for each drug in each cell line.
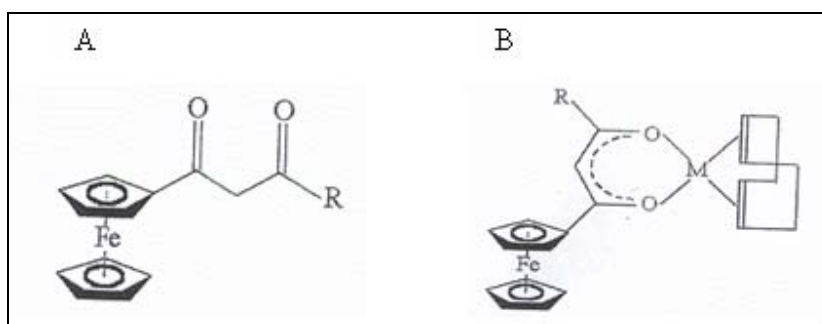
Figure 3.1: The chemical structures of Ferrocene (A) and Rhodium-ferrocene (B). R=CCl3. M=Rh.

3.2 Cell Culture

MCF-7, a breast cancer cell line and MCF-12A, a "normal" transformed breast cell line, were both obtained from the ATCC. MCF-7 cells were maintained in Dulbecco's modified Eagle's medium (Sigma) which was supplemented with 5% foetal calf serum (Adcock-Ingram). MCF-12A were maintained in a 1:1 mixture of Dulbecco's modified Eagle's medium (Sigma) and Ham's F12 medium (Sigma), with 20ng/ml human epidermal growth factor, 100ng/ml cholera toxin, 0.01mg/ml bovine insulin, 500ng/ml hydrocortisone (Sigma) and 5% foetal calf serum. Both cell lines were cultured in Nunc (Nunclon Δ) 75 cm^2 flasks and incubated at 37°C in a humidified atmosphere containing 5% CO_2. Cell passaging was performed using trypsin (Cambrex) to

release the cells from the surface of the flasks. Briefly, cells were washed once with phosphate buffered saline then incubated with trypsin for approximately five minutes. Serum-containing medium was then added in a ratio of 3:1 with trypsin and cells were collected by centrifugation (3000rpm). The supernatant was then discarded and cells were re-suspended in the appropriate medium.

Each cell line was seeded at a concentration of $2x10^5$ cells per well in Nunclon Delta (Nunc) six well plates (each with a surface area of $9.6cm^2$). An initial volume of 3ml of medium was added to the cells while they were allowed to attach for 24 hours, after which, a working volume of 1ml of medium was used in each well.

3.3 Cytotoxicity Testing

To determine the toxicity of the drugs, in a particular cell line, a standard MTT assay was carried out. Briefly, cell lines were seeded at 2.5×10^4 cells/ml, in 96-well plates containing the appropriate medium, and left to attach for 24 hours. Following this they are exposed to each drug, at varying concentrations (50µM, 25µM, 12.5µM, 6.2µM, 3.1µM, 1.5µM, 0.75µM and 0.37µM), for 7 days. The MTT assay was then performed according to the method used by Mossman (1983). All assays were performed in triplicate. The IC_{50} was then calculated by plotting drug concentration in relation to percentage inhibition of cell growth.

3.4 DNA Binding Assay

The DNA binding capabilities, of Ferrocene and Rhodium-ferrocene, were investigated using a restriction enzyme inhibition assay, as described by Skov *et al.* (1987), with modification. The pSV-β-Galactosidase Vector plasmid (Promega) 6821 bp in length (Figure 3.2) was linearised using Hind III (Roche).
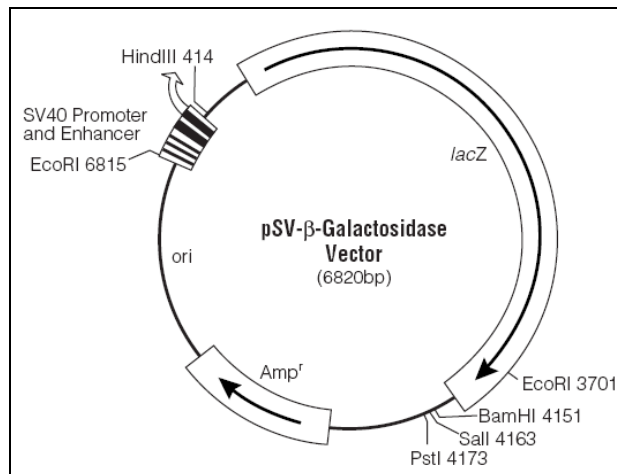
Figure 3.2: The Promega pSV-β-Galactosidase Vector circle map and sequence reference positions.

The DNA (100ng) in Tris-Cl (100mM) / EDTA (1mM), pH 8, was then exposed to either Ferrocene or Rhodium-ferrocene at varying concentrations, with each concentration in triplicate, for 1 hour at 37°C. After exposure, unbound drug was removed using a G50 Sephadex microspin-column (Amersham Biosciences). The eluted DNA was treated separately with 10 units of either PstI, BssHII, EcoRI, NarI, BamHI or EcoRV restriction enzymes in the appropriate buffer (Roche). EDTA was used to stop the enzymatic activity after 60 minutes.

The resulting solution was separated by gel electrophoresis, using a 1% agarose gel and stained with ethidium bromide. Following this, the gel was photographed and analysed by utilising the Kodak Digital Science Electrophoresis Documentation and Analysis System 120, with 1D Image Analysis Software (Kodak Digital Science). The inhibition of the restriction enzyme's cleavage, caused by the specific drug, was assessed quantitatively. The proportion of the uncleaved DNA was determined from densitometric scans of the agarose gels. The inhibited fraction (uncleaved) was determined by calculating the ratio between the intensity of the uncut band and the intensities of the total bands in the lane (uncut and two restriction products).

3.5 Cell Cycle Analysis

Propidium iodide (PI) flow cytometry is a method utilised to quantify the amount of DNA in a single cell. PI binds to DNA, and by counting each cell by flow cytometry, and measuring PI fluorescence, one may determine the amount of DNA per cell in a given population. This allows one to determine in which phase of cell division (mitosis) the cell is, at a particular point in time, or after a specific treatment.

Mitosis is divided into four phases, namely M phase, G1 phase, S phase and G2 phase. During M phase the nucleus and cells divide. G1 phase, also known as Gap 1, is an interval when transcription, translation and other cellular processes occur. The genome has a normal copy number at this point. The S phase, or synthesis phase, is when the cell's genome is replicated. G2, or Gap 2, is a secondary interval phase prior to mitosis (M phase) in which the cell contains double the usual compliment of genetic material (Brown, 2002).

Both exponentially growing cell lines were seeded at a concentration of $2x10^5$ cells per well in 6-well plates (Nunc), in a total volume of 3ml per well. The cells were left to attach for 24 hours, after which the medium was discarded and treatment began with a working volume of one millilitre. The working volume contained one of the two drugs at a concentration of five times the particular drug's IC_{50} for that specific cell line. This concentration was chosen to elicit an exaggerated effect in the cells, to determine the mechanism of action, that may be too subtle if lower concentrations are used. These concentrations being: 25.130µM for Rhodium Ferrocene in MCF-7 cells and 16.870µM in MCF-12A cells, and, 26.085µM for Ferrocene in MCF-7 cells and 22.175µM in MCF-12A cells. Each cell line was treated, separately, with Ferrocene and Rhodium-ferrocene for six, 12 and 18 hours. Treatments were performed in triplicate with mock-treated controls (equivalent amounts of DMSO and medium).

The influence the drugs have on the cell cycle was measured using propidium iodide flow cytometry (Brylan *et al.,* 1982; Crissman and Steinkamp, 1973). At the end of each time interval, adherent cells were collected by trypsinisation, and those in suspension by centrifugation at

3000rpm for five minutes. The cells were then washed twice with cold phosphate buffered saline (PBS), collected by centrifugation (3000rpm for 10 minutes) and fixed in ethanol for 15 minutes on ice. The fixed cells were collected by centrifugation and incubated for 15 minutes at 37°C with RNase (Sigma), at a concentration of 500 units per ml in 1.12% (w/v) sodium citrate (Sigma). The samples were treated with propidium iodide (Sigma), at a concentration of 0.05mg/ml, and incubated at room temperature for 30 minutes. These samples were then analysed using a Coulter Epics XL-MCL flow cytometer, with 2×10^4 events (cells) measured for each sample.

3.6 Cell Death Analysis

The way in which cells die as a result of drug treatment, provides valuable insight into the molecular action of the drugs. Apoptosis is characterised by a number of morphological features, such as changes in the plasma membrane. Phosphatidylserine (PS) is translocated from the inner to the outer membrane leaflet during early apoptosis. Annexin V has a high affinity for PS, and by utilising its binding activity, it can be used as a probe (conjugated to a fluorochrome) to detect apoptosis by flow cytometry. By staining with propidium iodide in conjunction with annexin V, one is able to distinguish between apoptosis and necrosis. PI is not taken up by the early apoptotic cell because the integrity of its membrane is maintained, thus making it impermeable. The permeability of necrotic membranes, however, allows for the uptake of PI (Homburg *et al.*, 1995; Koopman *et al.*, 1994; Martin *et al.*, 1995; Vermes *et al.*, 1995). It must be noted that during flow cytometric analysis of the cell cycle, one permeabilises the cell membrane to allow entry of PI; whereas during cell death analysis one does not actively permeabilise the cell membrane.

To establish which mode of cell death, apoptosis or necrosis, is induced by the drugs, a standard Annexin V binding assay was carried out and analyzed by flow cytometry. Following treatment with each drug in each cell line for six and 12 hours, as described previously, cells were detached from the growth surface by trypsinisation and washed twice with ice cold PBS. The cells were then collected by centrifugation and re-suspended in 1X binding buffer (10mM Hepes/NaOH,

pH7.4, 140mM NaCl and 2.5 mM $CaCl_2$) at a concentration of $1x10^6$ cells/ml. 5µl Annexin V-FITC (BD Biosciences) and 10µl propidium iodide (0.05mg/ml) was added to the buffered cells. The solution was vortexed gently and incubated for 15 minutes at room temperature, in the dark. A 1:5 dilution was made using 1Xbinding buffer, and this was subsequently analysed using a Coulter Epics XL-MCL flow cytometer, with 2×10^4 events (cells) measured for each sample. Cisplatin was used (5X IC_{50}) as a positive control.

3.7 Gene Expression

For gene expression analyses, both cell lines were seeded into six well Nunc ($9.6cm^2$) culture dishes, at a concentration of $4x10^5$ cells per dish in a total volume of 3ml. Cells were left to attach for 24 hours, after which the medium was discarded and treatment commenced. Each cell line was treated as before at 5xIC_{50} with Ferrocene or Rhodium-ferrocene in triplicate, with three mock-treated controls for the six treatments of six and 12 hours.

3.7.1 RNA extraction

RNA was extracted from cells using the RNeasy mini kit (Qiagen), with slight modification. After the treatment interval had expired the medium was discarded and cells were washed (in the dish) twice with cold 1xPBS. Buffer RLT (Qiagen) was added to each dish and after pipetting back and forth, the lysate was collected. The efficacy of the lysis was monitored under an inverted light microscope.

The solution was vortexed and homogenized using the Qiashredder kit (Qiagen). Briefly, the lysate is placed in a proprietary column and centrifuged at 13 000 rpm for five minutes. An equal volume of 70% ethanol is added to the lysate, after which it was vacuumed through an RNeasy column using the QiaVac vacuum manifold system (Qiagen). Columns were then washed with buffer RW1 by centrifugation at 13 000 rpm for one minute. 27 Kunitz units of RNase free DNase (Qiagen), in nuclease-free water, was added to each column and incubated at room temperature for 15 minutes. Columns were washed again with RW1 and then twice with buffer

RPE. Finally, RNA was eluted with RNase free water by centrifugation at 13 000 rpm for one minute. RNA was immediately stored at -70°C for later use.

The concentration and purity of each sample was measured by UV/vis spectrophotometry using a Nanodrop Spectrophotometer (Thermo). The wavelength (nm) ratios of 260/230 and 260/280 were used to indicate purity.

3.7.2 cDNA synthesis

RNA was converted into cDNA using Superscript II Reverse Transciptase (Invitrogen) according to the manufacturer's protocol. Briefly, 500μg/ml Oligo(dT), random hexamers (Roche), PCR grade water and the RNA were combined and incubated at 65°C for five minutes. The solution was then chilled on ice and centrifuged briefly. To this, 5xFirst Strand Buffer (Invitrogen), 0.1M DTT (Invitrogen) and RNAsin (Promega) were added. This was mixed thoroughly and incubated at 25°C. 400 Units of Superscript II was then added and the mixture was incubated at: 25°C for 10 minutes, 42°C for 50 minutes and 70°C for 15 minute. Upon completion of cDNA synthesis, the solution was incubated at 90°C for 30 seconds to destroy residual RNA. All incubation steps were carried out using an ABI 2700 thermal cycler.

3.7.3 Absolute Gene Expression Quantification of Selected Genes

A number of genes relevant to DNA damage and cell cycle progression were chosen from the literature (Table 3.1). In addition to these a number of house-keeping genes were chosen to determine normalization factors between the experiments.

Primers for these genes were designed using online software (www.roche-applied-science.com) for the Universal Probe Library System (Roche) and synthesized by Invitrogen. The Universal Probe Library concept is based on the use of short hydolysis probes, labeled at the 5' end with fluorescein and at the 3' end with a dark quencher dye. The library consists of 165 different probes, from which a probe matching a particular assay is selected. Due to the shortness of the probe, specificity is conferred by the PCR primer binding characteristics. Upon amplification, the

probe is hydrolysed by Taq polymerase, thereby freeing the fluorescent reporter from the influence of the quencher dye. The level of fluorescence is therefore directly proportional to the concentration of PCR amplicons and is measured by a real-time thermal cycler.

Standard Curve Creation

To supply the DNA required to create standard curves for each gene, the targets were amplified from total human RNA (Invitrogen) which was reverse transcribed into cDNA, as described previously. Each target was amplified separately, at various annealing temperatures to determine the optimum reaction characteristics. The reactions consisted of 112ng cDNA, nuclease free water, PCR buffer (Invitrogen), dNTP (0.025mM each), $MgCl_2$ (3mM) forward and reverse primer (0.2μM each) and one unit Taq Polymerase (Invitrogen) to a total volume of 20μl. The reaction mixtures were amplified on an ABI 9700 thermal cycler under the following conditions: 94°C for 3 minutes; followed by 30 cycles of 94°C for 1 min, 48-62°C for 1 min, 72°C for 1 min, and finally, 72°C for 7 minutes.

The PCR products were then run on a polyacrylamide gel consisting of 40% PAGE stock (37:1, Merck), distilled water, 10x TBE, TEMED (Bio-Rad) and 10% ammonium persulphate (Merck). Gels were cast in a vertical gel electrophoresis unit (Bio-Rad) and run at 300V until the loading marker reached the bottom of the gel. The gels were stained with ethidium bromide diluted in TBE (01.% v/v) for 15 minutes with shaking and visualized using the Kodak Digital Science Electrophoresis Documentation and Analysis System 120, with 1D Image Analysis Software (Kodak Digital Science). The results were visually inspected for the presence of a single delineated band without the presence of non-specific amplification products or primer dimers. The concentration of the PCR products were measured using the Nanodrop spectrophotometer at 260 nm.

The amplicons were diluted ten-fold, in water, by six orders of magnitude using the MagnaPure LC liquid handling system (Roche). The diluted target cDNA was used as template in a real-time PCR reaction consisting of 2X mastermix (Finnzyme DynamoProbe qPCR kit), forward and

reverse primer (0.2µM each), gene specific Universal Probe Library probe (Table 3.1) and nuclease free water. The reactions were run on a Roche Lightcycler version 2.0 and detected in channel one.

Table 3.1: Genes, probe numbers and expected amplicons sizes for the Lightcycler reactions.

Gene Name	Probe Number	Forward Primer	Reverse Primer	Amplicon Size
Cyclins				
CycA2	84	ggtactgaagtccgggaacc	gaagatccttaaggggtgcaa	83
CycB1	34	cgcctgagcctattttggt	gcacatccagatgtttccatt	61
INK				
P15 tran. var. 1	17	cggggactagtggagaagg	ctgcccatcatcatgacct	104
P15 tran. var. 2	44	ttgtacaggagtctccgttgg	gtgagagtggcagggtctg	113
P16 common	29	ttcccccactaccgtaaatg	ccagaaaactccaacacagtga	109
P18 var.1 and full	65	gactatcccttcggcgaga	aaggctcggccattctttag	122
P19 common	49	gacctccagggagcctagaa	actcattctaccttcttattgatttgg	125
Kip				
P27 not spanning	39	ccctagagggcaagtacgagt	agtagaactcgggcaagctg	60
P57	55	ctcctttccccttcttctcg	tccatcgtggatgtgctg	103
Other				
P21 tran var1+2	**32**	tcactgtcttgtaccccttgtgc	ggcgtttggagtggtagaaa	127
CDC25A common	2	ctccgagtcaacagattcagg	ttcaaggttttctttactgtccaa	70
CHK1	71	tgacttccggcttttctaagg	tgtggcaggaagccaaac	112
CHK2 common	1	gaggctgcggagagtgtg	gactcccgagacatcacgac	60
TP53	12	aggccttggaactcaaggat	ccctttttggacttcaggtg	85
APAF	**14**	aaaactcctgttgccgtttc	ctgagctgtcaaccatgagc	117
Wee1	2	ggcgatagtcgttttcttgc	cgcaaaaatatctgcttttggt	75
Myt1 tran var 1+2	**56**	tgaggtccaggagggagac	cacttccaggatggtgagg	106
RAD50	9	gcttctgataaaaggcggaat	gcgaatgatgagtgaggctaa	120
BCL2	**75**	tacctgaaccggcacctg	gccgtacagttccacaaagg	72
GAPDH	60	agccacatcgctcagacac	gcccaatacgaccaaatcc	66
Actin B	11	attggcaatgagcggttc	ggatgccacaggactccat	76
HPRT 5mRNA	73	tgaccttgatttattttgcatacc	cgagcaagacgttcagtcct	102
PBGD	60	tcagactgtgctgaggcaac	gactccagactcctccagtca	63
PARP	22	tgatgtggaaagtatgaagaaagc	ggcatcttctgaaggtcgat	60

Absolute Quantification

The RNA extracted from MCF-7 and MCF-12A cells exposed to either Ferrocene or Rhodium Ferrocene (for six and 12 hours) was subject to Lightcycler analysis using the Universal Probe Library assays. House keeping gene expression levels were quantified by comparison to an external standard curve, initially, to establish the variability between the various sample concentrations as well as to determine the stability of these genes' expression. Following this, each gene target (Table 3.1) was quantified by comparison to a standard curve, in each drug exposure iteration.

Specific focus was placed on the housekeeping genes Actin B, GAPDH and HPRT to establish normalization factors. The data was then evaluated using the REST (Relative Expression Software Tool) package to determine variability in regulation (Pfaffl *et al.*, 2002).

3.7.4 Relative Quantification of Gene Expression by qPCR Array Analysis

3.7.4.1 Cell-cycle Focused qPCR Array Analysis

cDNA from the triplicate experiments were pooled for each drug exposure, in each cell line for the six and twelve hour exposures. Each pooled triplicate was analysed using RT^{2}Profiler cell cycle analysis PCR Arrays (SABiosciences). The arrays were run according to the manufacturer's instructions. Briefly, cDNA was added to 2X SABiosciences Master mix and water. This was then added to 84 wells of the array, with each well containing a cell cycle or DNA damage specific lyophilised primer. Wells H1 to H6 contained primers for house keeping genes, which enable data normalization. To estimate the linear dynamic range of the reaction, wells H6 to H10 contain primer for a single housekeeping gene (β-Actin). A 10-fold serial dilution of the initial master mix was made and diluted with cDNA-free 1xPCR master mix and was added to these wells. Control systems, such as a "no reverse transcriptase control", in which a 1:100 dilution of RNA from the initial experiment was added, and a negative control, to which water and PCR mix was added, were in also place.

Plates were sealed with optical film (Applied Biosystems) and centrifuged at 3000 rpm for two minutes to remove any bubbles. The plates were then analysed on an ABI 7300 real-time thermal cycler using the following thermal profile: 95°C for 15 minutes; followed by 40 cycles of 95°C for 15 seconds and 60°C for 1 minute. Detection occurred after extension in the SYBR Green channel.

The baselines and thresholds were then set, manually, with identical values for all experiments using the ABI 7300 software. The data were exported as an Excel (Microsoft) file, and array based analyses were completed using a Microsoft Excel-based macro supplied by the

manufacturer (SABiosciences). The macro is based on the ΔΔCt method of relative expression analysis.

3.7.4.2 DNA Damage Focused qPCR Array Analysis

To determine the effect of the two drugs on DNA damage specific gene regulation, Real-time PCR arrays from SABiosciences were used. Pooled triplicate cDNA from each time interval, for a specific drug, in a particular cell line were analysed in duplicate according to the manufacturer's protocol. Briefly, cDNA was added to 2X SABiosciences Master mix and water. 25µl of this solution was then added, using a multi-channel pipette, to each of the 96 wells. The plates were then centrifuged at 3000 RPM for two minutes and analysed with an ABI 7300 Real-time thermal cycler (Applied Biosystems) using the following thermal profile: 95°C for 10 minutes; followed by 40 cycles of 95°C for 15 seconds and 60°C for 1 minute. Detection occurred after extension in the SYBR Green channel.

The baselines and thresholds were then set, manually, with identical values for all experiments using the ABI 7300 software. The data were exported as an Excel (Microsoft) file, and array based analyses were completed using a Microsoft Excel-based macro supplied by the manufacturer (SABiosciences). The macro is based on the ΔΔCt method of relative expression analysis.

3.8 Data Analysis

Gene expression data from the DNA damage arrays was evaluated using the Ingenuity Pathway Analysis (IPA) software platform from Ingenuity Systems that was obtained on a trial basis (www.ingenuity.com). This software package is a web-based tool that operates using a Java platform. Gene expression data was uploaded in Microsoft Excel format and analysed using the Core Analysis functionality. Briefly, data was loaded using standard identifiers (GenBank and Unigene). The reference set was the Ingenuity Knowledge base and reference data sources include: Ingenuity Expert Information, Ingenuity Expert Findings, Ingenuity ExpertAssist Findings, micro-RNA – mRNA interactions, Argonaute and Tarbase. Protein interaction information was

also included in the reference set which included: BIND, BIOGRID, COGNIA and DIP. The species analysis was set to human with stringent filtration and the full tissue and cell line set was included, also with stringent filtration. Once set, these were saved as default settings and used for all analyses. The data is presented in conjunction with the gene expression data, for the sake of clarity and to avoid unnecessary duplication.

Gene ontology and associative studies were further carried out using the "Your Favourite Gene" resource hosted by Sigma-Aldrich (www.sigma-aldrich.com). Differentially regulated genes were located on this database and their properties are summarized.

CHAPTER 4: RESULTS AND DISCUSSION

4.1 Anti-Cancer Compounds

The Ferrocene and Rhodium-ferrocene compounds were chosen for in depth evaluation due, in part, to the proven efficacy of organometallic drugs in the treatment of cancer. A well known example being cisplatin which has been widely used since the mid 1970's (Siddik, 2003).

The basic Ferrocene compound has been extensively investigated in fields ranging from aerospace to medicine. The structure is an electron donor and in the biological environment is oxidised. The resulting cation may interact with proteins, containing donor groups such as tryptophan, forming charge transfer complexes. The ferricinium ion has also been found to interact with charge transfer reactions such as the NADH-mediated oxidative pathway. In addition to this, it is believed that a hydroxyl free-radical formed by the ferricinium ion is responsible for DNA damage. Interestingly, although consensus has been reached that Ferrocene-based molecules affect cellular DNA, it has not been agreed upon by which mechanism the drugs act. Neuse suggests that the ferrcinium ion does not interact with the DNA directly; rather, the catabolically generated reactive oxygen species is responsible for the DNA damage (Neuse, 2005).

A number of variants of Ferrocene and Rhodium-ferrocene structures have been synthesised by the Smuts group (Conradie *et al.*, 2002) and were found to be biologically active within the chemotherapy framework (personal communication Prof. C Medlen). The choice of the CCl_3 containing variant as a candidate was based on cyctotoxicity data and availability.

The first point of evaluation, when considering possible anticancer agents, is the level of cytotoxicity in various cell lines. Since these two drug candidates have been chosen for evaluation based on earlier cytotoxicity analyses by the group of Professor C Medelen (University of Pretoria), the cytotoxicity of the compounds in MCF-7 and MCF-12A cells should be used as a starting point of further cell-based analyses using these two cell lines.

4.2 Cytotoxicity Testing

Cytotoxicity analysis was carried out using a standard MTT assay, as first described by Mossman (1983). This is a colourimetric assay which is based on the reduction of a tetrazolium salt by active mitochondria, which leads to a measurable colour change in the medium. The degree of colour change therefore relates to the cell concentration in the test vessel. Briefly, the assay relies on mitochondrial dehydrogenase from viable cells to cleave the tetrazolium rings of the pale yellow MTT. This forms insoluble dark blue formazan crystals which accumulate within the cells. Once cells are permebealised by the addition of a detergent, the crystals are released and solubilised. The resulting colour change may then be quantified using a spectrophotometer.

Table 4.1 illustrates the cytotoxicity values of the two drugs in the two cell lines presented as an IC_{50} value. This unit indicates the concentration of a particular drug that is able to inhibit the growth of 50% of the cells within a test population.

Table 4.1: IC50 values for Ferrocene and Rhodium-ferrocene in MCF-7 and MCF-12A cells.

Cell Line	Ferrocene	Rhodium-ferrocene
MCF 7	5.217µM	5.026µM
MCF 12A	4.435µM	3.374µM

From these data it is clear that both drugs are more toxic in the normal cell line when compared to the cancerous cell line. Although this is not the ideal situation, an *in vitro* assay such as this is not always a true reflection of the tumour micro-environment and the particular response it may show to a specific drug. As an example, vascularisation, the presence of multiple cell types as well as micro-environment interactions may affect the toxicity of a particular drug (i.e. ADME principles).

From the cytotoxicity assays, it has been shown that both compounds are biologically active. From this point however, the mechanism of action is not clear. Based on chemical structures and the activity of similar metallocene compounds it is predicted that they would have DNA-

binding potential. Therefore, through the use of naked (protein free), linearised DNA, exposed to both compounds, it may be shown that the drugs interact with DNA.

4.3 DNA Binding Assay

When linearised vector DNA was exposed to each drug at varying concentrations and digested with a number of restriction enzymes it was found that both drugs bind DNA at the PstI restriction site. This means that Ferrocene and Rhodium-ferrocene inhibit the restriction activity of PstI by binding at its recognition site (CTGCAG) and effectively blocking the enzyme's ability to cleave the DNA.

From the agarose gel (Figure 4.1) it was found that the amount of uncut DNA increased as the drug concentrations increased. This means that as drug concentration increases, the enzyme cleaves less DNA, leading to a more concentrated single high molecular weight band on the agarose gel. This relationship, plotted in Figure 4.1, indicates the inhibitory activity of the drugs, in increasing concentrations, on PstI restriction. The restriction activities of BamHI and EcoRV (results not shown), on the other hand, were only inhibited at exceptionally high drug concentrations (>100µM).
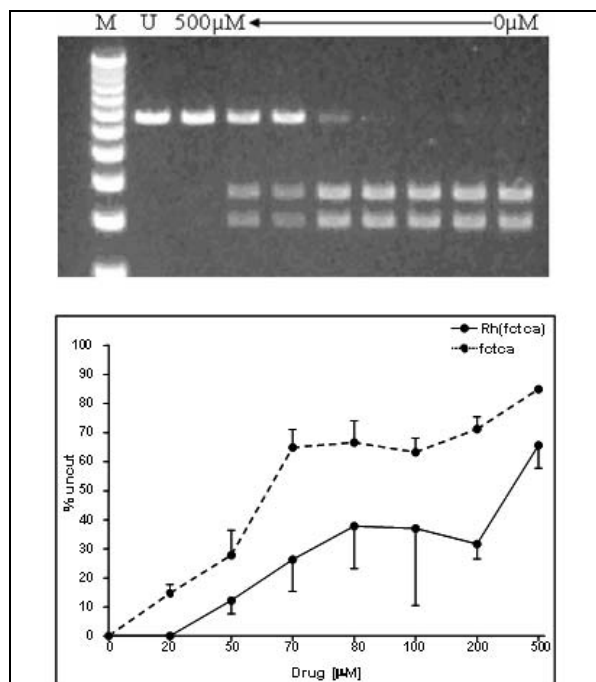
Figure 4.1: (Top) 1% agarose gel electrophoresis of the restriction products of PstI and pSV-β-Galactosidase vector after exposure to increasing concentrations of Ferrocene. (Bottom) Inhibitory action of varying concentrations of Ferrocene [fctca] and Rhodium-ferroc ferrocene [Rh(fctca)] on PstI restriction activity. All experiments were performed in triplicate.*

*M= 10Kb molecular marker; U=uncut DNA.

From Figure 4.1 it is clear that Ferrocene inhibits PstI activity (i.e. a higher percentage of uncut DNA) at lower concentrations than Rhodium-ferrocene. The reason for this may be due to the steric hindrance caused by the bulkier Rhodium side-chain, of the Rhodium-ferrocene molecule, when interacting with DNA. From these data, an initial indication that these two drugs' activity is based on DNA binding is confirmed. If the drug had interacted with a system of less than three base pairs one would expect that multiple restriction enzymes' cleavage sites would be affected. This was not the case and it could be postulated that the stereochemistry of the PstI site is such that the drugs interact with the DNA molecule in a very defined way.

The following analyses, on a cellular and molecular level would give further credence to this hypothesis. It has been shown that the drugs interact with "naked DNA", further investigations would reveal if the drugs are able to cross the nuclear membrane and affect cellular DNA, thereby exercising their cytotoxic action. In the same vein, an interaction with DNA would affect

not only the metabolism of the cell but also the synthesis of new DNA, which occurs during the cell cycle.

4.4 Cell Cycle Analysis

An example of the propidium iodide flow cytometric data is presented in Figure 4.2. The first peak of each figure denotes cells in the G1/G0 population while the second peak denotes those in G2. The trough between the peaks represents the cells in S phase. By comparing these populations in the exposed and mock-treated cells one can detect perturbations in the transitions between the cell cycle phases, as a result of the drug exposure.
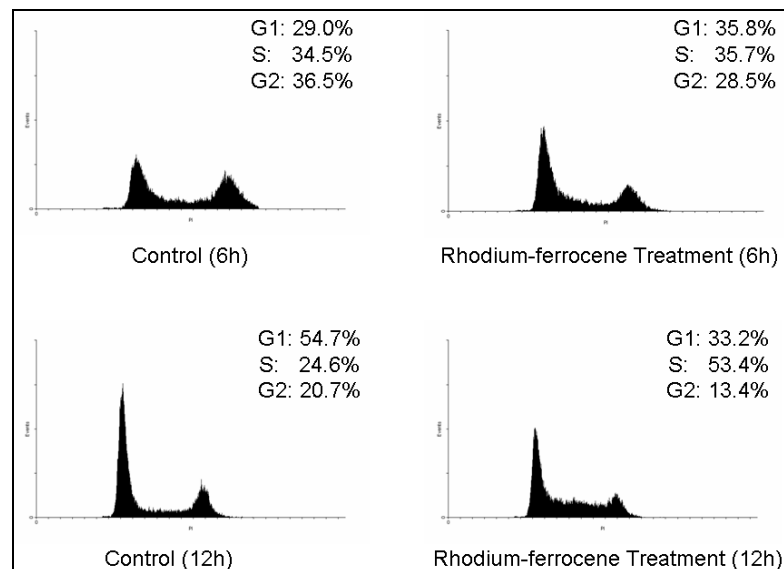
Figure 4.2: An example of flow cytometric data illustrating MCF 12A cells treated with Rhodium-ferrocene for six and 12 hours, with mock-treated controls. The cell percentage in each mitotic phase is printed above each distribution.

Averages for the triplicate experiments were calculated, with standard deviations, showing the effect of each drug on the cell cycle at a specific time interval (Table 4.2). Statistical differences between each population were calculated using Analysis of Variance. Additionally, the ratio between cells in G1 phase versus those in G2 was determined to gauge the progression through mitosis.

Table 4.2: Percentage of MCF-7 and MCF-12A cells in cell cycle phases following treatment with Ferrocene (Fc) of Rhodium-ferrocene (RhFc) for either six, 12 or 18 hours. The ratio of cells leaving the cell cycle versus those entering is presented as a G2/G1 ratio. Values are the means of three independent experiments +- SEM.

MCF-7				
Treatment Duration		**G1**	**S**	**G2**	**G2/G1 ratio**
	Control	47.1±0.80	31.6±0.90	21.3±0.10	0.452±0.01
6hrs	Fc	47±0.50	31.5±0.25	21.5±0.25	0.458±0.01
	RhFc	51.4±0.63*	28.3+0.68*	20.3±0.58	0.396±0.01*
	Control	44.1±1.31	39.9±0.80	16±0.77	0.366±0.03
12hrs	Fc	40.6±1.01	46.3+1.20*	13.1±0.49*	0.321±0.01
	RhFc	49.5±1.01*	39.4±1.20	11.1±0.49*	0.223±0.00*
	Control	44±5.31	31.2±7.10	24.8±1.88	0.572±0.04
18hrs	Fc	37.3±2.13	29.3±2.56	33.4±0.96*	0.903±0.05*
	RhFc	31±1.40	37.6±3.30	31.4±4.70	1.027±0.20
MCF12A				
Treatment Duration		**G1**	**S**	**G2**	**G2/G1 ratio**
	Control	29±1.25	34.5±0.91	36.5±1.36	1.265±0.09
6hrs	Fc	34.3±0.50*	37.5±0.66	28.2±0.21*	0.825±0.01*
	RhFc	35.8±1.44*	35.7±1.16	28.5±1.70*	0.804±0.07*
	Control	54.7±1.93	24.6±2.08	20.7±0.69	0.380±0.02
12hrs	Fc	28±2.99*	56.7±1.51*	15.3±1.73*	0.573±0.14
	RhFc	33.2±0.91*	53.4±1.22*	13.4±0.65*	0.404±0.02
	Control	41.2±4.74	34.9±0.91	23.9±4.15	0.625±0.19
18hrs	Fc	42.6±6.32	34.9±1.37	22.5±5.18	0.601±0.25
	RhFc	39.3±3.44	37.2±1.30	23.5±4.54	0.627±0.17

*Significantly different from control by Analysis of Variance

These averages are represented as stacked columns in Figures 4.3 and 4.4, for each drug in each cell line. Differences in the number of cells in each mitotic phase, between treated and mock-treated as well as the cancerous and non-cancerous cells become apparent.
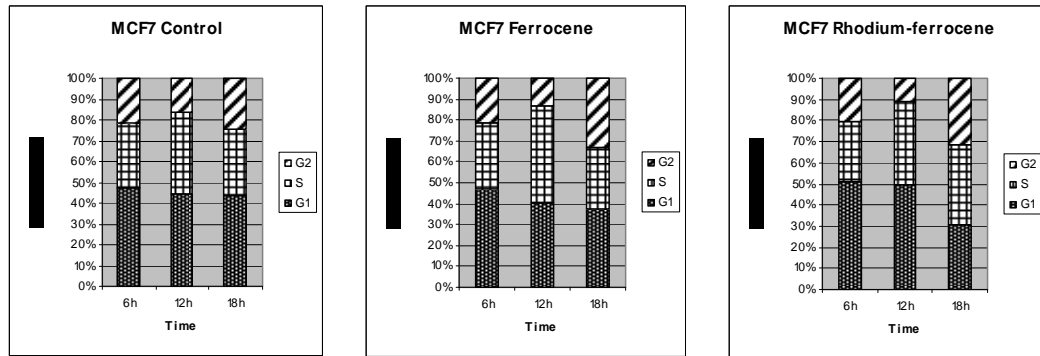
Figure 4.3: Stacked columns illustrating the effect of Ferrocene and Rhodium Ferrocene treatment on MCF-7 DNA content over time, as compared to a mock-treated control. Exponentially growing cells were exposed for 6, 12 and 18 hours and stained with propidium iodide.
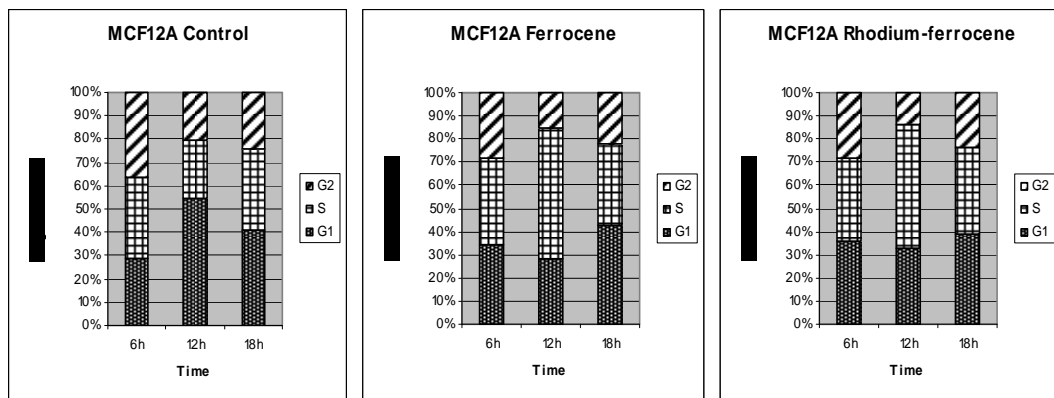
Figure 4.4: Stacked columns illustrating the effect of Ferrocene and Rhodium Ferrocene treatment on MCF-12A DNA content over time, as compared to a mock-treated control. Exponentially growing cells were exposed for 6, 12 and 18 hours and stained with propidium iodide.

MCF-7 cells treated with Ferrocene (Figure 4.3) for six hours showed no significant response when compared to the mock-treated control. After 12 hours, however, the cells appeared to be partially delayed in S phase. MCF-12A cells exposed to Ferrocene (Figure 4.4) for six hours, on the other hand, accumulated in the G1 and S phases. The delay in the G1 phase proved to be transient, and after 12 hours, cells accumulated in the S phase. This delay seen in MCF-12A cells was of a greater magnitude than that of the MCF-7 cells. An 18 hour exposure of MCF-7 cells to Ferrocene resulted in a marked accumulation in the G2/M phase. MCF-12A cells exposed to

Ferrocene for 18 hours, however, appeared to have resumed normal cycling showing no similar accumulation in the G2/M phase.

When MCF-7 cells were treated with Rhodium-ferrocene (Figure 4.3), for six hours, a small percentage appeared to accumulate in the G1 and S phases of the cell cycle. After a 12 hour exposure, cells were still able to progress from G1 to S phase, but became delayed in the S phase. When MCF-12A cells were treated with Rhodium-ferrocene for six hours their response was similar to that of the MCF-7 cells, only more pronounced. After 12 hours MCF-12A cells showed an S phase delay, with the G1 population still able to progress to the S phase. The S phase delay seen in MCF-12A cells was more pronounced than that of the MCF-7 cells. After an 18 hour Rhodium-ferrocene exposure MCF-7 cells accumulated in the G2/M phase, whereas MCF-12As were cycling as normal. These findings are indicative of the normal cell's ability to overcome genomic insult, whereas these mechanisms have been lost due to selection pressure in cancerous cells.

From the flow cytometry results it is clearly demonstrated that both drugs inhibit progression through mitotic phases. The G1/S and S phase accumulation may be due to inhibition of the DNA synthetic process or inhibition of the initiation of the synthetic process. If cells accumulated in G2 one would assume chromosomal segregation and subsequent division is affected. We have shown that both drugs bind naked DNA, and with these flow cytometry data, it is clear that the drugs are inhibiting progression through the cell cycle by interacting with cellular DNA. This can be placed in the context of the DNA damage checkpoints. Through treatment with these drugs it has been determined that the cells are halted in various phases of the cell cycle, where these checkpoints exert their influence. This cell cycle inhibition is indicative of checkpoint activation, as the cell either attempts to repair DNA damage or enters a cell death program.

From this point, we have shown that both drugs are cytotoxic and are able to inhibit progression through the cell cycle, most likely as a result of interaction with cellular DNA. It is pertinent at

this stage to determine the mechanism of cell death induced by the two compounds, and if there is a difference between the two cell lines.

4.5 Cell Death Analysis

Whether a cell undergoes apoptosis or necrosis, as a result of treatment, indicates which pathways the specific treatment affects. These tests also indicate the metabolic characteristics of the treated cell, i.e. the impact treatment has on ATP levels and production (Kroemer *et al.*, 2004). This is because apoptosis is an energy dependent process, whereas necrosis usually occurs as a result of an energy deficit.

In Figure 4.5 a flow cytometric analysis of cells stained with propidium iodide and Annexin V is pictured. The intensity of each particular fluorophore is indicative of the particular phase of cell death or the level of viability. Cells in the first quadrant are viable and are not excessively stained with Annexin V or PI; which indicates that the cell membrane is intact and PS has not crossed the membrane. Cells in the second quadrant have non-permeable membranes, preventing PI from crossing, and have transitioned PS which indicates early apoptosis. In the third quadrant one finds necrotic or late apoptotic cells, which have permeable membranes (PI is able to cross) and PS has translocated (allowing Annexin V to bind). By analysing cells treated with a particular compound in this way, one is able to determine the mechanism of cell death.
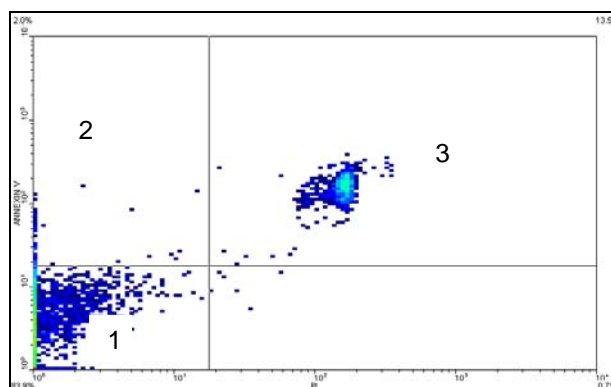
Figure 4.5: An example of Annexin V propidium iodide flow cytometry data to determine the mechanism of cell death. The y-axis represents Annexin V staining intensity and x-axis represents PI staining intensity. Quadrant 1: viable cells. Quadrant 2: early apoptotic cells. Qaudrant 3: late apoptotic or necrotic cells.

MCF-7 and MCF-12A cells exposed for six hours to Ferrocene, or to Rhodium-ferrocene, showed no defined apoptotic or necrotic responses. The majority of cells were found to be in Quadrant 1 (unstained by either fluorophore) which indicates that at this time point the cells were still viable. When reflecting on the data generated during cell cycle analysis, the cells are undergoing checkpoint activation, which prevents progression through the cell cycle. It therefore stands to reason that cell death is not initiated yet since checkpoint initiation allows the cell to assess the extent of the DNA insult, attempt repair, or if repair is not possible, to initiate a cell death programme.

MCF-7 cells treated with Ferrocene and Rhodium-ferrocene (separately) for 12 hours, however, display a late apoptotic/necrotic response (Figure 4.6). The cells at this point are positive for both annexin V and PI, which indicates apoptotic signalling in conjunction with membrane damage. MCF-12A cells exposed for 12 hours, on the other hand, show no significant signs of apoptosis or necrosis for either of the drugs (results not shown). This may be explained by the fact that the detection and repair mechanisms of MCF-12A are still intact, as described previously. The delay in cell death is most likely due to the MCF-12A cell's ability to halt cell cycle progression and initiate a repair mechanism. If repair is not possible, cell death may occur at a later time point. MCF-7 cells on the other hand have, as a feature of their cancerous state, lost a number of these mechanisms, which may result in the cells succumbing to the genotoxic insult faster than the MCF-12A cells.
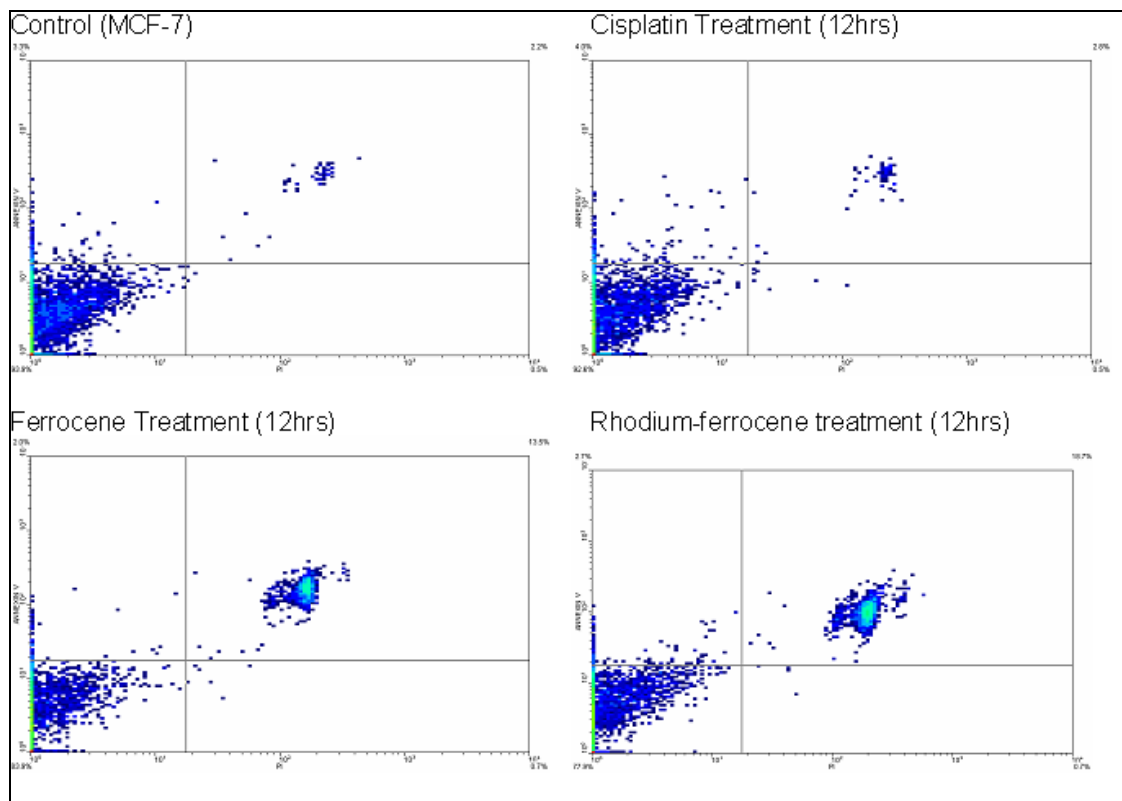
Figure 4.6: Annexin V (y axis) and propidium iodide (x axis) flow cytometric analysis of MCF-7 cells exposed to Ferrocene or Rhodium-ferrocene for 12 hours with a mock-treated control as well as a positive control (cisplatin at 5xIC50).

One of the main hallmarks of cancer are the perturbations found in the apoptotic machinery. Signalling pathways that regulate progression through the cell cycle (e.g. stop cell progression between phases) tend to be affected in cancer. These changes in turn affect the cells' progression through apoptosis, thereby conferring an evolutionary advantage (Borst *et al.*, 2004). Drugs that selectively damage DNA may therefore be effective chemotherapeutic agents, since the cancerous cells are less able to halt cell cycle progression, and repair the damage, than normal cells.

From Figure 4.6 it is clear that both drugs elicit a late apoptotic/necrotic response in MCF-7 cells. This can be seen in the dual staining of PI and annexin V, after treatment, which is indicative of the loss of membrane integrity. The cells appear to proceed straight to late

apoptosis without a clear early apoptotic phase (annexin V positive and PI negative). This can be seen in the absence of any noticeable early apoptotic population after a six hour exposure to the drugs. Interestingly, this response does not occur in the normal cell line (MCF-12A) after a 12 hour treatment interval. This may be due to the normal cells' ability to invoke a more robust arrest and repair programme than the cancerous cell line. MCF-7 cells may be unable to repair the drug-induced damage, continuing to replicate, thus leading to an increase in genomic instability, and, ultimately their demise. This becomes apparent when comparing the cell cycle analysis results with the cell death results. The absence of a drug-induced delay in cell cycle progression, at 12 hours, in the cancerous cell line goes hand-in-hand with the presence of a late apoptotic/necrotic response at this time.

Necrosis has long been thought of as a passive process whereby cells die as a result of an external insult. Recent data suggests, however, that there are examples of necrosis that occur normally and are regulated (programmed) events (Proskuryakov *et al.*, 2003). Zong *et al.* (2004) suggest that, as a result of alkylating DNA damage, certain cells undergo a "self-determined cell fate". In their study it was found that the apoptotic mediators p53, Bax/Bak and the caspases were not required for this form of cell death. The DNA repair protein, poly(ADP-ribose) polymerase (PARP), was found to be a key player in this form of cell death. In this case, cell death was found to be dependent on the effect of PARP driven consumption of β-nicotinamide adenine dinucleotide (NAD) on cellular metabolism. The cells died as a result of an energy deficit, and because cancer cells rely on aerobic glycolysis, Zong and colleagues suggest that this may be the mechanism by which DNA-damaging agents selectively target cancer cell. The role PARP plays in the response to our drug candidates is not known, but, it has been established that Ferrocene and Rhodium-ferrocene induce necrosis.

It is well known that the release of the cytosolic contents into the extra-cellular space, as a result of necrosis, leads to an immune response. The inflammatory response associated with necrosis may be advantageous, from a therapeutic standpoint, as it prevents the accumulation of aberrant or damaged cells (Zong *et al.*, 2004). Many of the mechanisms that control apoptosis

are lost in cancer cells. Therefore, chemotherapeutic drugs that induce necrosis may have therapeutic value on a number of levels. The therapeutic efficacy of our two candidates will become clearer, as more in depth molecular studies are performed.

It can be postulated that the molecular activity of these two candidates disrupt the metabolic functions of the cell on multiple levels. Due to their ubiquitous DNA binding activity and hence their possible effect on transcription, the drugs may cause an energy deficit which could ultimately lead to necrosis. In order to further elucidate the drugs' effect on DNA regulation, gene expression studies were performed. These would provide greater insight into the drugs' mechanism of action, as well as the cell's response to drug exposure.

4.6 Gene Expression Analysis

4.6.1 RNA extraction and cDNA synthesis

The purity and concentration of the RNA was measured using the Nanodrop Spectrophotometer (Thermo) prior to cDNA synthesis and was found to be within acceptable limits. That is to say that the absorbance ratio reported by the instrument indicated that there was no extraneous ethanol or protein present in the samples. The RNA concentrations for the triplicate experiments for both drugs in both cell lines are listed in Appendix 2. The fidelity of the extraction procedure can therefore be accepted and cDNA synthesis could proceed. Interestingly the cancerous cell line yielded more RNA than the normal cell line per experiment. The reason for this is unclear; it may be due to increased expression levels, differences in cell membrane permeability or differences between cell passage times.

The RNA was diluted and reverse transcribed into cDNA and the concentration and purity was measured as described previously. Having found that all samples were of sufficient concentrations and purity, the samples were used for gene expression analysis.

4.6.2 Absolute Gene Expression Quantification of Selected Genes

When performing gene expression experimentation, in various formats, it is common practice to use so called "housekeeping genes" to normalize data. This normalization corrects experimental errors arising from: pipetting, RNA extraction, cDNA synthesis etc. (Banda *et al.*, 2008). Housekeeping genes are thought to be stably and ubiquitously expressed (Zhu *et al.,* 2008). Unfortunately, as described by Turnbridge and colleagues (2011) the selection of the genes must be done on a case by case basis, as it has been found that expression stability is dependent on a number of factors (e.g. tissue type, disease, treatment etc.).

In order to determine the fidelity of the data and the experimental conditions two commonly used housekeeping genes were evaluated to determine their stability. The Lightcycler expression data from β-actin and GAPDH from the two time intervals, in both cell lines, for Ferrocene and Rhodium-ferrocene were analysed using the REST software package. Absolute quantitation data generated from each gene's standard curve was used as input data and both genes were found to be stable across all experiments with a 95% confidence interval. This data therefore provided confidence for the gene expression experiments that were to follow, since the same experimental material was used for the array analyses. If the selected housekeeping genes were not stable across the various experiments the correction factor applied to the expression values of the other genes would be incorrect, thereby leading to inaccurate relative expression values.

In order to perform absolute quantification of selected genes, a dilution series was created from the amplification product of the particular gene. These were then amplified using SYBR green chemistry with the Lightcycler and crossing thresholds were determined (Figure 4.7). The crossing thresholds are then related to input concentrations, in order to generate a calibration curve.
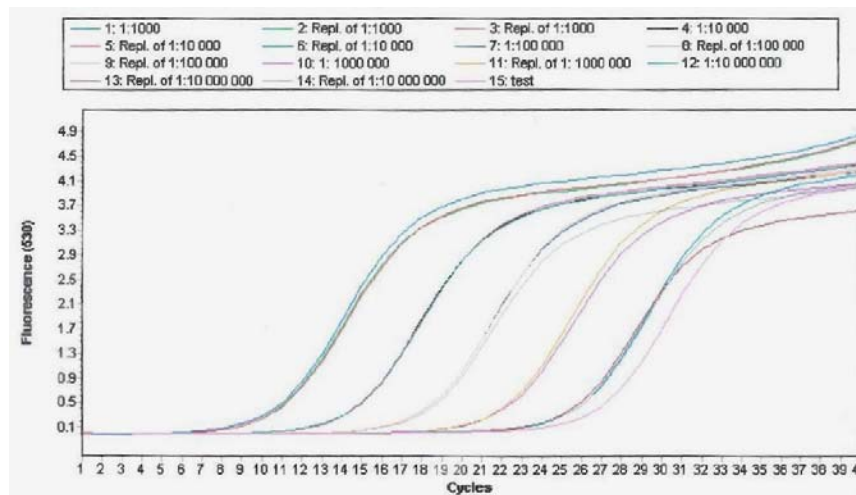
Figure 4.7: Lightcycler amplification curve of 10 fold serially diluted βActin cDNA used to generate a standard concentration curve for absolute quantification of the target gene. Targets were analysed in triplicate with x-axis indicating cyle number and the y-axis denoting fluorescence intensity (530nm).*

*Concentration ranges from sample 1 (0.172ng/µl) to sample 12 (0.0172pg/µl). "Test" indicates a positive control sample.

The amplification curve for serially diluted βActin cDNA (Figure 4.7) shows that the experimental triplicates were reproducible; yielding a linear calibration curve.

Although standard curves were generated for each target, in order to perform absolute quantification, data still had to be normalised relative to housekeeping genes. From these data, and relative expression studies performed using REST, we found no significant gene expression changes in the panel of genes chosen for evaluation.

Most significantly PARP, as described earlier, was found to be unaffected with regards to gene expression. The Lightcycler amplification data showed stable expression through out timecourses, treatment and cell lines. An excerpt from this data set is picture in Figure 4.8.
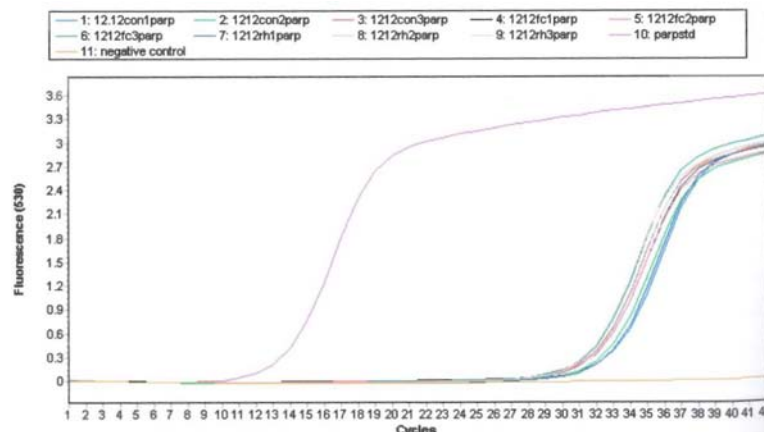
Figure 4.8: Lightcycler amplification curve for the detection of PARP cDNA in the reverse transcribed RNA extract of MCF-12A cells, exposed for 12 hours to either Ferrocene or Rhodium Ferrocene. Targets were analysed in triplicate with x-axis indicating cyle number and the y-axis denoting fluorescence intensity (530nm). Both a positive (PARP cDNA – 0.025ng/µl) and negative (no template) control is included.

From Figure 4.8 it is clear that the crossing thresholds for the various treatments are similar to the mock-treated control. Upon normalisation and comparison to calibration curves for the gene, it was found that there is no significant differential regulation of PARP.

The PARP protein has been identified as a key role-player in necrosis and apoptosis. Therefore if it is involved, in this study paradigm, it is most likely on a protein as opposed to a transcriptional level, as it has been shown that *PARP* expression is not affected at the time interval when necrosis/ late apoptosis is taking place (12 hours in MCF-7 cells).

4.6.3 Relative Quantification of Gene Expression by qPCR Array Analysis

4.6.3.1 Cell-cycle Focused qPCR Array Analysis

Due to the apparent effects induced by both drugs as seen in the flow cytometric data, it was decided to evaluate a panel of cell cycle-regulating genes in order to establish the mechanism of action of the two drugs. MCF-7 and MCF-12A cells were exposed to either drug at six or 12 hours and evaluated for expression changes as compared to a mock-treated control.

As an alternative to microarray analysis, SABiosciences offers a targeted expression analysis platform that can be utilised to screen specific genes relevant to a particular study. By

narrowing the range of genes to specific candidates one may infer perturbations in specific pathways. In addition to this validation (i.e. by real-time PCR) is not required, as is the case in microarray analysis.

The SABiosciences system consists of a 96-well plate with each well containing a lyophilised primer pair directed at a particular gene target or a control system (positive or negative control). The primers are designed in such a way that they have similar annealing temperatures and reaction efficiencies. The amplified PCR product is detected using SYBR Green, a DNA intercalating dye that fluoresces when bound to double stranded DNA. The fluorescence is therefore directly proportional to the DNA concentration.

Data was evaluated with the ΔΔCt method (Livak and Schmittgen, 2001) in which there is an inverse proportional relationship between the threshold cycle (Ct) and the gene expression level (L); therefore:

$$L = 2^{-Ct}$$

When one normalises the gene of interest (GOI) against that of a housekeeping gene (HKG) it may be represented as:

$$2^{-Ct(GOI)} \div 2^{-Ct(HKG)} = 2^{-[Ct(GOI)-Ct(HKG)]} = 2^{-\Delta Ct}$$

When an experimental sample is compared to a control sample:

$$2^{-\Delta Ct(experiment)} \div 2^{-\Delta Ct(control)} = 2^{-\Delta\Delta Ct}$$

As stated previously, the cDNA from the triplicate experiments was pooled, which was done as a normalisation procedure that allows one to avoid data bias resulting from sample variability. The variability experienced during the experimental procedure (seeding, treating and sampling) is therefore effectively accounted for during pooling. Bakay and colleagues (2002) expand on this paradigm. They studied variability in gene expression projects with microarrays and found the greatest level of variability occurring during the sampling procedure. The authors used biopsy samples from different patients and found that pooling eliminated a great deal of experimental bias. In this study we used two single homogenous cell lines, which would lead one to believe that pooling could be even more effective in this case.

Table 4.3 depicts the effect of Ferrocene treatment on MCF-7 cells at six and 12 hours. Generally, between a two and threefold change in certain genes was observed; with only two genes exhibiting a large fold change.

Table 4.3: Cell Cycle Array relative expression data for Ferrocene exposures of six and twelve hours in MCF-7 cells as compared to mock-treated controls.*

Gene Name	Gene Abbreviation	Fold Change*
Six Hour Ferrocene Treatment in MCF-7 Cells		
V-abl Abelson murine leukemia viral oncogene homolog 1	ABL1	2.07
DIRAS family, GTP-binding RAS-like 3	DIRAS3	-7.42
Cyclin-dependent kinase 5, regulatory subunit 1 (p35)	CDK5R1	2.01
Hect domain and RLD 5	HERC5	-2.37
Antigen identified by monoclonal antibody Ki-67	MKI67	-2.04
Twelve Hour Ferrocene Treatment in MCF-7 Cells		
V-abl Abelson murine leukemia viral oncogene homolog 1	ABL1	3.43
Anaphase promoting complex subunit 4	ANAPC4	2.30
Cyclin T2	CCNT2	2.87
Cyclin-dependent kinase inhibitor 1B (p27, Kip1)	CDKN1B	-2.20
RAD9 homolog A (S. pombe)	RAD9A	8.11

* Up-regulation is indicated by values in green whereas down-regulation is indicated by red text.

At six hours, in MCF-7 cells treated with Ferrocene, ABL is up-regulated. This proto-oncogene is responsible for cell differentiation, division, adhesion as well as stress response (OMIM *189980). The gene's expression continues to be elevated at 12 hours. Whether this is an attempt by the cancerous cell to continue division or if it is a direct response to treatment is not clear.

DIRAS3 appears to be markedly down-regulated at six hours. This gene is part of the Ras superfamily and has been associated with growth suppression and is therefore considered a putative tumour suppressor. Interestingly, it has been found to be absent or aberrant in breast epithelial cancers (OMIM *605193). If the gene is functional in MCF-7s the response may represent an attempt to continue the cell cycle regardless of genomic insult.

HERC5, a cyclin regulator, that is itself regulated by p53 (Mitsui *et al.*, 1999) is down regulated. The protein was found to induce cyclins in the absence of p53; in this case we assume that due

to its down-regulation, the division promoting cyclins are also down-regulated. MKI-67 is a protein that is expressed by proliferating cells at various stages of the cell cycle (OMIM *176741). Its down-regulation may be indicative of cell-cycle inhibition and its communication to adjacent cells within the experimental infrastructure. Although the flow cytometric cell cycle analysis shows no perturbations at this point, these gene expression data may point to the cell's preparation to halt cell cycle progression.

At 12 hours ANAPC4, a member of the anaphase promoting complex, is up-regulated. CCNT2 is also up-regulated at this point. This protein forms part of a complex with CDK-9 and functions to transition from abortive to productive elongation (OMIM *606947). These cell division promoting signals are counterintuitive to the expected cell cycle arrest, yet it may represent the cancerous cell's inability to arrest division following genomic insult, or, it may be a response gleaned from a subset of the cellular population that cannot be applied to the whole experimental group.

A noteworthy expression response at this point is the large up-regulation of RAD9A. This protein is phosphorylated as a result of DNA damage and plays a role in damage induced signalling (Volkmer and Karnitz, 1999). This is the first indication of the drug's DNA damaging effect from a gene expression analysis standpoint. When reflecting back on the flow cytometric data, at this point the MCF-7 cells are accumulating in S-phase as a result of Ferrocene treatment. This correlation between the perturbation of DNA synthesis, and expressed genes relating to DNA damage, lend further weight to the hypothesis that Ferrocene's mechanism of action (cytotoxicity) is as a result of its interaction with DNA.

The effect of Ferrocene on the "normal" cell line, MCF-12A, at six and 12 hours is illustrated in Table 4.4. The MCF-12A cells (normal transformed) show a lower expression response when compared to MCF-7 cells (cancerous). This changes at 12 hours when the "normal" cell line exhibits a marked increase in expression activity.

Table 4.4: Cell Cycle Array relative expression data for Ferrocene exposures of six and twelve hours in MCF-12A cells as compared to mock-treated controls.*

Gene Name	Gene Abbreviation	Fold Change
Six Hour Ferrocene Treatment in MCF-12A Cells		
Cyclin G2	CCNG2	2.88
CHK2 checkpoint homolog (S. pombe)	CHEK2	-3.67
Antigen identified by monoclonal antibody Ki-67	MKI67	-2.01
Twelve Hour Ferrocene Treatment in MCF-12A Cells		
Anaphase promoting complex subunit 4	ANAPC4	2.27
Ataxia telangiectasia mutated (includes complementation groups A, C and D)	ATM	-3.60
BCL2-associated X protein	BAX	-13.62
Cyclin B1	CCNB1	2.48
Cyclin F	CCNF	7.12
Cyclin-dependent kinase inhibitor 1B (p27, Kip1)	CDKN1B	-2.71
Growth arrest and DNA-damage-inducible, alpha	GADD45A	4.41
Hect domain and RLD 5	HERC5	-2.16
RAD17 homolog (S. pombe)	RAD17	2.09
RAD51 homolog (RecA homolog, E. coli) (S. cerevisiae)	RAD51	8.07
RAD9 homolog A (S. pombe)	RAD9A	11.57
SERTA domain containing	SERTAD1	2.62
Transcription factor Dp-1	TFDP1	3.84
Transcription factor Dp-2 (E2F dimerization partner 2)	TFDP2	2.22
Ubiquitin-activating enzyme E1 (A1S9T and BN75 temperature sensitivity complementing)	UBE1	2.22

* Up-regulation is indicated by values in green whereas down-regulation is indicated by red text.

When comparing MCF-7 and MCF-12A expression levels and the number of genes that are differentially expressed, a greater response is found in the normal cell line, at a later stage, when compared to the cancerous cells. This may be due to the fact that the normal cell line responds on a non-transcriptional level (e.g. protein phosphorylation) at the early stages of a genomic insult, followed by initiation of growth arrest and repair mechanisms. When relating back to the cell-death analyses, at 12 hours MCF-7 cells have entered necrosis whereas MCF-12A cells did not. This may mean that the expression changes in the normal line are an attempt to repair the damage, while at the same time the MCF-7 cells were overcome by the drugs, due to their lack of DNA repair functionality, and entered necrosis.

A number of expression similarities between the two cell lines are present as seen in the regulation of MKI67, ANAPC4 and RAD9A. But with that said, the normal cell line exhibits a

marked DNA-damage induced response with the up-regulation of GADD45A and the RAD proteins.

A remarkable outlier in the data is the massively down-regulated BAX gene. BAX associates with BCL2 in the apoptotic pathway. When BAX concentration outweighs BCL2, the anti-apoptotic activity of BCL2 is overcome and the cell enters apoptosis (Oltvai *et al.*, 1993). This may represent the normal cell's attempt to delay the apoptotic program and initiate DNA repair.

The effect of Rhodium-ferrocene treatment of MCF-7 cells at six and 12 hours is depicted in Table 4.5. It is noteworthy to observe that Rhodium-ferrocene elicits a greater gene expression response in the cancerous cell line. This could be attributed to differences in cytotoxicity but it is more likely that there are slight differences in the drugs' mechanism of action.

Table 4.5: Cell Cycle Array relative expression data for Rhodium-ferrocene exposures of six and twelve hours in MCF-7 cells as compared to mock-treated controls.*

Gene Name	Gene Abbreviation	Fold Change*
Six Hour Rhodium-ferrocene Treatment in MCF-7 Cells		
ANAPC4	ANAPC4	2.54
BCL2-associated X protein	BAX	29.36
Cyclin C	CCNC	2.23
Cyclin F	CCNF	2.32
CDC20 cell division cycle 20 homolog (S. cerevisiae)	CDC20	2.04
Cyclin-dependent kinase 5, regulatory subunit 1 (p35)	CDK5R1	2.51
Cyclin-dependent kinase inhibitor 1B (p27, Kip1)	CDKN1B	-4.04
Growth arrest and DNA-damage-inducible, alpha	GADD45A	3.42
Hect domain and RLD 5	HERC5	-2.88
MAD2 mitotic arrest deficient-like 1 (yeast)	MAD2L1	2.54
RAD51 homolog (RecA homolog, E. coli) (S. cerevisiae)	RAD51	2.63
SERTA domain containing	SERTAD1	2.11
Twelve Hour Rhodium-ferrocene Treatment in MCF-7 Cells		
V-abl Abelson murine leukemia viral oncogene homolog 1	ABL1	2.33
Ataxia telangiectasia mutated (includes complementation groups A, C and D)	ATM	2.12
Cyclin-dependent kinase 2	CDK2	2.15
Cyclin-dependent kinase inhibitor 1B (p27, Kip1)	CDKN1B	-5.16
RAD9 homolog A (S. pombe)	RAD9A	3.49

* Up-regulation is indicated by values in green whereas down-regulation is indicated by red text.

On average the response to the drug by MCF-7 cells is a general picture of up-regulated gene expression. Therefore one could assume that an energy dependent process is taking place. Whether ineffectual arrest and repair mechanisms are responsible for cell death leading to aberrant and unsustainable growth; or a general energy deficit leading to necrosis is unclear. Once again, the DNA damage related gene RAD9A is up-regulated.

Since necrosis was the endpoint, and it is generally characterised as the cell's inability to enter apoptosis, one could postulate that cell death is a result of the cells inability to repair genomic insult and an inability to initiate what repair mechanisms still exist, due to an energy deficit. Interestingly, genes associated with cell growth and division are up-regulated (e.g. cyclins and cyclin dependent kinases) which may be indicative of the cancerous cells' inability to halt cell cycle progression regardless of genomic integrity.

In stark contrast to the normal cell's response to Ferrocene; the cancerous cell's response to Rhodium Ferrocene shows a massively up-regulated response of the BAX gene. As alluded to previously, this protein forms part of the pro-apoptotic response. Therefore it may represent the first attempts to enter apoptosis as a result of treatment. Table 4.6 illustrates the effect of Rhodium-ferrocene on normal cells at six and 12 hours.

Table 4.6: Cell Cycle Array relative expression data for Rhodium-ferrocene exposures of six and twelve hours in MCF-12A cells as compared to mock-treated controls.*

Gene Name	Gene Abbreviation	Fold Change*
Six Hour Rhodium-ferrocene Treatment in MCF-12A Cells		
BCL2-associated X protein	BAX	-4.65
Cyclin D2	CCND2	2.57
CHK2 checkpoint homolog (S. pombe)	CHEK2	-4.08
RAD9 homolog A (S. pombe)	RAD9A	2.21
Twelve Hour Rhodium-ferrocene Treatment in MCF-12A Cells		
Ataxia telangiectasia mutated (includes complementation groups A, C and D)	ATM	-3.57
BCL2-associated X protein	BAX	2.39
Cyclin F	CCNF	2.08
Cyclin-dependent kinase inhibitor 1B (p27, Kip1)	CDKN1B	-5.29
Antigen identified by monoclonal antibody Ki-67	MKI67	-2.52
Nibrin	NBN	-2.84
RAD9 homolog A (S. pombe)	RAD9A	4.78
Ubiquitin-activating enzyme E1 (A1S9T and BN75 temperature sensitivity complementing)	UBE1	-2.06

* Up-regulation is indicated by values in green whereas down-regulation is indicated by red text.

When considering the "normal" cell's response to Rhodium-ferrocene, the majority of affected genes are in fact down-regulated. As opposed to a large or misplaced energy investment to remain viable the normal cell may be entering the apoptotic or necrotic program due to a down regulation in arrest and repair genes. From another point of view, the gene expression "snapshot" taken at this point in time may include a view of the cell population after genomic repair.

It is important to note that during these experiments the cells were not synchronised. This means that any gene expression profile is the response of a mixed population consisting of cells in different phases of the cell cycle. Although the expression picture would be a result of the majority of cells in a particular phase, certain genes may appear as outliers due to the response elicited by a minority of the population. There are a number of reasons why synchronisation was not used in this study. Synchronisation is a stress inducing process, which may result in aberrations in the data. In addition to this, the treatment of a mixed population more accurately simulates the *in vivo* response to a drug.

The cell cycle array data provided support for the data generated by flow cytometric analyses and once again illustrates that cell cycle perturbations are induced as a result of treatment with either of the compounds. Furthermore, certain DNA damage-related genes were affected, which prompted further investigation into genes and pathways specifically associated with DNA damage recognition and repair.

4.6.3.2 DNA Damage Focused qPCR Array Analysis

The DNA damage array used in the study was a later version of the cell cycle array and was therefore in a different format. The dilution series of the housekeeping genes were absent and a control system that relies on the use of the manufacturer's reverse transcriptase was introduced. Since Superscript (Invitrogen) was used these data points were discarded. In addition to this, three positive PCR wells are included to calculate the efficiency of the reactions as well as a "no reverse transcription" control. This final control is used to determine DNA contamination in the RNA extract. All arrays proved negative for this control (i.e. no DNA present in the RNA extract).

After duplicate arrays were run for each drug, in each cell line at each time, the thresholds and baselines were set on the ABI7300 to normalise analysis and avoid data bias. A two-fold up or down regulation response was chosen as the minimal reportable level. This was based on reproducibility data provided by the manufacturer (RT2 Profiler White-paper; www.SABiosciences.com). The genes probed by this array are listed in Appendix 3.

The representivity of genes up or down-regulated more than two-fold within the set of genes on the array may be visualised using "scatter plots" as pictured in Figures 4.9 to 4.12.
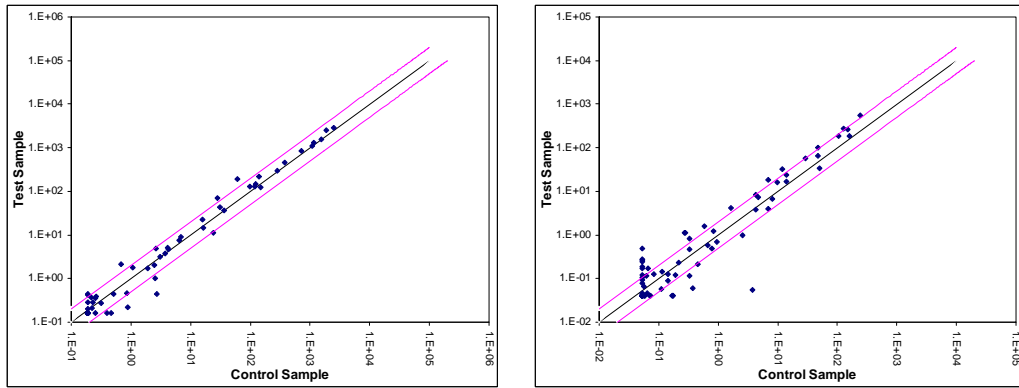
Figure 4.9: Scatter plots of gene expression fold change for MCF-7 cells exposed to Ferrocene for six (left) and 12 (right) hours. The black line indicates fold changes of one and pink lines represent an expression threshold set at two-fold.
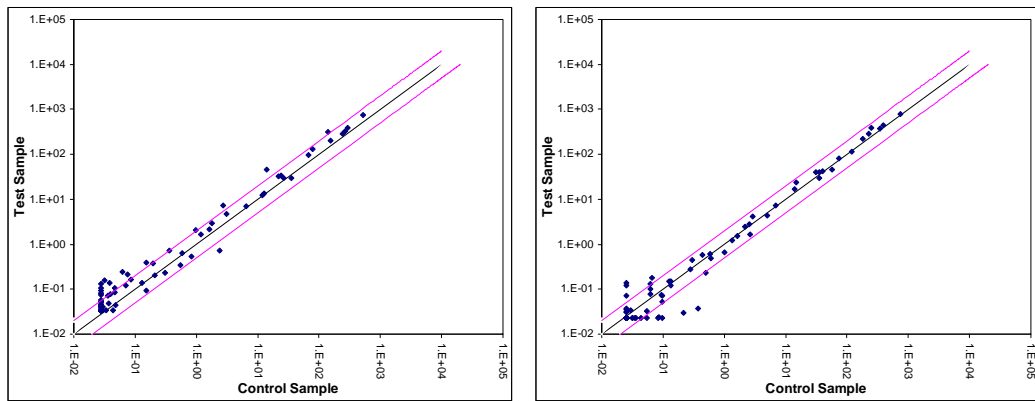
Figure 4.10: Scatter plots of gene expression fold change for MCF-12A cells exposed to Ferrocene for six (left) and 12 (right) hours. The black line indicates fold changes of one and pink lines represent an expression threshold set at two-fold.
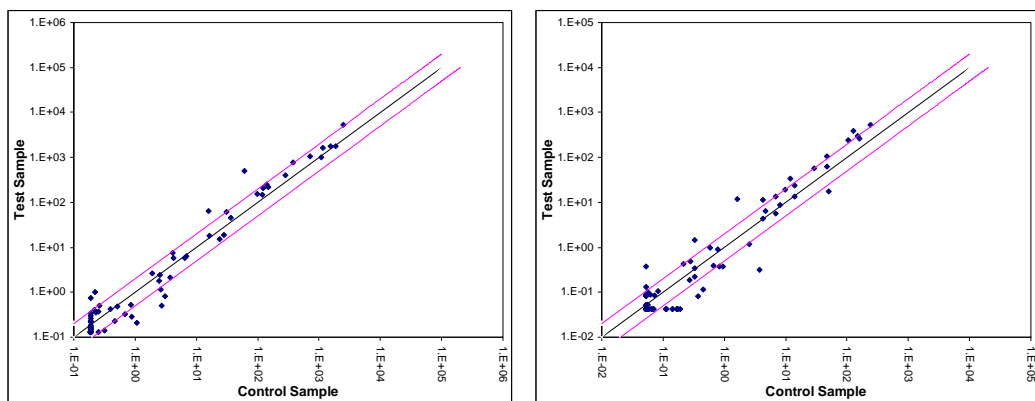
Figure 4.11: Scatter plots of gene expression fold change for MCF-7 cells exposed to Rhodium-ferrocene for six (left) and 12 (right) hours. The black line indicates fold changes of one and pink vertical lines represent an expression threshold set at two-fold.
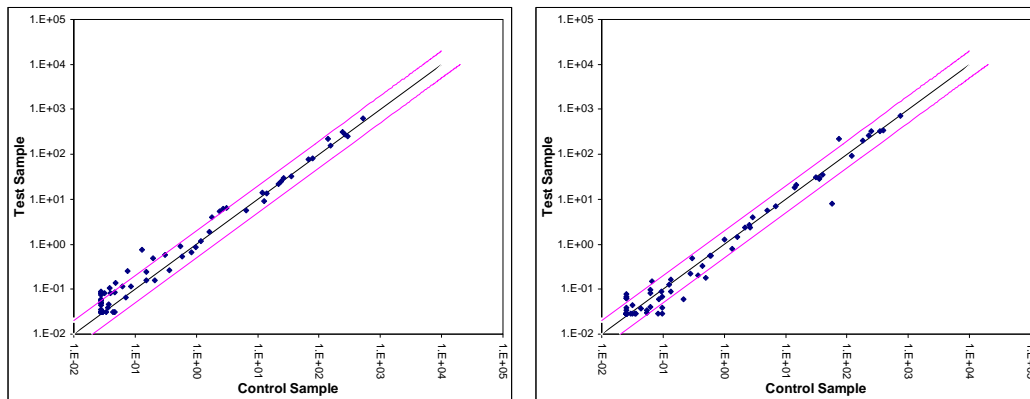
Figure 4.12: Scatter plots of gene expression fold change for MCF-12A cells exposed to Rhodium-ferrocene for six (left) and 12 (right) hours. The black line indicates fold changes of one and pink vertical lines represent an expression threshold set at two-fold.

When considering these data it is clear that a larger number of genes are differentially regulated in the cancerous cell line (MCF-7). In addition to this, the expression change in the normal cell line appears to occur earlier and to a greater extent than in the cancerous line. The reasons for this are unclear, yet one may speculate that the normal cell's DNA damage detection and repair mechanisms are more functional than the cancerous cells'. Table 4.7 illustrates the gene expression data for MCF-7 cells exposed to Ferrocene for six and twelve hours as related to mock-treated controls.

Table 4.7: DNA Damage Array relative expression data for Ferrocene exposures of six and twelve hours in MCF-7 cells as compared to mock-treated controls.*

Gene Name	Gene Abbreviation*	Fold* Change
Six Hour Ferrocene Treatment in MCF-7 Cells		
Ataxia telangiectasia mutated	ATM	2.21
Fanconi anemia, complementation group G	FANCG	-2.17
Growth arrest and DNA-damage-inducible, alpha	GADD45A	2.30
G-2 and S-phase expressed 1	GTSE1	-2.43
XRCC6 binding protein 1	XRCC6BP1	-2.50
8-oxoguanine DNA glycosylase	OGG1	-3.94
Proliferating cell nuclear antigen	PCNA	-6.11
RAD1 homolog (S. pombe)	RAD1	-2.83
RAD18 homolog (S. cerevisiae)	RAD18	2.54
Three prime repair exonuclease 1	TREX1	3.23
Xeroderma pigmentosum, complementation group C	XPC	3.07
Twelve Hour Ferrocene Treatment in MCF-7 Cells		
Ankyrin repeat domain 17	ANKRD17	2.25
Ataxia telangiectasia and Rad3 related	ATR	-2.87
CHK1 checkpoint homolog (S. pombe)	CHEK1	5.13
DNA-damage-inducible transcript 3	DDIT3	2.74
Flap structure-specific endonuclease 1	FEN1	2.55
X-ray repair complementing defective repair in Chinese hamster cells 6 (Ku autoantigen, 70kDa)	XRCC6	2.62
Growth arrest and DNA-damage-inducible, gamma	GADD45G	2.46
General transcription factor IIH, polypeptide 1, 62kDa	GTF2H1	2.66
General transcription factor IIH, polypeptide 2, 44kDa	GTF2H2	2.32
HUS1 checkpoint homolog (S. pombe)	HUS1	-4.03
Mitogen-activated protein kinase 12	MAPK12	2.01
Menage a trois homolog 1, cyclin H assembly factor (Xenopus laevis)	MNAT1	2.18
N-methylpurine-DNA glycosylase	MPG	4.08
Proliferating cell nuclear antigen	PCNA	-2.16
Apoptosis-inducing factor, mitochondrion-associated, 1	AIFM1	2.69
PMS2 postmeiotic segregation increased 2 (S. cerevisiae)	PMS2	3.95
RAD17 homolog (S. pombe)	RAD17	3.58
RAD51 homolog (RecA homolog, E. coli) (S. cerevisiae)	RAD51	4.53
RAD9 homolog A (S. pombe)	RAD9A	3.20
Sema domain, immunoglobulin domain (Ig), transmembrane domain (TM) and short cytoplasmic domain, (semaphorin) 4A	SEMA4A	-4.16
Uracil-DNA glycosylase	UNG	-4.25
Xeroderma pigmentosum, complementation group A	XPA	5.07
Xeroderma pigmentosum, complementation group C	XPC	-6.32
X-ray repair complementing defective repair in Chinese hamster cells 3	XRCC3	-2.60
Sterile alpha motif and leucine zipper containing kinase AZK	ZAK	2.12

* Up-regulation is indicated by values in green whereas down-regulation is indicated by red text.

Immediately, when compared to the cell-cycle array, it is apparent that genes concerned with DNA damage response are affected to a greater extent. This highlights the convenience of a

pathway/function focused approach to gene expression analysis. For the sake of brevity, only selected gene functions will be discussed here, in depth, to highlight and possibly extrapolate drug function.

ATM, one of the key effectors of the cell cycling checkpoints is up-regulated as a result of Ferrocene treatment. This protein phosphorylates p53, the "master" cell cycle regulator and has been found to be up-regulated after exposure to ionising radiation i.e. double stranded breaks (OMIM *607585). This could possibly point to the nature of the DNA damage induced by the drug in cancerous cells. The ionisation effect, as suggested by Neuse (2005) might be at play in addition to DNA binding thereby resulting in ionisation-induced DNA damage response. ATM has been implicated in the repair of double-stranded breaks by co-ordinating the DNA end repair complex (Bredemeyer, 2006).

ATM cascades its effect to the checkpoint kinases (CHK1 and CHK2). *CHK1* is found to be strongly up-regulated at 12 hours which is indicative of a marked attempt to halt cell cycle progression (CHK1 inhibits cyclin dependent kinases). This checkpoint activation may explain the accumulation of cells in the S-phase at this point, as found in the flow cytometric data. At this point, *ATR* (ataxia telangectasia-related) upstream of CHK1 and CHK2 is down-regulated, which may be as a result of feedback inhibition.

GADD45A is up-regulated as a result of treatment. This gene is initiated by p53 and binds PCNA (proliferating cell nuclear antigen) which is part of the cyclin dependent kinase complex and in these data it is found to be markedly down-regulated. GADD45A is involved in DNA excision repair and prevents the cell's entry into S phase (Smith *et al.*, 1998). S-phase regulation becomes apparent at 12 hours, from the flow cytometric data. GADD45A's involvement in DNA excision repair provides further insight into Ferrocene's mode of action. The excision induction may be to remove covalently bound drug or even ionisation damaged nucleotides, but, these data do clearly show the interaction of the drug with the DNA molecule.

It appears that the cancerous cell exposed to Ferrocene does attempt to affect repair mechanisms as seen in the up-regulation of the *RAD* genes whose proteins complex and associate with DNA, recruiting repair proteins to the molecule (OMIM *603761). In the cells' further attempt to repair DNA, *TREX1* is up-regulated. This protein associates with the SET complex and has 3' exonuclease activity. The protein complex removes modified, mismatched, fragmented and normal nucleotides from the 3'-terminus as a part of DNA metabolism (Mazur and Perrino, 1999; Chowdhury *et al.*, 2006). This activity may remove aberrant nucleotides as a result of exposure or it may represent early apoptotic/necrotic events, which is likely, since the initiation of necrosis for this treatment was confirmed at 12 hours through Annexin V flow cytometry.

XPC was found to be up-regulated at six hours. This protein complexes with HHR23B to form one of the earliest mechanisms to initiate nuclear excision repair (Sugasawa *et al.,* 1998). Up-regulation of *XPC* is indicative of further DNA damage induced by the drug. XPC has been found to be involved in the selective repair of cyclobutane pyrimidine dimers (Emmert *et al.*, 2000). This brings to mind the pyrimidine component of the PstI restriction site target of the drug. Interestingly the gene becomes strongly down-regulated after 12 hours. Further evidence of the cell's attempt to remove aberrant nucleotides can be seen in the up-regulation of *MPG* (3-methyladenine DNA glycosylase). The protein removes damaged DNA bases such as cytotoxic and mutagenic alkylation adducts of purines (Lau *et al.,* 1998). This is further illustration that multiple nucleotide damage is being induced by the drug.

The gene *SEMA4A* which codes for a soluble transmembrane protein and is involved in immune responses was found to be up-regulated (Kumanogoh *et al.,* 2002). As mentioned earlier, necrosis elicits an immune response. Additionally, after 12 hours, genes such as *PMS2* are strongly up-regulated. This protein has been associated with both DNA damage repair as well as DNA-damage-induced apoptosis. PMS2 associates with p73 in response to cisplatin treatment thus enhancing the apoptotic response (Shimodaira *et al.*, 2003). Thus one may infer correlation between organometallic drug sub-classes. Generally a picture of nuclear excision is seen in

which aberrant nucleotides are removed as is the case with up-regulation of *XPA* at 12 hours. The protein is associated with the nuclear excision repair complex and is implicated in anchoring and activation of endonucleases (Volker *et al.,* 2001). Interestingly, at 12 hours *RAD51* is up-regulated. This protein associates with BRCA1 and BRCA2 in a general DNA repair mechanism for double stranded breaks (Kato *et al.,* 2000). Therefore, these strand breaks (as well as those mentioned earlier in connection with ATM) are probably part of a post excision repair process in which strands are re-associated after repair.

From these data a clear picture of DNA damage induced by Ferrocene in MCF-7 cells emerges. The apparent response appears to be related to the excision of aberrant nucleotides. This may be a result of ionisation-induced damage by the drug free-radical or an attempt to remove covalently associated drug adducts.

When viewing data in a graphical representation of canonical pathways, the multiplicity of the genes' interactions become apparent. The gene expression results of Ferrocene treatment in MCF-7 cells at six hours, analysed using the IPA software, are pictured in Figure 4.13. The figure illustrates the influence of the drug treatment on the DNA replication, recombination, and repair, cell cycle and cell morphology network. This is the first indication of the extent of the influence the drug has on a number of genes and functions.

Figure 4.13: Gene network analysis of Ferrocene treated MCF-7 cells after six hours illustrating the influence on the DNA Replication, Recombination and Repair, Cell Cycle and Cell Morphology gene expression* networks.

*Green highlighted genes indicate up-regulation whilst red highlighting indicates down-regulation. Solid lines indicate direct interaction whereas dashed lines represent indirect interaction.

From Figure 4.13 it is clear that a number of genes are affected by the treatment. As illustrated previously, the strong influence of DNA damage signalling becomes apparent. The diversity of interactions caused by the drug exposure is evident. Many of the genes that affect p53 regulation, specifically the ATM cascade are upregulated. This is indicatibe of the cell's attempt to stop replication.

The ATM-mediated checkpoint (upregulated) which initiates CHEK2 (unchanged expression) is activated. This then initiates the XPC-driven nucleotide excision repair. *XPC* is upregulated in this experiment and the protein binds RAD23B, GTF2H1 and CETN2 (Your Favourite Gene – Appendix 4). This is indicative of the drug's mechanism of action.

Similarly, when considering Ferrocene treatment of MCF-7 cells after 12 hours, in Figure 4.14, the effect of treatment on DNA replication, recombination and repair and cell cycle gene expression pathways becomes clear. As stated previously, we note an increased number of up-regulated genes.

Figure 4.14: Gene network analysis of Ferrocene treated MCF-7 cells after 12 hours illustrating the influence on the DNA replication, recombination and repair and cell cycle gene expression* networks.

*Green highlighted genes indicate up-regulation whilst red highlighting indicates down-regulation. Solid lines indicate direct interaction whereas dashed lines represent indirect interaction.

Interestingly, at this point, *CHEK1* is upregulated as opposed to ATM-mediated CHEK2 initiation at six hours. RAD-17 (upregulated) associates with ATR to phosphorylate CHEK1 (Kastan and Bartek, 2004), thereby activating it. The multiple involvement of *ATR* and *ATM* may be due to redundancy or multiple effects induced by the drug.

Leading from the previous figure we note *XPC* down regulation where at six hours *XPC* was upregulated. This shows the progress of the excision repair pathway initiation over time. *GTF2H1* and *GTF2H2* are both up-regulated as a result. These proteins are associated with RNA-polymerase initiation and may represent an increase in transcription activity (OMIM *189972).

It appears that p53 is central to the drugs mechanism of action (Figure 4.14), yet it is not up-regulated. This may be explained by the fact that p53 is often dysregulated in cancers, or, regulation occurs on a protein level.

DDIT3, which is regulated by p53 is associated with endoplasmic reticulum stress (OMIM *126337) which may be as a result of drug treatment. The protein further regulates and is regulated by *MYC* (no regulation change in Figure 4.14), which sensitises cells to death receptor signalling (Lowe *et al.,* 2004).

XRCC6 is upregulated in Figure 4.14; it encodes p70 which is associated with DNA transport and repair. The protein binds double stranded DNA breaks and forms part of the double strand break repair mechanism (OMIM *152690).

Gene relationships and associations may be summarised, using the "Your Favourite Gene" (Sigma) tool. The gene in question is described in the context of genes, proteins and molecules that it regulates, is regulated by and binds to. In addition to this the functionality within the cell is also listed (Appendix 4).

Following examination of the cancerous cell's response, Table 4.8 illustrates the gene expression data for MCF-12A cells exposed to Ferrocene for six and twelve hours as related to mock-treated controls. These data should provide insight into the normal cell's response to treatment as opposed to the cancerous cell's response which is characterised by flawed molecular machinery.

Table 4.8: DNA Damage Array relative expression data for Ferrocene exposures of six and twelve hours in MCF-12A cells as compared to mock-treated controls.*

Gene Name	Gene Abbreviation	Fold Change*
Six Hour Ferrocene Treatment in MCF-12A Cells		
Ataxia telangiectasia and Rad3 related	ATR	2.87
Cell death-inducing DFFA-like effector a	CIDEA	2.60
Fanconi anemia, complementation group G	FANCG	-3.27
Flap structure-specific endonuclease 1	FEN1	2.10
Growth arrest and DNA-damage-inducible, alpha	GADD45A	2.84
General transcription factor IIH, polypeptide 2, 44kDa	GTF2H2	3.90
XRCC6 binding protein 1	XRCC6BP1	2.59
MutL homolog 1, colon cancer, nonpolyposis type 2 (E. coli)	MLH1	3.31
8-oxoguanine DNA glycosylase	OGG1	4.68
PMS1 postmeiotic segregation increased 1 (S. cerevisiae)	PMS1	3.63
Polynucleotide kinase 3'-phosphatase	PNKP	2.27
RAD17 homolog (S. pombe)	RAD17	3.68
RAD18 homolog (S. cerevisiae)	RAD18	2.66
Sema domain, immunoglobulin domain (Ig), transmembrane domain (TM) and short cytoplasmic domain, (semaphorin) 4A	SEMA4A	2.04
Sestrin 1	SESN1	2.00
SMT3 suppressor of mif two 3 homolog 1 (S. cerevisiae)	SUMO1	4.84
Three prime repair exonuclease 1	TREX1	3.26
Xeroderma pigmentosum, complementation group C	XPC	2.27
Twelve Hour Ferrocene Treatment in MCF-12A Cells		
APEX nuclease (multifunctional DNA repair enzyme) 1	APEX 1	-3.57
Ataxia telangiectasia and Rad3 related	ATR	2.13
Breast cancer 1, early onset	BRCA 1	-3.59
Cell death-inducing DFFA-like effector a	CIDEA	2.71
G-2 and S-phase expressed 1	GTSE1	-10.07
Immunoglobulin mu binding protein 2	IGHMBP2	-2.13
Inositol hexaphosphate kinase 3	IHPK3	-4.14
Nth endonuclease III-like 1 (E. coli)	NTHL1	2.89
8-oxoguanine DNA glycosylase	OGG1	-2.36
Proliferating cell nuclear antigen	PCNA1	-7.40
Xeroderma pigmentosum, complementation group A	XPA	5.41
X-ray repair complementing defective repair in Chinese hamster cells 1	XRCC1	4.87

* Up-regulation is indicated by values in green whereas down-regulation is indicated by red text.

Upon inspection of the six hour expression response one immediately notes a larger trend toward up-regulation when compared to MCF-7 cells. This is then followed by a lower number of affected genes at 12 hours when compared to MCF-7 cells and a trend towards down-regulation whereas the cancerous cell's genes are largely up-regulated at 12 hours.

When continuing the comparison the most noteworthy point of interest is the activation of *ATR* at six hours (*ATM* is activated in MCF-7). Up-regulation is continued until 12 hours after exposure. In the cancerous cell line it is down-regulated at this point. This may be indicative of a more prolonged arrest mechanism in the normal cell line. It may also serve to explain why cell death is detected earlier in the cancerous cells. This gene is part of the same checkpoint network that activates the checkpoint kinases (CHK1 and CHK2). Interestingly, ATR is associated with replication fork arrest, as described previously. This may be indicative of the influence of bound drug or drug-induced aberrations, on DNA replication. The endpoint however is another shared similarity with the up-regulation of *GADD45A*. These activated arrest and repair mechanisms serve to further explain the cell cycle progression inhibition detected in the flow cytometry data.

OGG1, a DNA glycosylase, is up-regulated at six hours. The protein removes 8-oxoguanine (8-oxoG), one of the major lesions in DNA induced by reactive oxygen species (Lu *et al.,* 1997). This is a strong argument for the chemical reactivity of the drug inducing free-radical-based damage to DNA.

SEM4A, coding for a protein responsible for immune response, is up-regulated as a result of treatment in MCF-12A cells whereas it is down-regulated in MCF-7 cells. *SUMO1* is up-regulated at six hours. This group of sumoylation proteins affect nuclear transport, protein stability, transcriptional regulation and apoptosis (Su and Li, 2002). A number of drugs and environmental stresses have been found to cause topoisomerase induced DNA damage. SUMO1 is recruited to DNA and has been implicated in repair mechanisms (Mao *et al.*, 2000).

As with the cancerous cells, Ferrocene was found to induce nucleotide excision repair in normal cells with the up-regulation of *TREX1*. This protein has 3-prime-to-5-prime exonuclease activity and removes mismatched, modified, fragmented and normal nucleotides to create appropriate 3' ends (Mazur and Perrino, 2001). *XPA* is markedly up-regulated at 12 hours and is further evidence of initiation of the excision complex. Further, *XRCC1* up-regulation is indicative of single strand break repair induced by ionising damage. *GTSE1*, a G2-phase marker (Monte *et al.*, 2000), was prominently down regulated at 12 hours. This shows the normal cell's ability to arrest the transition between the cell cycle phases as illustrated in the flow cytometry data. Similarly, *PCNA* is markedly down-regulated at 12 hours as was the case with MCF-7 treatment. From these data a number of similarities in expression patterns between MCF-12A and MCF-7 are present; yet the extent of the response in most cases is accentuated in the normal cell line.

The influence of Ferrocene on the MCF-12A cell's genetic networks is illustrated in Figure 4.15. As stated previously there is a marked increase in expression level and extent when compared to the cancerous cell line. Again, the centrality of p53 is noted as well as the involvement of DNA damage induced checkpoints.
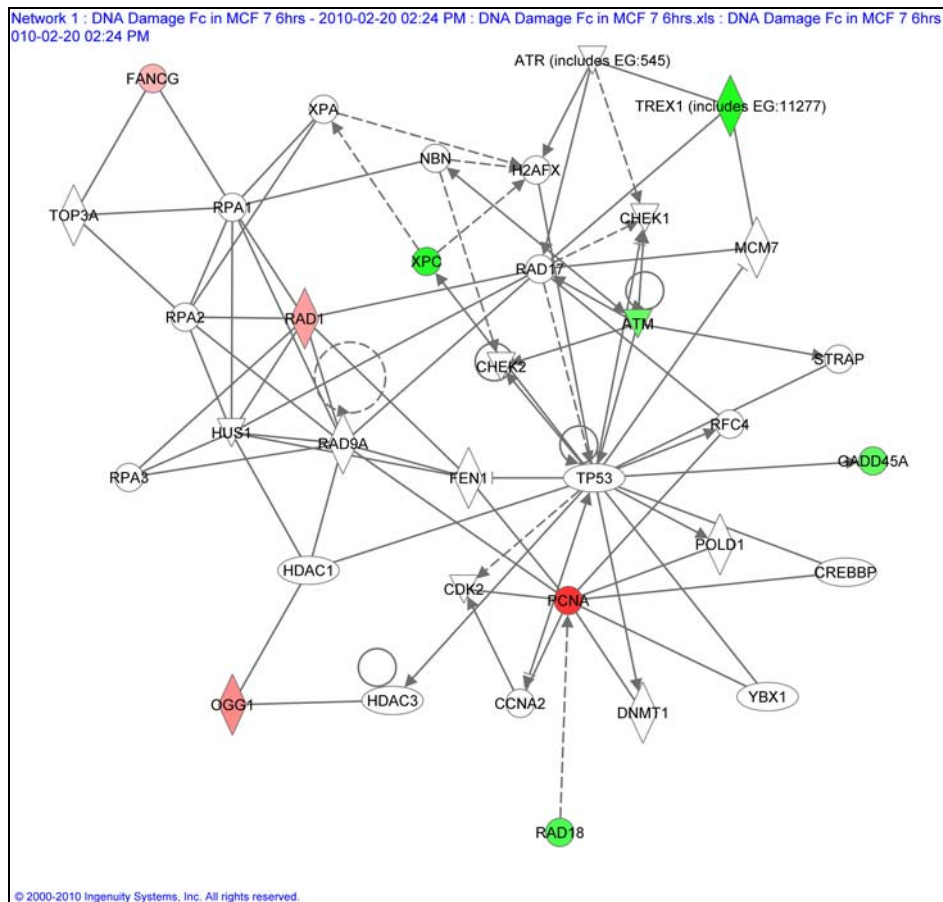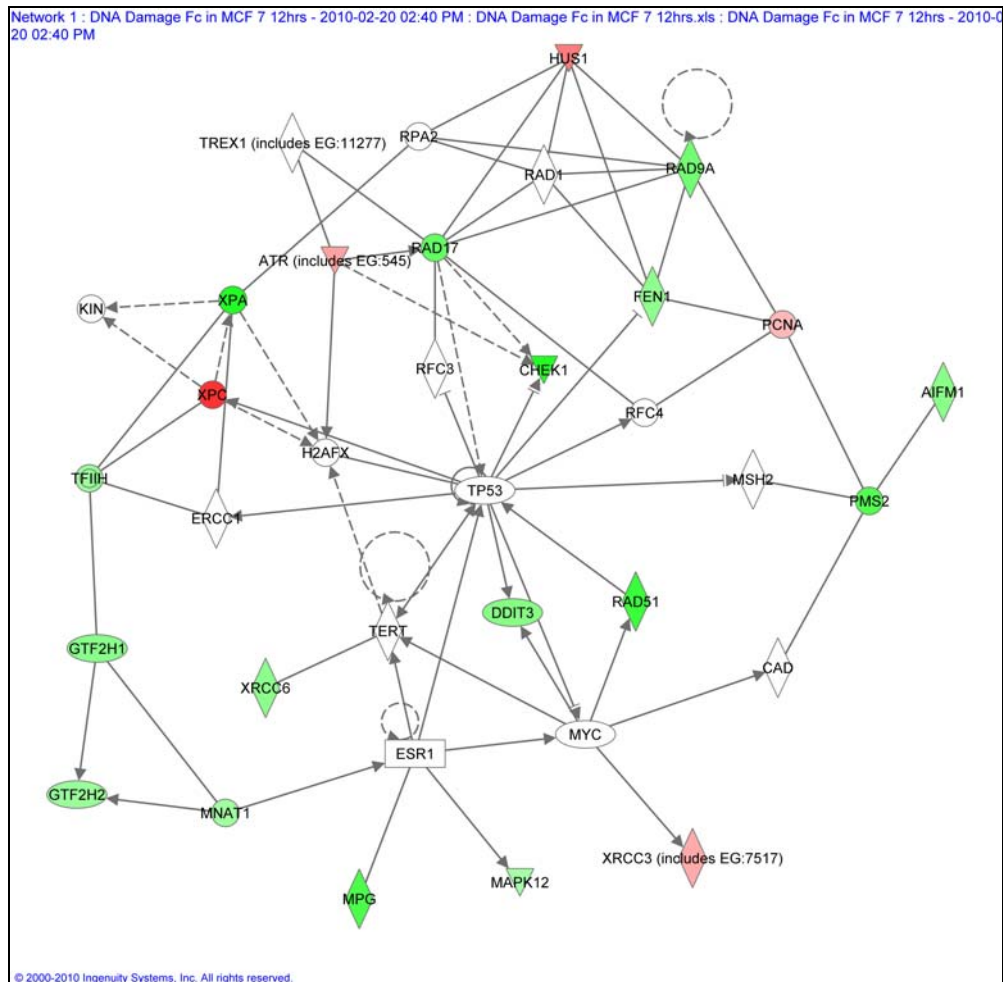
Figure 4.15: Gene network analysis of Ferrocene treated MCF-12A cells after six hours illustrating the influence on the DNA replication, recombination and repair and cell cycle gene expression* networks.

*Green highlighted genes indicate up-regulation whilst red highlighting indicates down-regulation. Solid lines indicate direct interaction whereas dashed lines represent indirect interaction.

From the figure, as before, we see the involvement of *XPC* and the nuclear excision pathway. *ATR*, appears to be the main initiator of checkpoint regulation in this treatment and is seen to cascade its effect to *TREX 1*, which is involved in three-prime exonuclease activity. This further

confirms the DNA damage induced by the drug. ATR must bind to RAD-17, which is upregulated, to phosphorylate CHEK1 (Kastan and Bartek, 2004). This highlights the veracity of the data, as multiple members of the same pathway are affected.

As with MCF-7 treatment, in Figure 4.15 *XPC* is upregulated. This illustrates the initiation of the excision repair pathway in the normal cell line after six hours of treatment with ferrocene.

The effect of Ferrocene treatment on the normal cell line after 12 hours may be seen represented graphically in Figure 4.16. Here the drug's influence on DNA replication, recombination, and repair, cell cycle and tumour morphology networks is illustrated.
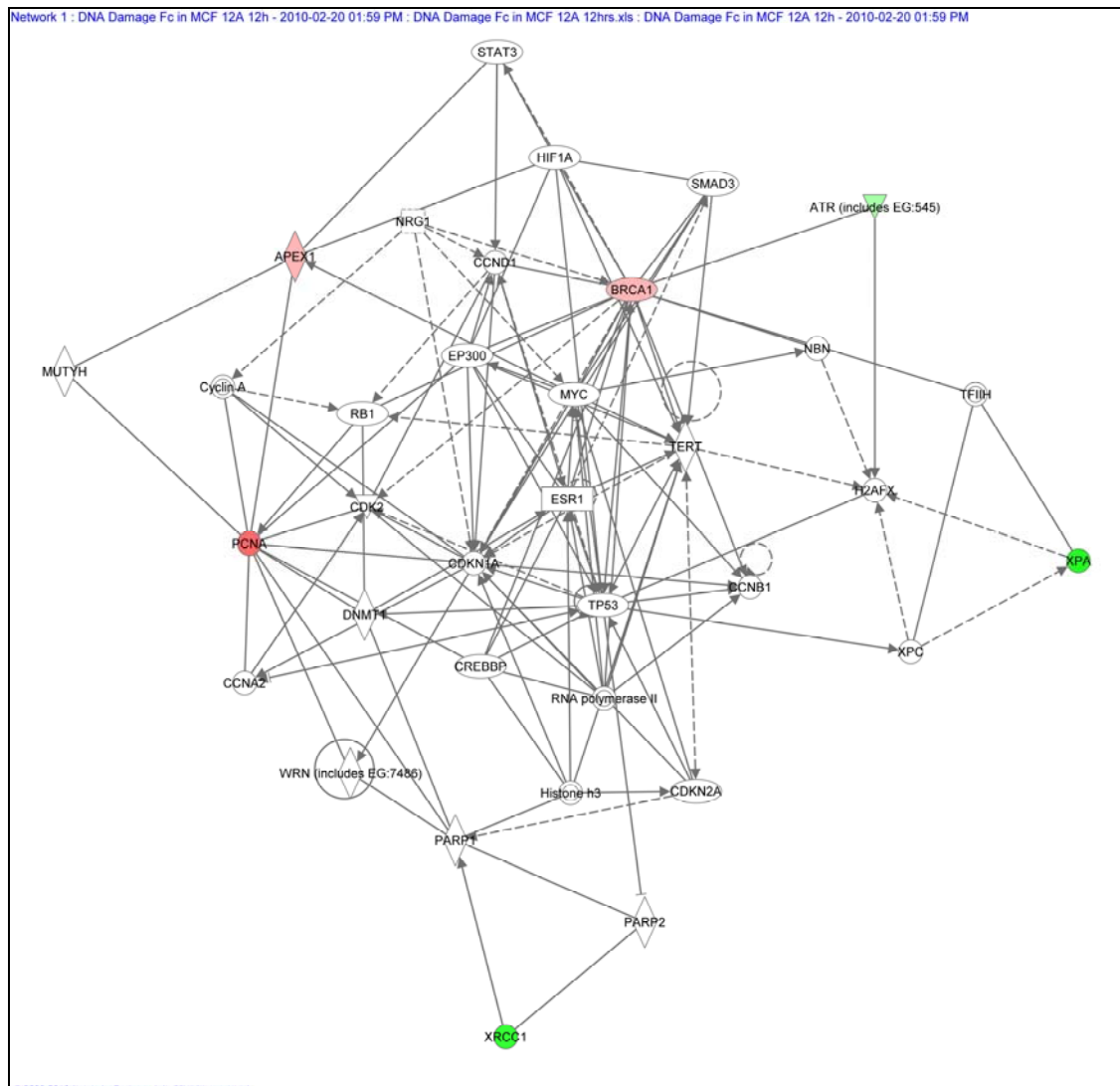
Figure 4.16: Gene network analysis of Ferrocene treated MCF-12A cells after 12 hours illustrating the influence on the DNA replication, recombination and repair and cell cycle gene expression* networks.

*Green highlighted genes indicate up-regulation whilst red highlighting indicates down-regulation. Solid lines indicate direct interaction whereas dashed lines represent indirect interaction.

The pathway analysis appears under represented with few genes pictured, yet it must be remembered that only a representative panel of marker genes were evaluated in the arrays, as opposed to whole genome analysis by microarray. Also, many software packages such as IPA would give multiple pathway outputs, even with just a single affected gene included, which may not be of statistical value. In the figure *XPA* is noted again and shows that excision repair is being attempted at this time point, as a result of drug treatment.

ATR is still up-regulated at 12 hours, which is indicative of continued checkpoint initiation and the maintenance of cell cycle arrest. *ATR* interacts indirectly with *XPA* through H2AFX, which is a histone protein family member. This protein associates with irradiation-induced double strand breaks and is part of the DNA repair program (OMOM *6011772).

The representation of the gene set however improves when considering the functions of the genes in the expression set. Gene relationships and associations may be summarised, using the "Your Favourite Gene" (Sigma) tool. The gene in question is described in the context of genes, proteins and molecules that it regulates, is regulated by and binds to. In addition to this the functionality within the cell is also listed (Appendix 4).

The expression data for Ferrocene, in both cell lines, at six and 12 hours was then compiled into the following summary (Table 4.9) to illustrate the differences and similarities between the cell lines' responses to Ferrocene treatment. This was done to enable convenient side by side comparisons, which is often not possible with gene tables or graphic pathway representations.

The normal cells affect an earlier gene expression response to the Ferrocene treatment whereas this occurs later in the cancerous cell line. There are noticeable similarities between the cell lines, regarding which genes are affected. Checkpoint initiation occurs in both cell lines and these data correlate well with flow cytometry data.

Table 4.9: Gene expression summary of MCF-7 and MCF-12A cells exposed to Ferrocene for six and twelve hours.*

Gene Name	Six Hours MCF-7	Twelve Hours MCF-7	Six Hours MCF-12A	Twelve Hours MCF-12A
Ankyrin repeat domain 17		2.25		
APEX nuclease (multifunctional DNA repair enzyme) 1				-3.57
Ataxia telangiectasia mutated	2.21			
Ataxia telangiectasia and Rad3 related		-2.87	2.87	2.13
Breast cancer 1, early onset				-3.59
CHK1 checkpoint homolog (S. pombe)		5.13		
Cell death-inducing DFFA-like effector a			2.60	2.71
DNA-damage-inducible transcript 3		2.74		
Fanconi anemia, complementation group G	-2.17		-3.27	
Flap structure-specific endonuclease 1		2.55	2.10	
X-ray repair complementing defective repair in Chinese hamster cells 6 (Ku autoantigen, 70kDa)		2.62		
Growth arrest and DNA-damage-inducible, alpha	2.30		2.84	
Growth arrest and DNA-damage-inducible, gamma		2.46		
General transcription factor IIH, polypeptide 1, 62kDa		2.66		
General transcription factor IIH, polypeptide 2, 44kDa		2.32	3.90	
G-2 and S-phase expressed 1	-2.43			-10.07
HUS1 checkpoint homolog (S. pombe)		-4.03		
Immunoglobulin mu binding protein 2				-2.13
Inositol hexaphosphate kinase 3				-4.14
XRCC6 binding protein 1	-2.50		2.59	
Mitogen-activated protein kinase 12		2.01		
MutL homolog 1, colon cancer, nonpolyposis type 2 (E. coli)			3.31	
Menage a trois homolog 1, cyclin H assembly factor (Xenopus laevis)		2.18		
N-methylpurine-DNA glycosylase		4.08		
Nth endonuclease III-like 1 (E. coli)				2.89
8-oxoguanine DNA glycosylase	-3.94		4.68	-2.36
Proliferating cell nuclear antigen	-6.11	-2.16		-7.40
Apoptosis-inducing factor, mitochondrion-associated, 1		2.69		
PMS1 postmeiotic segregation increased 1 (S. cerevisiae)			3.63	
PMS2 postmeiotic segregation increased 2 (S. cerevisiae)		3.95		
Polynucleotide kinase 3'-phosphatase			2.27	
RAD1 homolog (S. pombe)	-2.83			
RAD17 homolog (S. pombe)		3.58	3.68	
RAD18 homolog (S. cerevisiae)	2.54		2.66	
RAD51 homolog (RecA homolog, E. coli) (S. cerevisiae)		4.53		
RAD9 homolog A (S. pombe)		3.20		
Sema domain, immunoglobulin domain (Ig), transmembrane domain (TM) and short cytoplasmic domain, (semaphorin) 4A		-4.16	2.04	
Sestrin 1			2.00	
SMT3 suppressor of mif two 3 homolog 1 (S. cerevisiae)			4.84	
Three prime repair exonuclease 1	3.23		3.26	
Uracil-DNA glycosylase		-4.25		
Xeroderma pigmentosum, complementation group A		5.07		5.41
Xeroderma pigmentosum, complementation group C	3.07	-6.32	2.27	
X-ray repair complementing defective repair in Chinese hamster cells 1				4.87
X-ray repair complementing defective repair in Chinese hamster cells 3		-2.60		
Sterile alpha motif and leucine zipper containing kinase AZK		2.12		

*Text printed in green indicates greater than twofold up-regulation and text printed in red indicates greater than twofold down-regulation.

Although Ferrocene and Rhodium Ferrocene share structural similarity, their functional groups differ. It is therefore advisable to consider the drugs as separate entities when considering the cells' response. From this we can draw comparisons and infer the effect of the addition of the Rhodium moiety to the Ferrocene molecule. Table 4.10 depicts the gene expression data for MCF-7 cells exposed to Rhodium-ferrocene for six and twelve hours as related to mock-treated controls.

Table 4.10: DNA Damage Array relative expression data for Rhodium-ferrocene exposures of six and twelve hours in MCF-7 cells as compared to mock-treated controls.*

Gene Name	Gene Abbreviation	Fold Change
Six Hour Rhodium-ferrocene Treatment in MCF-7 Cells		
Ankyrin repeat domain 17	ANKRD17	2.12
Cell death-inducing DFFA-like effector a	CIDEA	4.60
Excision repair cross-complementing rodent repair deficiency, complementation group 1 (includes overlapping antisense sequence)	ERCC1	-2.29
X-ray repair complementing defective repair in Chinese hamster cells 6 (Ku autoantigen, 70kDa)	XRCC6	-2.27
Growth arrest and DNA-damage-inducible, gamma	GADD45G	4.07
Inositol hexaphosphate kinase 3	IHPK3	-5.21
Nedd4 binding protein 2	N4BP2	2.07
8-oxoguanine DNA glycosylase	OGG1	-3.06
Proliferating cell nuclear antigen	PCNA	-5.38
PMS2 postmeiotic segregation increased 2 (S. cerevisiae)	PMS2	-3.79
RAD1 homolog (S. pombe)	RAD1	-2.02
Retinoblastoma binding protein 8	RBPP8	3.82
Three prime repair exonuclease 1	TREX1	8.51
Xeroderma pigmentosum, complementation group C	XPC	-2.10
Twelve Hour Rhodium-ferrocene Treatment in MCF-7 Cells		
Ankyrin repeat domain 17	ANKRD17	2.16
BTG family, member 2	BTG2	-2.71
DNA-damage-inducible transcript 3	DDIT3	2.88
Excision repair cross-complementing rodent repair deficiency, complementation group 1 (includes overlapping antisense sequence)	ERCC1	-2.49
Flap structure-specific endonuclease 1	FEN1	4.53
Growth arrest and DNA-damage-inducible, gamma	GADD45G	7.27
Glycosylphosphatidylinositol anchored molecule like protein	GML	-11.95
G-2 and S-phase expressed 1	GTSE1	-4.61
HUS1 checkpoint homolog (S. pombe)	HUS1	-3.95
Inositol hexaphosphate kinase 3	IHPK3	-3.31
XRCC6 binding protein 1	XRCC6BP1	-2.20
Mitogen-activated protein kinase kinase 6	MAP2K6	6.95
Mitogen-activated protein kinase 12	MAPK12	2.69
Menage a trois homolog 1, cyclin H assembly factor (Xenopus laevis)	MNAT1	2.20
Proliferating cell nuclear antigen	PCNA	-3.83
Protein kinase, DNA-activated, catalytic polypeptide	PRKDC	-2.60
Sema domain, immunoglobulin domain (Ig), transmembrane domain (TM) and short cytoplasmic domain, (semaphorin) 4A	SEMA4A	-4.07
Sestrin 1	SESN1	2.03
Structural maintenance of chromosomes 1A	SMC1A	2.25
Tumor protein p53	TP73	-3.39
Three prime repair exonuclease 1	TREX1	-2.85
Uracil-DNA glycosylase	UNG	-4.17
Xeroderma pigmentosum, complementation group C	XPC	-4.61
X-ray repair complementing defective repair in Chinese hamster cells 3	XRCC3	-2.20
Sterile alpha motif and leucine zipper containing kinase AZK	ZAK	3.12

* Up-regulation is indicated by values in green whereas down-regulation is indicated by red text.

CIDEA (Cell death-inducing DFFA-like effector A), was found to be up-regulated after six hours of Rhodium-ferrocene treatment in MCF-7 cells. This protein has been found to activate apoptosis and induce DNA fragmentation (Inohara, 1998). Interestingly, although apoptosis appears to be initiated on a transcriptional level, it is not carried out, as seen by the cell death analysis by flow cytometry. This is most likely due to aberrations downstream of CIDEA. However, the cell's attempt to halt cell-cycle progression may be seen in the up-regulation of *GADD45G* at six hours and its continued up-regulation at 12 hours. The protein has been associated with G2/M arrest as well as apoptosis (Chung *et al.*, 2003). The *GADD45A* response seen in Ferrocene treatment appears to be absent in Rhodium-ferrocene treatment of the cancerous cells. *PMS2, XPC* and *OGG1*, which are up-regulated in Ferrocene treatment, are down-regulated by Rhodium-ferrocene. These proteins are associated with both DNA damage repair as well as DNA-damage-induced apoptosis. With that said however, *TREX1* is strongly up-regulated at six hours, which is indicative of 3'-exonuclease activity. The gene is then down-regulated at 12 hours which may indicate feedback inhibition.

FEN1, which is involved in DNA replication and has endonuclease activity is up-regulated. The protein also has a repair function in which 5-prime overhanging flaps are removed (Hosfield *et al.*, 1998). This may represent the cells' continued attempt to proceed with DNA synthesis in spite of damage, or, it may illustrate DNA repair. This would only be clear if protein associations are studied.

PCNA (proliferating cell nuclear antigen) which is part of the cyclin dependent kinase complex, is found to be markedly down-regulated in these data. This is indicative of cell cycle arrest. This is further substantiated by down-regulation of *GTSE1* which is found during the G2/M stage of the cell cycle. *HUS1*, coding for a protein involved in DNA damage checkpoints, on the other hand is down regulated. This may indicate further down-stream processing at 12 hours.

Interestingly a number of growth and division promoters are up-regulated at 12 hours. *MAP2K6* a mitogen activated kinase is markedly up-regulated. This protein is responsible for aspects of

cell signalling and compensating for certain environmental factors (Han *et al.*, 1996). Other signal transduction genes in the MAP kinase family are also up-regulated, such as *MAPK 12* and *ZAK*.

From these data we have found that Rhodium-ferrocene induces cell cycle arrest on a genetic level due to its DNA damaging properties. Repair mechanisms as a result of treatment are not as pronounced as in the case of Ferrocene, yet there are indications of excision repair initiation. This deficit in repair may serve to explain the higher toxicity level of Rhodium-ferrocene when compared to Ferrocene.

When evaluating the effect of Rhodium-ferrocene in MCF-7 from a pathway related standpoint, the involvement of multiple networks and signaling systems becomes apparent. Figure 4.17 illustrates the effect of six hours of treatment on DNA replication, recombination and repair and cell cycle networks. Once again, the centrality of p53 is noted. The gene is not differentially regulated; yet one could surmise that its effect is carried out on a protein level.

Figure 4.17: Gene network analysis of Rhodium-ferrocene treated MCF-7 cells after six hours illustrating the influence on the DNA replication, recombination and repair and cell cycle gene expression* networks.

*Green highlighted genes indicate up-regulation whilst red highlighting indicates down-regulation. Solid lines indicate direct interaction whereas dashed lines represent indirect interaction.

The figure shows a picture of general down-regulation, which is misleading, since many of the up-regulated genes are not included. This illustrates the fact that the drug affects multiple pathways within the cell.

116

TREX1 is up-regulated in the figure as was the case with earlier experiments (ferrocene treatment). The protein associates with the SET complex and has 3' exonuclease activity. The protein complex removes modified, mismatched, fragmented and normal nucleotides from the 3'-terminus as a part of DNA metabolism (Mazur and Perrino, 1999; Chowdhury *et al.*, 2006).

Genes associated with excision repair, such as *OGG1, XPC* and *XRCC6 are* down regulated in the figure. Either Rhodium-ferrocene induced damage is repaired through a different mechanism or the genomic insult is of such an extent that repair is not possible.

PCNA is strongly down-regulated at this point as has been the case with many of the previous experiments. The protein is associated with the CDK-complex and its down-regulation is associated with cell cycle arrest.

Following a 12 hour treatment of MCF-7 cells with Rhodium-ferrocene, the involvement of DNA replication, recombination and repair and cell cycle networks becomes clear (Figure 4.18).

Figure 4.18: Gene network analysis of Rhodium-ferrocene treated MCF-7 cells after 12 hours illustrating the influence on the DNA replication, recombination and repair and cell cycle gene expression* networks.

*Green highlighted genes indicate up-regulation whilst red highlighting indicates down-regulation. Solid lines indicate direct interaction whereas dashed lines represent indirect interaction.

TREX1 is down regulated at 12 hours (as opposed to up-regulation at six hours), which may be due to feedback inhibition. As mentioned earlier, *XPC* is down-regulated (Figure 4.17 and 4.18). The reason why excision repair is under represented in this treatment is unclear, but it may serve to highlight the difference in drug function between ferrocene and Rhodium-ferrocence.

DDIT3 which associated with endoplasmic reticulum stress (OMIM *126337) is up-regulated in the figure, which points to p53 involvement as a result of drug treatment.

Gene relationships and associations may be summarised, using the "Your Favourite Gene" (Sigma) tool. The gene in question is described in the context of genes, proteins and molecules that it regulates, is regulated by and binds to. In addition to this the functionality within the cell is also listed (Appendix 4).

As before, Rhodium-ferrocene induced changes in the normal cell line was explored to infer the response as well as illustrate differences when compared to the cancerous line. Table 4.11 illustrates the gene expression data for MCF-12A cells exposed to Rhodium-ferrocene for six and twelve hours as related to mock-treated controls.

Table 4.11: DNA Damage Array relative expression data for Rhodium-ferrocene exposures of six and twelve hours in MCF-12A cells as compared to mock-treated controls.*

Gene Name	Gene Abbreviation	Fold Change
Six Hour Rhodium-ferrocene Treatment in MCF-12A Cells		
Ataxia telangiectasia and Rad3 related	ATR	3.42
Alpha thalassemia/mental retardation syndrome X-linked (RAD54 homolog, S. cerevisiae)	ATRX	2.19
BTG family, member 2	BTG2	2.13
Cell death-inducing DFFA-like effector a	CIDEA	2.87
Fanconi anemia, complementation group G	FANCG	2.29
X-ray repair complementing defective repair in Chinese hamster cells 6 (Ku autoantigen, 70kDa)	XRCC6	2.84
Growth arrest and DNA-damage-inducible, gamma	GADD45G	2.06
Immunoglobulin mu binding protein 2	IGHMBP2	2.49
N-methylpurine-DNA glycosylase	MPG	5.71
Nibrin	NBN	2.90
8-oxoguanine DNA glycosylase	OGG1	3.07
PMS1 postmeiotic segregation increased 1 (S. cerevisiae)	PMS1	2.76
Protein kinase, DNA-activated, catalytic polypeptide	PRKDC	2.06
RAD18 homolog (S. cerevisiae)	RAD18	2.28
RAD50 homolog (S. cerevisiae)	RAD50	2.66
RAD9 homolog A (S. pombe)	RAD9A	2.03
SMT3 suppressor of mif two 3 homolog 1 (S. cerevisiae)	SUMO1	2.49
Twelve Hour Rhodium-ferrocene Treatment in MCF-12A Cells		
Ataxia telangiectasia mutated	ATM	2.79
Breast cancer 1, early onset	BRCA1	-2.96
Cyclin-dependent kinase 7	CDK7	2.53
Cell death-inducing DFFA-like effector a	CIDEA	2.28
Cryptochrome 1 (photolyase-like)	CRY1	3.03
X-ray repair complementing defective	XRCC6	2.51
Immunoglobulin mu binding protein 2	IGHMBP2	-2.84
Inositol hexaphosphate kinase 3	IHPK3	-3.42
Nth endonuclease III-like 1 (E. coli)	NTHL1	3.10
Proliferating cell nuclear antigen	PCNA	-3.68
Protein kinase, DNA-activated, catalytic polypeptide	PRKDC	-2.52
Three prime repair exonuclease 1	TREX1	-6.98

*Up-regulation is indicated by values printed in green whereas down-regulation is indicated by red text.

In MCF-12A cells exposed to Rhodium-ferrocene there is a marked trend towards transcriptional up-regulation. This is an energy dependant process and indicates active attempts to repair DNA damage.

Once again ATR is involved, as was the case with MCF-7 treatment, and as opposed to initial ATM up-regulation as a result of Ferrocene treatment. Interestingly *ATM* becomes up-regulated after 12 hours of treatment. A number of other similarities exist such as the up-regulation of

CIDEA and *GADD45G*, with *CIDEA* up-regulation continuing to 12 hours of exposure. This may represent the cells entry into the apoptotic program.

There are a number of marked reversals in behaviour though, such as the up-regulation of *OGG1* the DNA glycosylase, which is up-regulated at six hours. The protein removes 8-oxoguanine (8-oxoG), one of the major lesions in DNA induced by reactive oxygen species (Lu *et al.,* 1997). This shows the chemical reactivity of the drug in normal cells inducing free-radical-based damage to DNA. *MPG* (3- methyladenine DNA glycosylase) is strongly up-regulated at six hours. The protein removes damaged DNA bases such as cytotoxic and mutagenic alkylation adducts of purines (Lau *et al.,* 1998). From this, the molecular activity from both drugs appears to be the induction of ionisation based damage to DNA as well as bound aberrant DNA adducts.

Besides effect on purines, it appears that treatment with Rhodium-ferrocene at 12 hours increases *NTHL1* expression. This endonuclease plays a part in DNA base excision repair and has been found to remove oxidised ring saturated pyrimidine residues (Ocampo et al., 2002).

A marked difference at six hours is the involvement of the RAD proteins (RAD18, 50 and 9A). These proteins, as described earlier, are involved in the mediation of DNA damage repair complexes.

When MCF-12A cells are treated with Rhodium-ferrocene for six hours DNA replication, recombination and repair, cell cycle and gene expression networks are once again extensively affected (Figure 4.19).
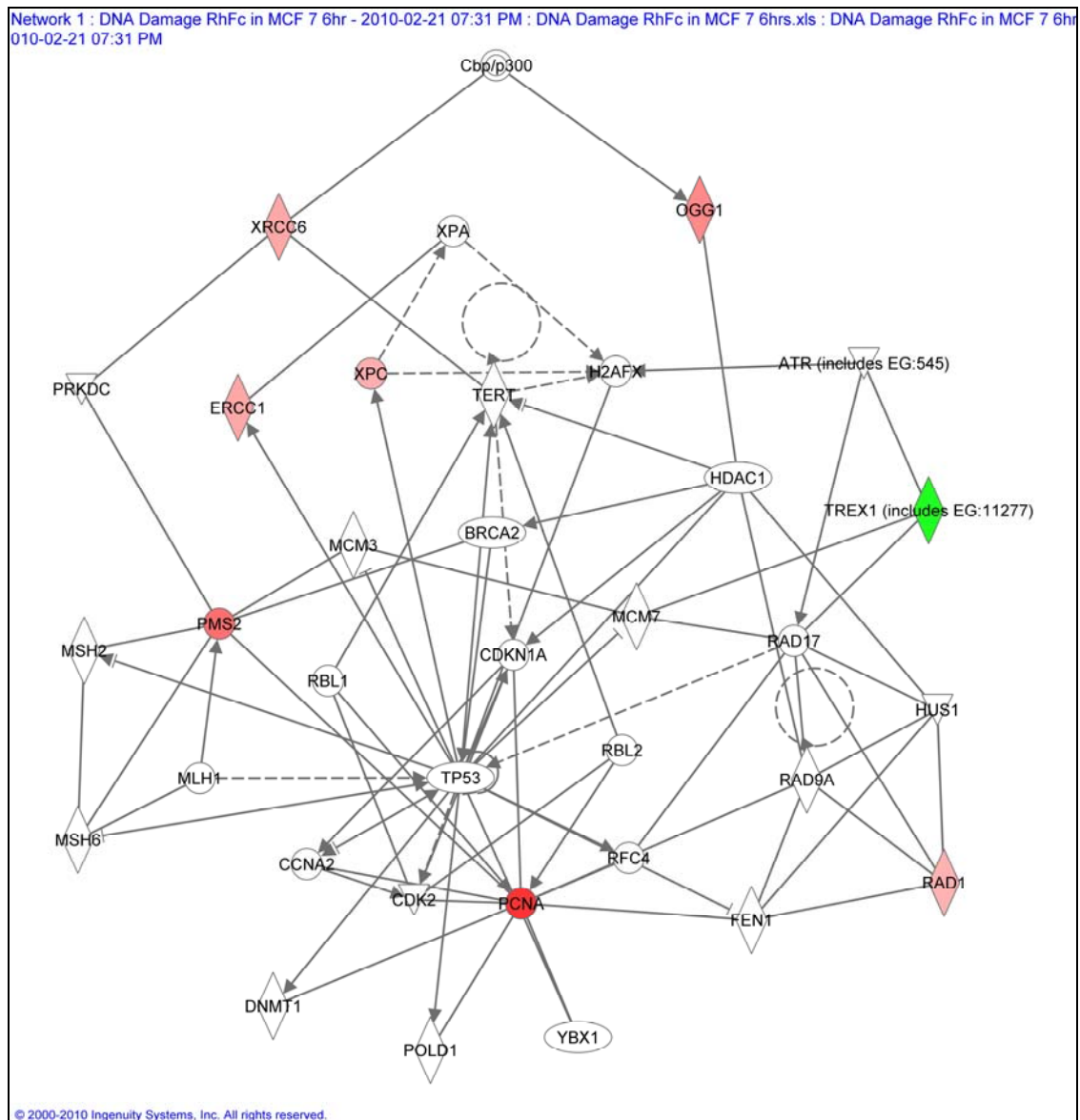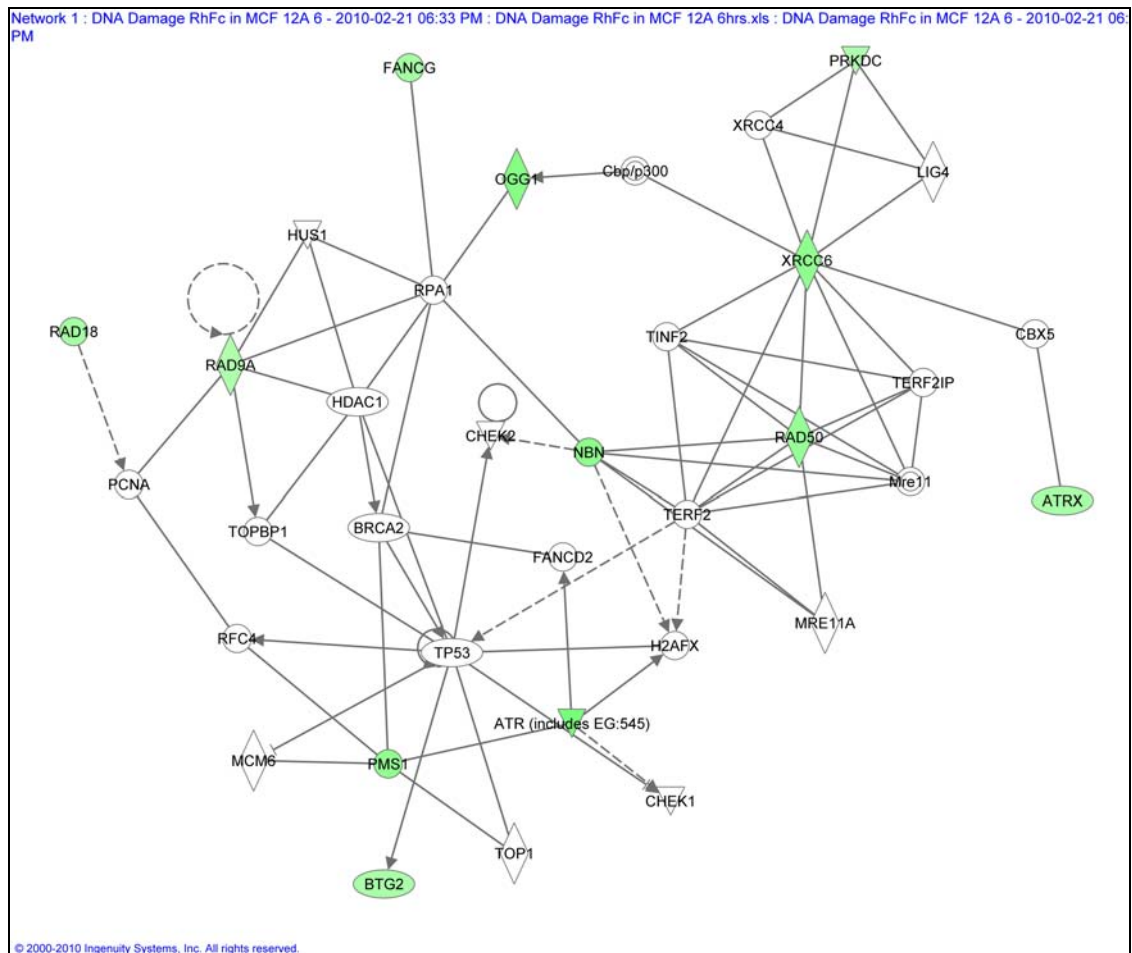
Figure 4.19: Gene network analysis of Rhodium-ferrocene treated MCF-12 cells after six hours illustrating the influence on the DNA replication, recombination and repair and cell cycle gene expression* networks.

*Green highlighted genes indicate up-regulation whilst red highlighting indicates down-regulation. Solid lines indicate direct interaction whereas dashed lines represent indirect interaction.

A picture of up-regulation is seen (Figure 4.19) which could indicate the activation of a functional DNA damage detection and repair response, which is lacking in the cancerous cell line. p53 is central to this process and it is noteworthy that aspects of the DNA damage checkpoints are initiated. This correlates well with the flow cytometry data and is indicative of the cells' attempt to repair damage prior to progressing through the cell cycle.

ATR is up-regulated in the figure which serves to highlight checkpoint initiation and the subsequent cell cycle arrest. Repair mechanisms, driven by genes such as *OGG1* and *XRCC6* are also evident in the figure.

The effect of Rhodium-ferrocene treatment on the normal cell line after 12 hours may be represented graphically from a systems network perspective (Figure 4.20), in which various aspects of DNA damage and detection pathways are involved.
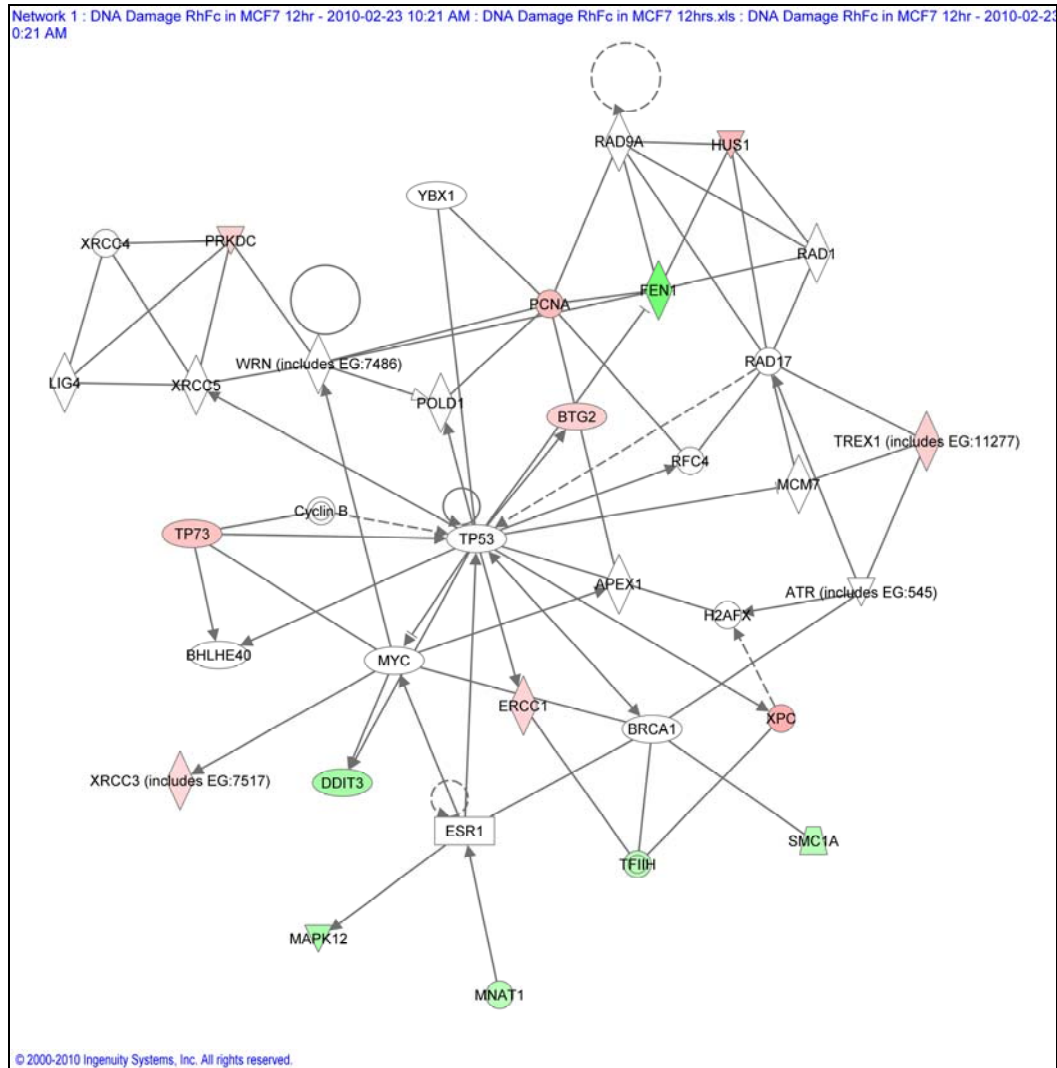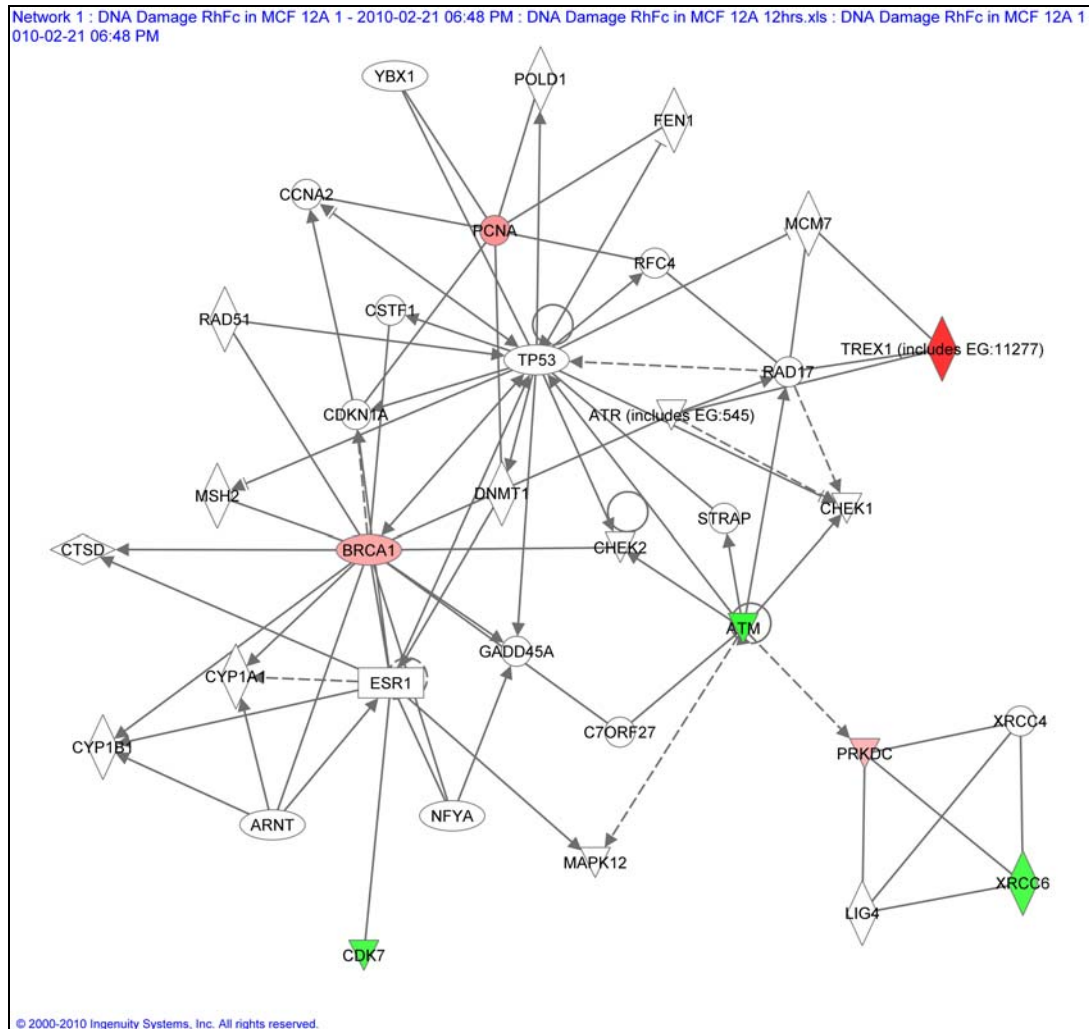

Figure 4.20: Gene network analysis of Rhodium-ferrocene treated MCF-12 cells after 12 hours illustrating the influence on the DNA replication, recombination and repair and cell cycle gene expression* networks.

*Green highlighted genes indicate up-regulation whilst red highlighting indicates down-regulation. Solid lines indicate direct interaction whereas dashed lines represent indirect interaction.

In the figure *ATM*-mediated regulation is shown as opposed to the *ATR*-driven checkpoints of Figure 4.19 at six hours. At the 12 hour treatment interval, the checkpoint mediators such as ATM are still upregulated. This shows that a prolonged effort to halt the cell cycle is carried out

by the "normal" cell line. At this point, the cancerous cell has entered a necrotic cell death program, while the "normal" cell line has not.

Down regulation of *PCNA* at 12 hours is indicative of the cells' attempt to halt cell cycle progression at the G1/S and G2/M interface. This substantiates what was found in the flow cytometry data.

It is likely that MCF-12A cells will succumb to the drugs through necrosis, yet from the data it seems this process takes longer than in the cancerous cell line. More robust arrest and repair mechanisms are in place in the "normal" cell line as well as functional apoptotic machinery. There have been indications of apoptotic initiation from the gene expression data, but it would most likely result in necrosis.

Gene relationships and associations may be summarised, using the "Your Favourite Gene" (Sigma) tool. The gene in question is described in the context of genes, proteins and molecules that it regulates, is regulated by and binds to. In addition to this the functionality within the cell is also listed (Appendix 4). The data was then compiled into a summary format (Table 4.12) to illustrate the difference between the cell lines' responses to the drug.

Table 4.12: Gene expression summary of MCF-7 and MCF-12A cells exposed to Rhodium-ferrocene for six and twelve hours.*

Gene Name	Six Hours MCF-7	Twelve Hours MCF-7	Six Hours MCF-12A	Twelve Hours MCF-12A
Ankyrin repeat domain 17	2.12	2.16		
Ataxia telangiectasia mutated				2.79
Ataxia telangiectasia and Rad3 related			3.42	
Alpha thalassemia/mental retardation syndrome X-linked (RAD54 homolog, S. cerevisiae)			2.19	
Breast cancer 1, early onset				-2.96
BTG family, member 2		-2.71	2.13	
Cyclin-dependent kinase 7				2.53
Cell death-inducing DFFA-like effector a	4.60		2.87	2.28
Cryptochrome 1 (photolyase-like)				3.03
DNA-damage-inducible transcript 3		2.88		
Excision repair cross-complementing rodent repair deficiency, complementation group 1	-2.29	-2.49		
Fanconi anemia, complementation group G			2.29	
Flap structure-specific endonuclease 1		4.53		
X-ray repair complementing defective repair in Chinese hamster cells 6 (Ku autoantigen, 70kDa)	-2.27		2.84	2.51
Growth arrest and DNA-damage-inducible, gamma	4.07	7.27	2.06	
Glycosylphosphatidylinositol anchored molecule like protein		-11.95		
G-2 and S-phase expressed 1		-4.61		
HUS1 checkpoint homolog (S. pombe)		-3.95		
Immunoglobulin mu binding protein 2			2.49	-2.84
Inositol hexaphosphate kinase 3	-5.21	-3.31		-3.42
XRCC6 binding protein 1		-2.20		
Mitogen-activated protein kinase kinase 6		6.95		
Mitogen-activated protein kinase 12		2.69		
Menage a trois homolog 1, cyclin H assembly factor (Xenopus laevis)		2.20		
N-methylpurine-DNA glycosylase			5.71	
Nedd4 binding protein 2	2.07			
Nibrin			2.90	
Nth endonuclease III-like 1 (E. coli)				3.10
8-oxoguanine DNA glycosylase	-3.06		3.07	
Poly(rC) binding protein 4				
Proliferating cell nuclear antigen	-5.38	-3.83		-3.68
PMS1 postmeiotic segregation increased 1 (S. cerevisiae)			2.76	
PMS2 postmeiotic segregation increased 2 (S. cerevisiae)	-3.79			
Protein kinase, DNA-activated, catalytic polypeptide		-2.60	2.06	-2.52
RAD1 homolog (S. pombe)	-2.02			
RAD18 homolog (S. cerevisiae)			2.28	
RAD50 homolog (S. cerevisiae)			2.66	
RAD9 homolog A (S. pombe)			2.03	
Retinoblastoma binding protein 8	3.82			
Sema domain, immunoglobulin domain (Ig), transmembrane domain (TM) and short cytoplasmic domain, (semaphorin) 4A		-4.07		
Sestrin 1		2.03		
Structural maintenance of chromosomes 1A		2.25		
SMT3 suppressor of mif two 3 homolog 1 (S. cerevisiae)			2.49	
Tumor protein p73		-3.39		
Three prime repair exonuclease 1	8.51	-2.85		-6.98
Uracil-DNA glycosylase		-4.17		
Xeroderma pigmentosum, complementation group C	-2.10	-4.61		
X-ray repair complementing defective repair in Chinese hamster cells 3		-2.20		
Sterile alpha motif and leucine zipper containing kinase AZK		3.12		

*Text printed in green indicates greater than twofold up-regulation and text printed in red indicates greater than twofold down-regulation.

Rhodium-ferrocene treated MCF-7 and MCF-12A cells show a clear DNA damage response. As stated previously, the cells were not synchronised. Therefore the data presents a mixed picture of the responses of various populations at different stages of the cell cycle. Certain replication inducing factors are up-regulated and may obfuscate the original intention of displaying the drug's inhibitory properties, but it must be borne in mind that these responses may be those of cells that have repaired the damage and proceeded with replication.

Although Ferrocene showed a clear picture of nuclear excision repair in both cell lines, this was not seen to such a large extent in Rhodium-ferrocene treated cells. With that said however, this pattern was still detected to some extent. Due to its increased toxicity, Rhodium-ferrocene may induce irreparable damage to the large majority of the population.

Many authors compare a treated experiment versus a mock-treated control in order to illustrate expression change as has been shown previously. It was however felt that a greater depth of understanding may be gained by viewing a change over time. To accomplish this we compare, in Table 4.13, the gene expression changes between six and 12 hours for the mock-treatment as related to the change between six and twelve hours for the treated cells. If the drugs had no effect one would expect the difference between the control expression change over time and the treatment expression change over time to be negligible. Viewing data in this way enables us to identify genes that are not up-regulated or down-regulated as they should be over time. Furthermore this approach may be explained as follows using a hypothetical example: if a gene is up-regulated at six hours in the treated population, and stays stable until 12 hours, while the expression of the gene increases in the mock-treated cells over time, it would appear that the gene is not differentially regulated at 12 hours (if this time point is considered separately from the earlier treatment). This conclusion would be false since the hypothetical gene is still being expressed, but its expression did not increase over time and the mock-treated expression has increased to match it. Alternatively, if the expression in the mock-treated sample decreased over time, and the treated sample stayed stable, there would be a false impression of gene activation (up-regulation). When expression data for *ATR* is considered, we see that expression

increases over time in mock-treated MCF-7 cells, but stays stable in Ferrocene and Rhodium-ferrocene treatment. This is reflected as down regulation when MCF-7 cells are exposed for 12 hours to Rhodium-ferrocene.

Table 4.13: A comparison between gene expression change from six to twelve hours for controls, Ferrocene (Fc) treatment and Rhodium-ferrocene (Rh) treatment in MCF-7 and MCF-12A cells.*

	MCF-7, 6hrs Control vs. MCF-7,12hrs Control	MCF-7,6hrs Fc vs. MCF-7,12hrs Fc	MCF-7, 6hrs Rh vs. MCF-7, 12hrs Rh	MCF-12A, 6hrs Control vs. MCF-12A, 12hrs Control	MCF-12A, 6hrs Fc vs. MCF-12A, 12hrs Fc	MCF-12A, 6hrs Rh vs. MCF-12A, 12hrs Rh
ABL1	1.16	-6.76	1.39	-1.05	-1.58	1.05
ANKRD17	-2.44	-2.63	-2.72	1.53	1.46	1.35
APEX1	1.16	-2.07	-1.66	1.98	-2.61	2.18
ATM	1.41	-2.99	-1.93	-1.05	-1.06	1.80
ATR	5.38	-1.65	1.64	-1.12	-1.19	-2.70
ATRX	1.09	-1.53	-1.13	1.30	1.17	-1.41
BRCA1	1.59	-1.33	2.44	3.18	-1.35	1.05
BTG2	2.48	2.13	-2.21	-1.05	1.48	-1.84
CCNH	-3.06	-4.45	-4.40	2.02	2.64	1.65
CDK7	1.16	-1.33	-1.07	-1.38	-1.14	1.63
CHEK1	1.16	4.98	1.18	-1.05	-1.06	1.05
CHEK2	1.16	-1.33	1.18	-1.05	-1.42	1.05
CIB1	1.29	-1.33	1.18	-1.05	-1.06	1.05
CIDEA	1.08	-1.85	-2.69	2.49	3.30	2.14
CRY1	-2.33	-2.39	-1.93	1.18	1.13	3.31
DDB1	1.16	-1.33	1.18	1.21	-1.06	1.63
DDIT3	-2.43	-1.70	-1.20	1.35	2.63	1.72
DMC1	1.16	1.92	1.18	-1.05	-1.06	1.05
ERCC1	1.54	-1.82	1.24	2.08	2.95	1.13
ERCC2	-3.03	-3.06	-1.65	1.56	1.92	1.44
EXO1	1.16	-1.33	-1.10	-1.25	-1.06	1.05
FANCG	1.19	1.45	1.35	1.16	5.29	-1.71
FEN1	-4.99	-3.77	-1.15	1.49	-1.22	1.08
XRCC6	-1.15	2.32	1.10	-1.81	-1.02	-1.89
GADD45A	1.23	-5.70	-1.70	3.74	1.19	1.44
GADD45G	-2.29	-3.04	-1.45	1.01	1.19	-1.40
GML	82.13	-1.30	6.40	-1.60	-1.06	1.05
GTF2H1	-5.17	-2.98	-4.49	1.25	1.90	1.22
GTF2H2	-2.30	-1.18	-1.58	2.36	-1.44	-1.14
GTSE1	2.03	-1.23	-2.77	2.63	-1.84	1.49
HUS1	3.62	-1.33	1.18	-1.05	-1.22	1.05
IGHMBP2	1.16	-1.26	-1.22	2.78	-1.14	-2.36
IHPK3	-1.83	-2.38	-1.32	-2.01	-6.33	-4.68
XRCC6BP1	1.37	3.67	-1.74	1.99	-1.06	1.06
LIG1	1.16	-1.33	1.18	-1.05	-1.06	1.05
MAP2K6	1.16	-1.33	10.35	-1.05	-1.06	1.05

127

	MCF-7, 6hrs Control vs. MCF-7,12hrs Control	MCF-7,6hrs Fc vs. MCF-7,12hrs Fc	MCF-7, 6hrs Rh vs. MCF-7, 12hrs Rh	MCF-12A, 6hrs Control vs. MCF-12A, 12hrs Control	MCF-12A, 6hrs Fc vs. MCF-12A, 12hrs Fc	MCF-12A, 6hrs Rh vs. MCF-12A, 12hrs Rh
MAPK12	-1.72	**-2.81**	-1.43	1.19	1.74	**2.37**
MBD4	-1.82	**-2.16**	-1.90	1.17	1.48	1.46
MLH1	1.16	-1.33	1.42	-1.05	**-2.94**	1.05
MLH3	-1.26	**-5.26**	**-2.30**	1.50	1.24	1.40
MNAT1	**-3.65**	**-3.64**	**-2.72**	1.51	1.80	1.23
MPG	1.34	**6.08**	1.31	1.12	1.49	**-3.91**
MRE11A	-1.15	1.09	1.49	1.04	**-2.23**	-1.19
MSH2	**-2.13**	**-3.55**	**-4.26**	1.56	1.69	1.35
MSH3	1.16	-1.33	1.18	-1.05	-1.06	1.05
MUTYH	1.16	-1.33	1.18	-1.05	-1.06	1.05
N4BP2	-1.93	**-3.45**	**-3.41**	1.67	1.21	1.33
NBN	1.16	-1.33	1.18	1.12	1.36	**-2.51**
NTHL1	1.36	**2.10**	**2.17**	-1.05	**2.95**	**2.88**
OGG1	**-3.92**	1.08	-1.84	**2.09**	**-4.15**	**-2.50**
PCBP4	1.16	-1.33	-1.14	-1.05	1.44	1.29
PCNA	-1.41	1.21	-1.14	**2.70**	**-4.04**	-1.66
AIFM1	**-2.58**	**-2.32**	-1.59	1.71	1.04	1.42
PMS1	1.04	**-6.27**	-1.24	1.74	1.03	1.09
PMS2	**-2.64**	-1.01	**2.19**	-1.26	1.26	-1.33
PMS2L3	1.16	-1.33	1.18	-1.05	-1.22	-1.54
PNKP	-1.60	**-2.27**	-1.05	1.75	1.26	1.40
PPP1R15A	1.16	-1.33	1.18	-1.05	-1.06	1.05
PRKDC	1.81	-1.56	**-2.36**	**2.64**	-1.09	-1.83
RAD1	**-2.11**	-1.33	-1.49	-1.05	-1.38	1.42
RAD17	1.16	1.69	1.18	-1.05	**-3.27**	1.05
RAD18	1.22	**-3.51**	1.68	1.99	-1.23	1.05
RAD21	1.16	-1.33	1.18	-1.05	-1.31	1.05
RAD50	1.16	-1.33	-1.48	1.19	-1.06	**-2.30**
RAD51	1.16	**4.40**	1.18	-1.05	-1.06	1.05
RAD51L1	**-2.45**	**-3.60**	**-2.13**	1.73	1.22	1.48
RAD9A	1.16	**3.11**	1.18	-1.05	-1.06	-1.76
RBBP8	1.16	-1.58	**-4.73**	1.93	1.30	1.28
REV1	1.16	-1.33	1.18	-1.05	-1.06	1.05
RPA1	1.27	-1.33	1.18	1.33	-1.25	1.05
SEMA4A	**3.74**	-1.33	-1.00	1.67	-1.81	1.23
SESN1	**-2.10**	**-4.18**	-1.65	-1.12	-1.16	**2.13**
SMC1A	**-2.61**	**-2.95**	-1.87	1.29	1.51	1.50
SUMO1	1.50	-1.79	1.10	**3.14**	-1.50	1.32
TP53	1.16	-1.33	1.18	-1.05	-1.06	1.05
TP73	**3.11**	1.32	1.18	-1.07	-1.14	-1.34
TREX1	**3.57**	**-6.91**	**-7.75**	**4.35**	1.39	-1.45
UNG	**3.82**	-1.33	1.18	-1.05	-1.06	1.05
XPA	1.16	**4.92**	1.18	-1.05	**5.51**	1.05
XPC	**2.29**	**-6.55**	-1.09	**2.92**	1.94	1.67
XRCC1	1.16	-1.33	1.18	-1.05	**4.18**	1.05

128

	MCF-7, 6hrs Control vs. MCF-7,12hrs Control	MCF-7,6hrs Fc vs. MCF-7,12hrs Fc	MCF-7, 6hrs Rh vs. MCF-7, 12hrs Rh	MCF-12A, 6hrs Control vs. MCF-12A, 12hrs Control	MCF-12A, 6hrs Fc vs. MCF-12A, 12hrs Fc	MCF-12A, 6hrs Rh vs. MCF-12A, 12hrs Rh
XRCC2	1.16	-1.33	1.18	-1.05	-1.06	1.05
XRCC3	2.84	-1.46	2.00	-1.34	1.54	-1.01
ZAK	-2.88	-2.73	-1.22	-1.09	1.36	1.49
B2M	1.16	-1.33	1.18	-1.05	-1.06	1.05
HPRT1	-2.38	-3.84	-2.81	1.22	1.98	1.29
RPL13A	1.54	-1.33	-1.01	-1.05	-1.06	1.05
GAPDH	1.16	8.95	1.11	-1.05	-1.06	1.05
ACTB	1.16	-1.33	2.18	-1.05	-1.68	-1.48

*Text printed in green indicates up-regulation and text printed in red indicates down-regulation.

From these data it is clear that the drugs not only affect expression when compared to control experiments, the rate and extent of change in expression between the treated samples is also affected. In addition to this the similarities of the unaffected genes are an indication of the robustness of the experiment. It shows that perturbations are a result of treatment and not experimental bias. There are a number of extreme outliers, though, which arise as a result of comparing a state of near zero expression (very high Ct values) to a state of expression (lower Ct values). This is an artefact of the analysis methodology.

The pathway graphics presented here it may appear that the pathways are under-represented, yet it must be remembered that only a panel of candidate genes were used for the analyses as opposed to a whole genome micro-array approach. When we compare the vast amount of pathway and functionality data generated from these few genes one sees the value of using representative candidates. One may only imagine the systems biology challenge to properly evaluate a microarray-based system for a similar experiment.

CHAPTER 5: CONCLUSIONS

Metallocene drugs have been used successfully as chemotherapeutic agents for a number of years. With that said though, these compounds do induce a number of severe side effects such as nephrotoxicity. In addition to this, their effects on general metabolism and cellular processes are still not fully understood. This has prompted the need for the development of other organometallic compounds with fewer side effects for the effective treatment of cancer. It is essential that a compound's mechanism of action is fully understood, prior to the onset of clinical trials, in order to predict possible side effects as well as efficacy. With this in mind, two novel chemotherapeutic compounds that were previously found to show promise as possible "new" drugs were investigated in this study.

The effects of two novel organometallic drugs, Ferrocene [ferrocenoyltrichloroacetone] and Rhodium-ferrocene [(1.5 cyclooctadiene)(1-ferrocenyl-4,4,4-trichloro- 1,3 butanedionate], on a transformed "normal" breast epithelial cell line (MCF-12A) and a cancerous breast epithelial cell line (MCF-7) were examined.

Due to the structure of the drugs it was expected that they would interact with or affect the cells' DNA, as is the case with similar organometallic compounds (e.g. cisplatin). This was shown to be true as an interaction between the drugs and naked, linearised, DNA at a specific residue (the PstI restriction site – CTGCAG) was found *in vitro*. This is indicative of a level of specificity, where in many cases this class of drug has a relatively broad mechanism of action.

It was then shown that as a result of drug exposure, progression through the cell cycle was affected. Most noticeably, a G1/S phase delay was caused by the two drugs in the normal cell line. A similar delay was present in the cancerous cell line, but to a much lesser extent. The observed S-phase arrest is indicative of the cells' inability to continue DNA synthesis and cell division, as a result of drug treatment. Cell cycle checkpoints are initiated, due to a genomic insult, and the cell attempts to affect a DNA repair program before normal cycling can proceed.

If repair is not possible the cell would then enter a cell death phase. The fact that the S-phase cell cycle inhibition occurred proves that the compounds are able to enter the cell and cross the cells' nuclear membrane to interact with intact natural DNA.

Continuing on a cellular level it was demonstrated that the drugs induced necrotic cell death in the cancerous cell line. This is usually a hallmark of a major metabolic catastrophe, which is often characterized by the production of reactive oxygen species, the activation of JNK (Jun N-terminal kinase) and/or PARP; which have been shown (Proskuryakov *et al.,* 2003; Festjens *et al.*, 2006; Zong *et al.*, 2004), to cause necrotic cell death in response to DNA damage. These results point to the wide ranging damage induced by the drugs, leading to the cell's inability to initiate a metabolically controlled cell-death program.

Cell-cycle based gene expression arrays containing DNA-damage specific genes as well as cell cycle control genes were used to investigate which pathways were involved in the observed cell cycle disruption. These showed an up-regulation of members of the *RAD* gene family (DNA damage related) and a down regulation of cyclins (associated with the inhibition of cell division). This clearly indicates the DNA damaging effect of the drugs, as well as attempts by the cell to halt cell cycle progression as a result of DNA damage.   These gene changes led us to focus specifically on DNA-damage related gene expression, through the use of gene array panels.

Generalized perturbations in the DNA-damage and repair mechanisms of the exposed cells were found. It was determined that Ferrocene elicited a strong excision repair response in both cell lines with up-regulation of genes such as *GADD45A, XPC* and *OGG1*. This could be expected as it was shown that Ferrocene binds to DNA, and it logically then follows that this would lead to excision repair being attempted. *GADD45A* is also associated with S-Phase arrest, which was highlighted during cell cycle analysis. The common DNA damage associated checkpoint genes (*ATM, ATR* and *CHEK1*) were initiated and the various effects the drug has on DNA metabolism, as shown by previous experiments, were validated.

Rhodium-ferrocene was found to be more toxic than Ferrocene in both cell lines. It also elicited a greater cellular response. The transcriptional response as a result of treatment showed similar mechanisms to Ferrocene, yet less pronounced excision repair. With that said though, genes associated with excision repair such as *TREX1* and *OGG1* that were up-regulated as a result of Ferrocene treatment were also differentially regulated in the case of Rhodium-ferrocene treatment. The larger molecule may not bind DNA *in vitro* as effectively as Ferrocene, due to steric hindrance, and may impart its toxicity by another (or additional) mechanism.

In this study, it has been revealed on every level that both Ferrocene and Rhodium-ferrocene damage DNA. This property validates the original hypothesis of the thesis and indicates that the main cytotoxicity of both drugs is due to their interaction with the cell's genome. The exact molecular interaction of the drugs has yet to be proven conclusively. Although we showed that the drugs do bind DNA, their free radical properties cannot be discounted. This is apparent in the number of ionization-induced DNA damage genes that were found to be dysregulated. These genes are associated with the recognition and repair of free radical induced DNA damage and strand breaks. The possibility does exist though that the drugs have a dual function: DNA damage by adduction and alkylation, as well as free radical-based damage. The free radical effect that these drugs may have on other components of the cell should not be discounted. Neuse (2005) outlined the interaction between the ferrocene ion and various proteins such as the topoisomerases which are involved in DNA synthesis and topology. This illustrates an indirect effect on DNA, through the inhibition of enzymes involved in DNA structure.

This concept of the interrelatedness between the drugs' effect on DNA as well as proteins associated with DNA synthesis and structure highlights the need to evaluate novel drug candidates using a systems biology approach. Each target must be considered within the context of genes or proteins that regulate it or that are regulated by the target. This may be achieved through the creation of gene/protein pathway networks (as seen in this work); which prove their utility by illustrating the diverse effect of the drugs in a concise manner.

Through this work and others like it, the importance of Systems Biology becomes apparent. Focusing on a single aspect of the cell such as gene expression may be counterproductive in furthering one's understanding of the drug's mechanism of action. The cascading, as well as the unique effects of a molecule on the genomic, proteomic and metabolomic regulation of the cell should be explored. The data generated from such an exercise would be vast, but, it would give a clearer picture of mechanisms of action. In addition to this, the interpretation of data should be considered. Describing individual gene functions in the context of a large gene panel is not always possible. Due to multiple evolutionary redundancies and multiple protein functions within the cell, relying on descriptions of single genes affected may confuse the reality of a molecule's function. Therefore, in this work, although single genes were considered, from a functional perspective; greater emphasis was placed on pathways as well as the networks that are influenced as a result of drug treatment. Computational analysis of pathway perturbations may prove to be more accurate in predicting a molecule's mechanism of action if the functionality of an affected gene, or pathway, is considered in the context of a system.

From these data the cellular and molecular effects of Ferrocene and Rhodium-ferrocene on a normal and cancerous cell line were shown. However, there are a plethora of avenues that still require exploration; that are unfortunately beyond the scope of this research. We have shown direct changes in transcription but have not explored post translational regulation such as protein phosphorylation. This type of signaling occurs without changes in gene expression or the subsequent protein concentration. It may occur seconds after exposure and represents an energy efficient method of cell signaling that should be explored in depth.

Finally, the metabolomic effect of the drugs should be explored. These changes can be seen as the endpoint of transcriptional and proteomic changes. The multiplicity of metabolic pathways and their interactions within and between cells would present a behemoth challenge computationally; yet it would give the final answer in terms of a drug's function.

CHAPTER 6: REFERENCES

1. Bakay, M., *et al.,* 2002, Sources of variability and effect of experimental approach on expression profiling data interpretation, *BMC Bioinformatics*, 3: 4.

2. Bakkenist, C., Kastan, M., 2003, DNA damage activates ATM through intermolecular autophosphorylation and dimmer dissociation, *Nature,* 421: 499-506.

3. Banda, M., *et al.,* 2008, Evaluation and validation of housekeeping genes in response to ionizing radiation and chemical exposure for normalizing RNA expression in real-time PCR, *Mutation Research,* 649: 126-134.

4. Barradas, M., Monjas, A., Diaz-Mecco, M., Serrano, M., Moscat, J., 1999, The down-regulation of the pro-apoptotic protein Par-4 is critical for Ras-induced survival and tumour progression, *EMBO J.,* 18: 6362-6369*.*

5. Baguley, B., 2010, Multidrug resistance in cancer, *Biomedical and Life Sciences*, 596: 1-14.

6. Bonni, A., *et al.*, 1999, Cell survival promoted by the ras-MAPK signalling pathway by transcription dependant and independent mechanisms, *Science*, 286: 1358-1362.

7. Borst, P., *et al.*, 2000, A family of drug transporters: the multidrug resistance-associated proteins, *J.Natl. Cancer Inst.*, 92: 1295-1302.

8. Borst, P. and Rottenberg, S., 2004, Cancer cell death by programmed necrosis?, *Drug resistance updates,* 7: 321-324.

9. Boyd, M., Paull, K.D., 1995, Some practical considerations and applications of the National Cancer Institute in vitro drug discovery screen, *Drug Development Research*, 34: 91-109.

10. Braylan, R.C., Benson, N.A., Nourse, V., Kruth, H.S., 1982, Correlated analysis of cellular DNA, membrane antigens, and light scatter of human lymphoid cells, *Cytometry,* 2: 337-343.

11. Bredemeyer, A. L., 2006, ATM stabilizes DNA double-strand-break complexes during V(D)J recombination, *Nature,* 442: 466-470.

12. Bredel, M., Jacoby, E., 2004, Chemogenomics an emerging strategy for rapid target and drug discovery, *Nat Rev*, 5: 262-275.

13. Brown, E.J., Baltimore, D., 2003, Essential and disposable roles of ATR in cell cycle arrest and genome maintenance, *Gen. Dev.*, 17: 615-628.

14. Brown, T. A., (Ed.) Genomes, 2nd ed., Wiley (2002) New York.

15. Browne, L., *et al.*, 2002, Chemogenomics-pharmacology with genomic tools, *Targets*, 1: 59-65.

16. Burkhart, C.A., 2001, The role of beta-tubulin isotypes in resistance to antimitotic drugs, *Biochem. Biophys. Acta*, 1471: O1-O9.

17. Busino, L., *et al.,* 2003, Degradation of Cdc25A by β-TrCP during S phase and in response to DNA damage, *Nature,* 426: 87-91.

18. Carson, P. R., *et al.*, 2001, Chemogenomic approaches to drug discovery, *Current Opinion in Chemical Biology*, 5: 464-470.

19. Cheung, C., *et al.,* 2010, Cancer cells acquire mitotic drug resistance properties through beta tubulin mutations and alterations in the expression levels of beta tubulin isotypes, *PloS one*, 5: e12564.

20. Chowdhury, D., *et al.*, 2006, The exonuclease TREX1 is in the SET complex and acts in concert with NM23-H1 to degrade DNA during granzyme A-mediated cell death, *Molec. Cell,* 23: 133-142.

21. Chung, H., *et al.,* 2003, Gadd45-gamma expression is reduced in anaplastic thyroid cancer and its reexpression results in apoptosis, *J. Clin. Endocr. Metab.,* 88: 3913-3920.

22. Clarke, P.A., *et al.*, 2004, Gene expression microarray technologies in the development of new therapeutic agents, *European Journal of Cancer*, 40: 2560-2591.

23. Conradie, J., Lamprecht, G., Otto, S., Swarts, J., 2002, Synthesis and characterization of Ferrocene containing β-diketanato complexes of Rhodium(I) and Rhodium(III), *Inorganica Chimica Acta*, 328: 191-203.

24. Cortez, D., Guntuku, S., Quin, J., Elledge, S., 2001, ATR and ATRIP: partners in checkpoint signaling, *Science,* 294: 1713-1716.

25. Cotton, R., Horaitis, O., 2002, The *HUGO* mutation database initiative, *Pharmacogenom J.*, 2: 16-19.

26. Craciunescu, D., *et al.*, 1991, Pharmacological and toxicological studies on new Rh(I)organometallic complexes, *In Vivo*, 5: 329-332.

27. Crissman, H.A., Steinkamp, J.A., 1973, Rapid simultaneous measurement of DNA, protein, and cell volume in single cells from large mammalian cell populations, *J Cell Biol,* 59: 766.

28. Csikasz-Nagy, A., *et al.,* 2006, Analysis of a generic model of eukaryotic cell cycle regulation, *Biophysical Journal*, 90: 4361-4379.

29. Datar, S., Jacobs, H., dela Cruz, A., Lehner, C., Edgar, B., 2000, The *Drosophila* cyclin B-CDK2 complex promotes cellular growth, *EMBO J.,* 19: 4543-4554.

30. DeVita, V., Chu, E., 2008, A history of cancer chemotherapy, *Cancer Research,* 68:8643-53.

31. Ebbell, B, 1936, The papyrus ebers: the greatest Egyptian medical document, Levin and Munksgaard, Copenhagen, pp 110, 111, 124.

32. Eckhardt, S., 2002, Recent progress in the development of anticancer agents, *Curr. Med. Chem.*, 2: 419-439.

33. Ed., Pazdur, R., Hoskins, W., Lawrence, R., Lawrence, D., 2005, Cancer management: a multidisciplinary approach, 9th ed., 21-37.

34. Emmert, S., Kobayashi, N., Khan, S. G., Kraemer, K. H., 2000, The xeroderma pigmentosum group C gene leads to selective repair of cyclobutane pyrimidine dimers rather than 6-4 photoproducts, *Proc. Nat. Acad. Sci.,* 97: 2151-2156.

35. Engedal, N., Saatcioglu, F., 2001, Ceramide-induced cell death in the prostate cancer cell line LNCaP has both necrotic and apoptotic features, *The Prostate*, 46: 289-297.

36. Ezhevsky, S., Becker-Hapack, M., Davis, P., Dowdy S., 2001, Differential regulation of retinoblastoma tumour suppressor protein by G1 cyclin-dependant kinase complexes *in vivo, Mol. Cell Biol.,* 21: 4773-4784.

37. Fan, S., *et al.*, 1995, Disruption of p53 function sensitises breast cancer MCF7 cells to cisplatin and pentoxifylline, *Cancer Res.,* 55: 1649-1654.

38. Festjens, N., Van den Berghe, T., Van den Abeele, P., 2006, Necrosis, a well orchestrated form of cell demise: signalling cascades, important mediators and concomitant immune response, *Biochim. Biophys. Acta,* 1757: 1371-1387.

39. Fiamani, V., *et al.*, 1990, Antitumour effect of the new Rhodium(II) complex: Rh(Form)2(O2CCF3)2H2O)2(Form=N,N' –di-p-tolylformamidinate, *J. Chemotherapy*, 2: 319-326.

40. Fiers, W., *et al.*, 1999, More than one way to die: apoptosis, necrosis and reactive oxygen damage, *Oncogene*, 18: 7719-7730.

41. Fromm, M.F., 2002, The influence of *MDR1* polymorphisms on p-glycoprotein expression and function in humans, *Adv. Drug Deliv. Rev.*, 54: 1295-1310.

42. Fuertes, M., Castilla, J., Alonso, C., Perez, J., 2003, Cisplatin biochemical mechanism of action: from cytotoxicity to induction of cell death through interconnections between apoptotic and necrotic pathways, *Current Medicinal Chemistry*, 10: 257-266.

43. Gagna, C., *et al.*, 2004, Cell biology, chemogenomics and proteomics, *Cell Biology International*, 28: 755-764.

44. Giannakakou, P., *et al.*, 1997, Paclitaxel-resistant human ovarian cancer cells have mutant beta-tubulins that exhibit impaired paclitaxel-driven polymerisation, *J. Biol. Chem.*, 272: 17118-17125.

45. Goldberg, M., *et al.,* 2003, MDC1 is required for the intra-S-phase DNA damage checkpoint, *Nature,* 421: 952-956.

46. Gottlieb, T., Oren, M., 1998, p53 and apoptosis, *Sem. in Cancer Biology*, 8: 359-368.

47. Greener, M., 2005, QSAR: prediction beyond the fourth dimension, *Drug Discovery and Development*, 8: 44-47.

48. Halestrap, A., 2005, A pore way to die, *Nature*, 434: 578-579.

49. Han, J., *et al.,* 1996, Characterization of the structure and function of a novel MAP kinase kinase (MKK6), *J. Biol. Chem*, 271: 2886-2891.

50. Hanahan, D., Weinberg, R., 2000, The hallmarks of cancer, *Cell*, 100: 57-70.

51. Hanahan, D., Weinberg, R., 2011, Hallmarks of cancer: the next generation, *Cell*, 144: 646-674.

52. Ho, A., Dowdy, S., 2002, Regulation of G_1 cell cycle progression by oncogenes and tumor suppressor genes, *Curr. Opin. Gen. Dev.,* 12: 47-52.

53. Hollstein, M., *et al.* 1991, p53 mutations in human cancer, *Science*: 49-53.

54. Hosfield, D. J., Mol, C. D., Shen, B., Tainer, J. A., 1998, Structure of the DNA repair and replication endonuclease and exonuclease FEN-1: coupling DNA and PCNA binding to FEN-1 activity, *Cell*, 95: 135-146.

55. Houtgraaf, J., Vermissen, J., van der Giessen, W., 2006, A concise review of DNA damage checkpoints and repair in mammalian cells, *Cardio. Revasc. Med.,* 7: 165-172.

56. Hu, M., *et al.,* 2004, IkappaB kinase promotes tumourigenisis through inhibition of forkhead FOXO3A, *Cell,* 117: 225-237.

57. Huang, Y., *et al.*, 2004, Membrane transporters and channels: role of the transportome in cancer chemosensitivity and chemoresistance, *Cancer Research*, 64: 4294-4301.

58. Inohara, N., 1998, CIDE, a novel family of cell death activators with homology to the 45 kDa subunit of the DNA fragmentation factor, *EMBO J.*, 17: 2526-2533.

59. Johnson, P.H., *et al.*, 2002, Multiplex gene expression analysis for high- throughput drug discovery: screening and analysis of compounds affecting genes over expressed in cancer cells, *Mol. Cancer Ther.*, 1: 1293-1304.

60. Jorgensen, W.L., 2004, The many roles of computation in drug discovery, *Science*, 303: 1813-1818.

61. Kastan, M. and Bartek, J., 2004, Cell-cycle checkpoints and cancer, *Nat.,* 432: 316-323.

62. Kastan, M., Lim, D., 2000, The many substrates and functions of ATM, *Mol. Cell Biol.,* 1: 179-186.

63. Kato, M., 2000, Identification of Rad51 alteration in patients with bilateral breast cancer, *J. Hum. Genet.,* 45: 133-137.

64. Kelly, T., Brown, G.W., 2000, Regulation of chromosome replication, *Ann. Rev. Biochem.,* 69: 829-880.

65. Kim, C.H., *et al.*, 2000, Biphasic effects of dithiocarbamates on the activity of nuclear factor –kappa B, *Eur. J. Pharmacol.*, 392: 133-136.

66. Klebl, B.M., 2004, Chemical kinomics-a target gene family approach in chemical biology, *Drug Discovery Today: Technologies*, 1: 25-34.

67. Koopman, G., Reutelingsperger, C., Kuijten, G.A.M., Keehen, R., Pals, S., van Oers, M.H.J., 1994, Annexin V for flow cytometric detection of phosphatidylserine expression on B cells undergoing apoptosis, *Blood*, 84: 1415-1420.

68. Kopf-Maier, P., 1994, Complexes of metals other than platinum as anti-tumoural agents, *European Journal of Clinical Pharmacology*, 47: 1-16.

69. Kroemer, G., 2004, Cell death and cancer: an introduction, *Oncogene,* 23: 2744-2745.

70. Kruh, G.D., 2003, Introduction to resistance to anticancer agents, *Oncogene*, 22: 7262-7264.

71. Kumanogoh, A., 2002, Class IV semaphorin Sema4A enhances T-cell activation and interacts with Tim-2, *Nature,* 419: 629-633.

72. Lau, A. Y., *et al.,* 1998, Crystal structure of a human alkylbase-DNA repair enzyme complexed to DNA: mechanisms for nucleotide flipping and base excision*, Cell,* 95: 249-258.

73. Lee, W., *et al.*, 2005, Cancer pharmacogenomics: powerful tools in cancer chemotherapy and drug development, *The Oncologist*, 10: 104-111.

74. Lipinski, M.M., Jacks, T., 1999, The retinoblastoma gene family in differentiation and development, *Oncogene,* 18: 7873-7882.

75. Livak, K., Schmittgen, T., 2001, Analysis of relative gene expression data using real-time quantitative PCR and the $2^{-\Delta\Delta Ct}$ method, *Methods,* 25: 402-408.

76. Longley, D.B., Johnston, P.G., 2005, Molecular mechanisms of drug resistance, *Journal of Pathology*, 205: 275-292.

77. Lowe, S., *et al.,* 2004, Intrinsic tumour suppression, *Nat*, 432 : 307-315.

78. Lu, R., *et al.,* 1997, A mammalian DNA repair enzyme that excises oxidatively damaged guanines maps to a locus frequently lost in lung cancer, *Curr. Biol.*, 7: 397-407.

79. Luo, J., Solomini, N., Elledge, 2009, Principles of cancer therapy: oncogene and non-oncogene addiction, *Cell,* 136: 823-837.

80. Ma, X., *et al.*, 1999, Inhibition of p38 mitogen-activated protein kinase decreases cardiomyocyte apoptosis and improves cardiac function after myocardial ischemia and reperfusion, *Circulation,* 99: 1685-1691.

81. Macleod, K, 2000, Tumour suppressor genes, *Cur opin in Gen and Dev*, 10: 81-93.

82. Mao, Y., Sun, M., Desai, S. D., Liu, L. F., 2000, SUMO-1 conjugation to topoisomerase I: a possible repair response to topoisomerase-mediated DNA damage, *Proc. Nat. Acad. Sci.,* 97: 4046-4051.

83. Marechal, E., 2008, Chemogenomics: a discipline at the crossroad of high throughput technologies, biomarker research, combinatorial chemistry, genomics, chemoinformatics, bioinformatics and artificial intelligence, *Cominatorial Chemistry and High Throughput Screening,* 11: 583-586.

84. Marron, B., Jayawickreme, C.K., 2003, Going to the well no more: lawn format assays for ultra-high-throughput screening, *Current Opinion In Chemical Biology*, 7: 395-401.

85. Martin, J.S., *et al.,* 1995, Early redistribution of plasma membrane phosphatidylserine is a general feature of apoptosis regardless of the initiating stimulus: inhibition by over expression of Bcl-2 and Abl, *J. Exp. Med.,* 182: 1545-1556.

86. Massague, J., 2004, G1 cell-cycle control and cancer*, Nature,* 432: 298-305.

87. Maxwell, P.J., *et al.*, 2003, Identification of 5-flouracil inducible target genes using cDNA microarray profiling, *Cancer Res.*, 62: 3377-3381.

88. Mazur, D., Perrino, F. W., 2001, Structure and expression of the TREX1 and TREX2 3-prime-to-5-prime exonuclease genes, *J. Biol. Chem,* 276: 14718-14727.

89. Meyer, C., *et al.,* 2000, *Drosophila* CDK4 is required for normal growth and is dispensable for cell cycle progression, *EMBO,* 19: 4533-45442.

90. Mitsui, K., *et al.,* 1999, A novel human gene encoding HECT domain and RCC1-like repeats interacts with cyclins and is potentially regulated by the tumor suppressor proteins, *Biochem. Biophys. Res. Commun,* 266: 115-122.

91. Mochizuki, T., *et al.*, 2002, Akt protein kinase inhibits non-apoptotic programmed cell death induced by ceramide, *J Biol. Chem.* 277: 2790-2797.

92. Monks, A., *et al.*, 1991, Feasibility of a high-flux anticancer drug screen using a diverse panel of cultured human tumour cell lines, *J. Natl. Cancer Inst.*, 83: 757-766.

93. Monte, M., *et al.,* 2000, Cloning, chromosome mapping and functional characterization of a human homologue of murine Gtse-1 (B99) gene, *Gene,* 254: 229-236.

94. Morgan, D., 1997, Cyclin-dependant kinases: engines, clocks and microprocessors, *Ann. Rev. Cell Div. Bio.*, 13: 261-291.

95. Mossman, T., 1983, Rapid colorimetric assay for cellular growth and survival: Application to proliferation and cytotoxicty assays, *J Immuno Methods,* 65: 55-63.

96. Musumarra, G., *et al.*, 2002, Short cuts in genome-scale pharmacology research from multivariate analysis of the national cancer institute gene expression database, *Biochem. Pharmacol.*, 2: 259-271.

97. Murray, A.W., Recycling the cell cycle: cyclins revisited, *Cell,* 116: 221-234.

98. Nelson, D., White, E., 2004, Exploiting different ways to die, *Genes and Development*, 18: 1223-1226.

99. Neuse, E., 2005, Macromolecular Ferrocene compounds as cancer drug models, *Journal of Inorganic and Organometallic Polymers and Materials*, 15: 2-32.

100. Nicotera, P., Melino, G., 2004, Regulation of the apoptosis-necrosis switch, *Oncogene*, 23: 2757-2765.

101. Nishizuka, S., *et al.*, 2003, Proteomic profiling of the NCI60 cell linesusning new high-density reverse-phase lysate microarrays, *PNAS*, 24: 14229-14234.

102. Nurse, P., 2000, A long twentieth century of the cell cycle and beyond, *Cell*, 100: 71-78.

103. Nyberg, K., Michelson, R., Putnam, C., Weinert, T., 2002, Toward maintaining the genome: DNA damage and replication checkpoints, *ANNU. Rev. Genetics,* 36: 617-656.

104. Ocampo, M., *et al.*, 2002, Targeted deletion of mNth1 reveals a novel DNA repair enzyme activity, *Molec. Cell Biol,* 22: 6111-6121.

105. Oltvai, Z. N., Milliman, C. L., Korsmeyer, S. J., 1993, Bcl-2 heterodimers in vivo with a conserved homolog, Bax, that accelerates programmed cell death, *Cell,* 74: 609-619.

106. Parker, W., 2010, Enzymology of purine and pyrimidine antimetabolites used in the treatment of cancer, *Chemical Reviews*, 109: 2880-2893.

107. Paweletz, C.P., *et al.*, 2001, Reverse phase protein microarrays which capture disease progression show activation of the pro-survival pathways at the cancer invasion front, *Oncogene*, 20: 1981-1989.

108. Pawson, T., 2004, Specificity in signal transduction: from phosphotyrosine-SH2 domain interactions to complex cellular systems, *Cell,* 116: 191-203.

109. Pfaffl, M., Horgan, G., Dempfle, L., 2002, Relative expression software tool (REST) for groupwise comparison and statistical analysis of relative expression results in real-time PCR, *Nucleic Acids Research*, 30: e36.

110. Pitot, H.C, 2002, Fundamentals of oncology, 4th ed., Marcel Dekker, New York

111. Prasanth, S., Mendez, J., Prasanth, K., Stilman, B., 2004, Dynamics of pre-replication complex proteins during the cell division cycle, *Phil. Trans. R. Soc. London,* 359: 7-16.

112. Proskuryakov, S., *et al.* 2003, Necrosis: a specific form of programmed cell death? *Exp. Cell. Res.* 283: 1-16.

113. Ravichandran, K, 2003, Recruitment signals from apoptotic cells: invitation to a quiet meal, *Cell*, 113: 817-820.

114. Ray, S., *et al.*, 2005, Small-molecule-mediated stabilisation of familial amyotrophic lateral sclerosis-linked superoxide dismutase mutants against unfolding and aggregation, *PNAS*, 102: 3639-3644.

115. Reilly, T.P., *et al.*, 2001, Expression profiling of acetaminophen liver toxicity in mice using microarray technology, *Biochemical and Biophysical Research Communications*, 282: 321-328.

116. Reinhold, W.C., *et al.*, 2003, Apoptotic susceptibility of cancer cells selected for camptothecin resistance: gene expression profiling, functional analysis and molecular interaction mapping, *Cancer Res.*, 63: 1000-1011.

117. Sancar, A., *et al.,* 2004, Molecular mechanisms of mammalian DNA repair and the DNA damage checkpoints, *Annu Rev Biochem,* 73: 39-85.

118. Sauseville, E., Holbeck, S., 2004, Transcription profiling of gene expression in drug discovery and development: the NCI experience, *European Journal of Cancer*, 40: 2544-2549.

119. Scherf, U., *et al.*, 2000, A gene expression database for the molecular pharmacology of cancer, *Nat. Genetics*, 24: 236-244.

120. Schessinger, J., Lemon, M.A., 2003, SH2 and PTB domains in tyrosine kinase signalling, *Sci STKE*, 191: RE12.

121. Searfoss, G.H., Ryan, T.P., Jolly, R.A., 2005, The role of transcriptome analysis in pre-clinical toxicology, *Current Molecular Medicine*, 5: 53-64.

122. Shimodaira, H., *et al.*, 2003, Interaction of mismatch repair protein PMS2 and the p53-related transcription factor p73 in apoptosis response to cisplatin, *Proc. Nat. Acad. Sci.*, 100: 2420-2425.

123. Shiloh, Y., Kastan, M., 2001, ATM: genome stability, neuronal development and cancer cross paths, *Adv. Cancer Res.,* 83: 209-254.

124. Shoemaker, R.H., *et al.*, 2002, Application of high through-put, molecular targeted screening to anti-cancer drug discovery, *Current Topics in Medicinal Chemistry*, 2, 229-246.

125. Shoichet, B.K., *et al.*, 2002, Lead discovery using molecular docking, *Current Opinions in Chemical Biology*, 6: 439-446.

126. Siddik, Z., 2003, Cisplatin: mode of cytotoxic action and molecular basis of resistance, *Oncogene*, 22: 7265-7279.

127. Skov, K., *et al.* (1987), Assessment of DNA binding of platinum-radio-sensitiser complexes by inhibition of restriction enzymes. Chem. Biol. Interactions. 62: 117-128.

128. Smith, M., *et al.,* 1994, Interaction of the p53-regulated protein Gadd45 with proliferating cell nuclear antigen, *Science,* 266: 1376-1380.

129. Sparreboom, A., *et al.*, 2003, Pharmacogenomics of ABC transporters and its role in cancer chemotherapy, *Drug Resistance Updates*, 6: 71-84.

130. Su, H.-L., Li, S. S.-L., 2002, Molecular features of human ubiquitin-like SUMO genes and their encoded proteins, *Gene,* 296: 65-73.

131. Sugasawa, K., *et al.,* 2006, Xeroderma pigmentosum group C protein complex is the initiator of global genome nucleotide excision repair, *Molec. Cell,* 2: 223-232.

132. Turnbridge, E., Eastwood, S., Harrison, P., 2011, Change relative to what? Housekeeping genes and normalization strategies in human brain gene expression studies, *Biological Psychiatry,* 69: 173-179.

133. Tu, S., 2010, History of Cancer, *Cancer Treatment and Research,* 154: 19-31.

134. Vermes, I., Haanen, C., Steffens-Nakken, H., Reutelingsperger, C., 1995, A novel assay for apoptosis: Flow cytometric detection of phosphatidylserine expression on early apoptotic cells using fluorescein labelled Annexin V, *J. Immunol. Meth.,* 184: 39-51.

135. Vermeulen, K., Bockstaele, D., Bereman, Z., 2003, The cell cycle: a review of regulation, deregulation and therapeutic targets in cancer, *Cell Prolif.,* 36: 131-149.

136. Vivanco, I., Sawyers, C.L., 2002, The phosphatidylinositol 3-kinase AKT pathway in human cancer, *Nature Rev. Cancer*, 2: 489-501.

137. Volker, M., *et al.,* 2001, Sequential assembly of the nucleotide excision repair factors in vivo, *Molec. Cell,* 8: 213-224.

138. Volkmer, E., Karnitz, L.M., 1999, Human homologs of Schizosaccharomyces pombe Rad1, Hus1, and Rad9 form a DNA damage-responsive protein complex, *J. Biol. Chem,* 274: 567-570.

139. Walker, M.G., 2001, Drug target discovery by gene expression analysis: cell cycle genes, *Current Cancer Drug Targets*, 1: 73-83.

140. Webster, P., 2005, Biomarkers save clinical trial costs, *Drug Discovery and Development*, 8: 15.

141. Wegner, S. *et al.,* 2000, Alternative splicing in the regulatory region of the human phosphatases CDC25A and CDC25C, *European Journal of Cell Biology*, 79: 810-815.

142. Weinberg, R., 1995, The retinoblastoma protein and cell cycle control, *Cell,* 81: 323-330.

143. Weinstein, J.N., Buolamwini, J.K., 2000, Molecular targets in cancer drug discovery: cell based profiling, *Current Pharmaceutical Design*, 6: 473-483.

144. World Health Organisation Fact Sheet No. 297, 2008, nt. http://www.who.int/cancer/en/index.html

145. Wuster, A., Babu, M., 2008, Chemogenomics and biotechnology, *Trends in Biotechnology,* 26: 252-258.

146. Young, R.C., *Ed.* Rubin, S., 1996, Chemotherapy of gynaecologic cancers, Lippencott-Raven, 1-16.

147. Zembutsu, H., *et al.*, 2002, Genome wide cDNA microarray screening to correlate gene expression profiles with sensitivity of 85 human tumour xenografts to anti-cancer drugs, *Cancer Res.*, 62: 518-527.

148. Zong, W., *et al.* 2004, Alkylating DNA damage stimulates a regulated form of necrotic cell death, *Genes and Development*, 18: 1272-1282.

149. Zhou, Y., *et al.*, 2002, Transcriptional regulation of mitotic genes by campothectin induced DNA damage: microarray analysis of dose and time dependent effects, *Cancer Res.*, 62: 1688-1695.

150. Zhu, J., He, F., Hu, S., Yu, J., 2008, On the nature of human housekeeping genes, *Trends in Genetics*, 24: 481-484.

151. Zou, L., Cortez, D., Elledge, S., 2002, Regulation of ATR substrate selection by Rad17-dependent loading of Rad9 complexes onto chromatin, *Genes and Dev.*, 16: 198-208.

APPENDIX 1:

GENE AND PROTEIN ABBREVIATIONS

4E-BP	factor-4E (eIF-4E)-binding protein
53BP1	p53 binding protein 1
ABCB1	ATP-binding cassette, sub-family B (MDR/TAP), member 1
ABCC1	ATP-binding cassette, sub-family C (CFTR/MRP), member 1
ABCC2	ATP-binding cassette, sub-family C (CFTR/MRP), member 2
ABCC3	ATP-binding cassette, sub-family C (CFTR/MRP), member 3
ABCC4	ATP-binding cassette, sub-family C (CFTR/MRP), member 4
ABCC5	ATP-binding cassette, sub-family C (CFTR/MRP), member 5
ABCG2	ATP-binding cassette, sub-family G (WHITE), member 2
Akt1	v-akt murine thymoma viral oncogene homolog 1
AMPK	protein kinase, AMP-activated, alpha 1 catalytic subunit
Apaf-1	apoptotic peptidase activating factor 1
AP-1	adaptor-related protein complex AP-1
APC	adenomatous polyposis coli
ARF	ADP-ribosylation factor
ATF3	activating transcription factor 3
ATM	ataxia telangiectasia mutated
ATR	ataxia telangiectasia mutated and Rad3 related
ATRIP	ATR-interacting protein
Bad	BCL2-associated agonist of cell death
Bak	BCL2-antagonist/killer
Bax	BCL2-associated X protein
Bcl-2	B-cell CLL/lymphoma 2
Bcl-XL	BCL2-like 1
BID	BH3 interacting domain death agonist
BNIP3	BCL2/adenovirus E1B 19kDa interacting protein 3
BRCA1	breast cancer 1
β-TrCP	beta-transducin repeat containing
BUB 1β	budding uninhibited by benzimidazoles 1 homolog (yeast)
CAD	Caspase activated DNase
CDC25A	cell division cycle 25 homolog A (S. pombe)
CDK9	cyclin-dependent kinase 9
CHK1	CHK1 checkpoint homolog (S. pombe)
CHK2	CHK2 checkpoint homolog (S. pombe)
C-JUN	jun oncogene
c-Myc	myc myelocytomatosis viral oncogene homolog
cPLA2	Ca^{2+}-dependent phospholipase A2
DPD	Dihydropyrimidine dehydrogenase
DR5	Death receptor 5
E2F	E2F transcription factor
ELF-1	E74-like factor 1 (ets domain transcription factor)
FANCD2	Fanconi anaemia protein D2
Fas	Fas (TNF receptor superfamily, member 6)
FOXO	forkhead box O
GSK3-β	glycogen synthase kinase 3 beta
HDAC	Histone deacetylase
HGF/SF	Hepatocyte growth factor/scatter factor
HOXB-13	Homeodomain transcription factor

Hsp70	Heat-shock protein 70
HSPA1A	heat shock 70kDa protein 1A
IFN-γ	Interferon gamma
IL-1	Interleukin 1
IL-1β	Interleukin 1 beta
JNK	mitogen-activated protein kinase
JUN	jun oncogene
LRG-21	activating transcription factor 3
LKB1	serine/threonine kinase 11
MAP	microtubule-associated protein
MAPK	mitogen-activated protein kinase
MDC1	mediator of DNA damage checkpoint 1
MDM2	Mdm2 p53 binding protein homolog (mouse)
MDR1	ATP-binding cassette, sub-family B (MDR/TAP), member 1
Miz1	interacting zinc-finger protein
MNK	ATPase, Cu++ transporting, alpha polypeptide
NBS1	Nijmegan breakage syndrome 1
NF-kB	nuclear factor kappa B
NOXA	Phorbol-12-myristate-13-acetate-induced protein 1
p15Ink4b	cyclin-dependent kinase inhibitor 2B (p15, inhibits CDK4)
p21	cyclin-dependent kinase inhibitor 1A (p21, Cip1)
p21Cip1	cyclin-dependent kinase inhibitor 1A (p21, Cip1)
p27Kip1	cyclin-dependent kinase inhibitor 1B (p27, Kip1)
p38MAPK	mitogen-activated protein kinase 14
p53	tumor protein p53
p63	tumor protein p63
p73	tumor protein p73
p90rsk	ribosomal protein S6 kinase, 90kDa, polypeptide 1
PAR-4	Proteinase activated receptor 4 precursor
PARP	Poly (ADP-ribose) polymerase
PIKKs	PI(3)K (phosphatidyl-inositol-3-OH kinase)-like kinases
PML	promyelocytic leukemia
P-gp	P-glycoprotein
PTEN	phosphatase and tensin homolog
PUMA	p53 up-regulated modulator of apoptosis
RAD17	RAD17 homolog (S. pombe)
Rb	Retinoblastoma
Rheb	Ras homolog enriched in brain
RPA	Replication protein A
SP2	Splicing protein 2
TNFα	Tumour necrosis factor alpha
TNFR	Tumour necrosis factor receptor
TSC2	tuberous sclerosis 2
TRAIL	tumor necrosis factor (ligand) superfamily, member
S6K	ribosomal protein S6
SLC29A1	ENT equilibrative nuclear transporter
SMC1	structural maintenance of chromosome 1
SOCS	Suppressor of cytokine signalling

Upa   Urikinase
uPAR   Urikinase receptor
XBP-1   X-box binding protein 1

APPENDIX 2:

RNA PURITY DATA

Table A2.1: Nanodrop spectrophotometer data for RNA concentration, 260/230 and 260/280 of MCF-12A cells exposed to Ferrocene or Rhodium-ferrocene at six and 12 hours. Sample ID (cell line-time-control/experiment-replicate).

Sample ID	ng/ul	260/230	260/280
MCF-12A Exposure at Six Hours			
12.6Con1	126.8	2.04	2.09
12.6Con2	124.24	2.36	2.09
12.6Con3	120.71	2.14	2.12
12.6Fc1	122.57	2.18	2.11
12.6Fc2	136.74	2.32	2.10
12.6Fc3	119.46	2.32	2.08
12.6Rh1	124.42	2.15	2.12
12.6Rh2	140.81	2.28	2.11
12.6Rh3	100.08	1.72	2.06
MCF-12A Exposure at Twelve Hours			
12.12Con1	132.34	2.16	2.10
12.12Con2	183.18	2.20	2.12
12.12Con3	143.41	2.16	2.11
12.12Fc1	143.08	2.17	2.10
12.12Fc2	145.93	2.21	2.12
12.12Fc3	146.05	2.18	2.10
12.12Rh1	161.11	2.18	2.10
12.12Rh2	137.88	2.20	2.09
12.12Rh3	150.21	2.19	2.11

Table A2.2: Nanodrop spectrophotometer data for RNA concentration, 260/230 and 260/280 of MCF-7 cells exposed to Ferrocene or Rhodium-ferrocene at six and 12 hours. Sample ID (cell line-time-control/experiment-replicate).

Sample ID	ng/ul	260/230	260/280
MCF-7 Exposure at Six Hours			
7.6Con1	205.29	2.24	2.10
7.6Con2	172.16	2.26	2.09
7.6Con3	227.51	2.24	2.10
7.6Fc1	214.81	2.27	2.10
7.6Fc2	214.93	2.26	2.09
7.6Fc3	200.99	2.23	2.10
7.6Rh1	182.58	1.88	2.10
7.6Rh2	173.52	2.21	2.11
7.6Rh3	188.24	2.14	2.10
MCF-7 Exposure at Twelve Hours			
7.12Con1	279.30	2.07	2.10
7.12Con2	285.00	2.21	2.11
7.12Con3	276.22	2.24	2.11
7.12Fc1	261.44	2.26	2.12
7.12Fc2	312.80	2.19	2.11
7.12Fc3	267.66	2.21	2.11
7.12Rh1	266.63	2.20	2.10
7.12Rh2	229.84	2.21	2.10
7.12Rh3	256.31	2.19	2.11

APPENDIX 3:

SABIOSCIENCES DNA DAMMAGE ARRAY GENES

Table A3.1: Genes (symbol, name and description) included in the SABiosciences DNA Damage Real-time PCR Array.

Symbol	Description	Gene Name
ABL1	C-abl oncogene 1, receptor tyrosine kinase	ABL/JTK7
ANKRD17	Ankyrin repeat domain 17	GTAR/NY-BR-16
APEX1	APEX nuclease (multifunctional DNA repair enzyme) 1	APE/APE-1
ATM	Ataxia telangiectasia mutated	AT1/ATA
ATR	Ataxia telangiectasia and Rad3 related	FRP1/MEC1
ATRX	Alpha thalassemia/mental retardation syndrome X-linked (RAD54 homolog, S. cerevisiae)	ATR2/MRXHF1
BRCA1	Breast cancer 1, early onset	BRCAI/BRCC1
BTG2	BTG family, member 2	PC3/TIS21
CCNH	Cyclin H	CAK/p34
CDK7	Cyclin-dependent kinase 7	CAK1/CDKN7
CHEK1	CHK1 checkpoint homolog (S. pombe)	CHK1
CHEK2	CHK2 checkpoint homolog (S. pombe)	CDS1/CHK2
CIB1	Calcium and integrin binding 1 (calmyrin)	CIB/KIP
CIDEA	Cell death-inducing DFFA-like effector a	CIDE-A
CRY1	Cryptochrome 1 (photolyase-like)	PHLL1
DDB1	Damage-specific DNA binding protein 1, 127kDa	DDBA/UV-DDB1
DDIT3	DNA-damage-inducible transcript 3	CEBPZ/CHOP
DMC1	DMC1 dosage suppressor of mck1 homolog, meiosis-specific homologous recombination (yeast)	DMC1H/HsLim15
ERCC1	Excision repair cross-complementing rodent repair deficiency, complementation group 1 (includes overlapping antisense sequence)	COFS4/UV20
ERCC2	Excision repair cross-complementing rodent repair deficiency, complementation group 2 (xeroderma pigmentosum D)	COFS2/EM9
EXO1	Exonuclease 1	HEX1/hExoI
FANCG	Fanconi anemia, complementation group G	FAG/XRCC9
FEN1	Flap structure-specific endonuclease 1	FEN-1/MF1
XRCC6	X-ray repair complementing defective repair in Chinese hamster cells 6 (Ku autoantigen, 70kDa)	CTC75/CTCBF
GADD45A	Growth arrest and DNA-damage-inducible, alpha	DDIT1/GADD45
GADD45G	Growth arrest and DNA-damage-inducible, gamma	CR6/DDIT2

Symbol	Description	Gene Name
GML	Glycosylphosphatidylinositol anchored molecule like protein	LY6DL
GTF2H1	General transcription factor IIH, polypeptide 1, 62kDa	BTF2/TFIIH
GTF2H2	General transcription factor IIH, polypeptide 2, 44kDa	BTF2/BTF2P44
GTSE1	G-2 and S-phase expressed 1	B99
HUS1	HUS1 checkpoint homolog (S. pombe)	Hus1
IGHMBP2	Immunoglobulin mu binding protein 2	CATF1/HCSA
IHPK3	Inositol hexaphosphate kinase 3	INSP6K3/IP6K3
XRCC6BP1	XRCC6 binding protein 1	KUB3
LIG1	Ligase I, DNA, ATP-dependent	MGC117397
MAP2K6	Mitogen-activated protein kinase kinase 6	MAPKK6/MEK6
MAPK12	Mitogen-activated protein kinase 12	ERK3/ERK6
MBD4	Methyl-CpG binding domain protein 4	MED1
MLH1	MutL homolog 1, colon cancer, nonpolyposis type 2 (E. coli)	COCA2/FCC2
MLH3	MutL homolog 3 (E. coli)	HNPCC7
MNAT1	Menage a trois homolog 1, cyclin H assembly factor (Xenopus laevis)	MAT1/RNF66
MPG	N-methylpurine-DNA glycosylase	AAG/APNG
MRE11A	MRE11 meiotic recombination 11 homolog A (S. cerevisiae)	ATLD/HNGS1
MSH2	MutS homolog 2, colon cancer, nonpolyposis type 1 (E. coli)	COCA1/FCC1
MSH3	MutS homolog 3 (E. coli)	DUP/MRP1
MUTYH	MutY homolog (E. coli)	MYH
N4BP2	Nedd4 binding protein 2	B3BP
NBN	Nibrin	AT-V1/AT-V2
NTHL1	Nth endonuclease III-like 1 (E. coli)	NTH1/OCTS3
OGG1	8-oxoguanine DNA glycosylase	HMMH/HOGG1
PCBP4	Poly(rC) binding protein 4	LIP4/MCG10
PCNA	Proliferating cell nuclear antigen	MGC8367
AIFM1	Apoptosis-inducing factor, mitochondrion-associated, 1	AIF/PDCD8
PMS1	PMS1 postmeiotic segregation increased 1 (S. cerevisiae)	DKFZp781M0253/HNPCC3
PMS2	PMS2 postmeiotic segregation increased 2 (S. cerevisiae)	HNPCC4/PMS2CL

Symbol	Description	Gene Name
PMS2L3	Postmeiotic segregation increased 2-like 3	PMS2L9/PMS5
PNKP	Polynucleotide kinase 3'-phosphatase	PNK
PPP1R15A	Protein phosphatase 1, regulatory (inhibitor) subunit 15A	GADD34
PRKDC	Protein kinase, DNA-activated, catalytic polypeptide	DNAPK/DNPK1
RAD1	RAD1 homolog (S. pombe)	HRAD1/REC1
RAD17	RAD17 homolog (S. pombe)	CCYC/HRAD17
RAD18	RAD18 homolog (S. cerevisiae)	RNF73
RAD21	RAD21 homolog (S. pombe)	HR21/HRAD21
RAD50	RAD50 homolog (S. cerevisiae)	RAD50-2/hRad50
RAD51	RAD51 homolog (RecA homolog, E. coli) (S. cerevisiae)	BRCC5/HRAD51
RAD51L1	RAD51-like 1 (S. cerevisiae)	R51H2/RAD51B
RAD9A	RAD9 homolog A (S. pombe)	RAD9
RBBP8	Retinoblastoma binding protein 8	CTIP/RIM
REV1	REV1 homolog (S. cerevisiae)	REV1L
RPA1	Replication protein A1, 70kDa	HSSB/REPA1
SEMA4A	Sema domain, immunoglobulin domain (Ig), transmembrane domain (TM) and short cytoplasmic domain, (semaphorin) 4A	CORD10/RP35
SESN1	Sestrin 1	PA26/SEST1
SMC1A	Structural maintenance of chromosomes 1A	CDLS2/DKFZp686L19178
SUMO1	SMT3 suppressor of mif two 3 homolog 1 (S. cerevisiae)	DAP-1/GMP1
TP53	Tumor protein p53	LFS1/TRP53
TP73	Tumor protein p73	P73
TREX1	Three prime repair exonuclease 1	AGS1/AGS5
UNG	Uracil-DNA glycosylase	DGU/DKFZp781L1143
XPA	Xeroderma pigmentosum, complementation group A	XP1/XPAC
XPC	Xeroderma pigmentosum, complementation group C	XP3/XPCC
XRCC1	X-ray repair complementing defective repair in Chinese hamster cells 1	RCC
XRCC2	X-ray repair complementing defective repair in Chinese hamster cells 2	DKFZp781P0919
XRCC3	X-ray repair complementing defective repair in Chinese hamster cells 3	XRCC3
ZAK	Sterile alpha motif and leucine zipper containing kinase AZK	AZK/MLK7

Symbol	Description	Gene Name
B2M	Beta-2-microglobulin	B2M
HPRT1	Hypoxanthine phosphoribosyltransferase 1 (Lesch-Nyhan syndrome)	HGPRT/HPRT
RPL13A	Ribosomal protein L13a	RPL13A
GAPDH	Glyceraldehyde-3-phosphate dehydrogenase	G3PD/GAPD
ACTB	Actin, beta	PS1TP5BP1

APPENDIX 4:

"YOUR FAVOURITE GENE" ANALYSIS OF DNA DAMAGE

ARRAY DATA

Table A4.1: DNA Damage Array relative expression data for Ferrocene exposures of six and twelve hours in MCF-7 cells as compared to mock-treated controls. Selected aspects of gene association (regulation, binding and cellular function) are summarised from the "Your Favourite Gene" resource (www.sigma-aldrich.com).*

Gene Name	Gene Abbreviation	Regulates	Regulated By	Binds	Role in Cell
Six Hour Ferrocene Treatment in MCF-7 Cells					
Ataxia telangiectasia mutated	ATM	TP53 CHEK2 NBN	ATM NBN NBS1-Rad50-MRE11	TP53 BRCA1 NBN	▪ Apoptosis ▪ DNA damage response ▪ Survival
Fanconi anemia, complementation group G	FANCG	EIF2AK2 FANCA FANCD2	mitomycin C hydrogen peroxide FANCA	FANCA FANCF FANCE	▪ DNA damage response ▪ Cell death ▪ Biogenesis
Growth arrest and DNA-damage-inducible, alpha	GADD45A	MAP3K4 P38 MAPK MAPK14	TP53 MYC BRCA1	TP53 PCNA CDC2	▪ Apoptosis ▪ G2/M phase transition ▪ Growth
G-2 and S-phase expressed 1	GTSE1	GTSE1	TP53 GTSE1 Cdh1/APC	FZR1 CDH1	▪ No Data
XRCC6 binding protein 1	XRCC6BP1	No Data	No Data	CDKN2C	▪ No Data
8-oxoguanine DNA glycosylase	OGG1	8-hydroxyguanine 4,6-diamino-5-N-formamidopyrimidine 2,6-diamino-4-hydroxy-5-formamidopyrimidine	heavy metal OGG1 PPARA	Cbp/p300 HDAC2 HDAC3	▪ Cell viability ▪ Excision repair ▪ Apoptosis
Proliferating cell nuclear antigen	PCNA	POLD1 LIG1 Pol delta	beta-estradiol E2F1 RB1	CDKN1A FEN1 GADD45A	▪ Proliferation ▪ Cell cycle progression ▪ Homologous

Gene Name	Gene Abbreviation	Regulates	Regulated By	Binds	Role in Cell
					recombination (repair)
RAD1 homolog (S. pombe)	RAD1	LIG1	RPA2 Collagen Caco2 cells	RAD9A HUS1 RAD17	▪ DNA damage response ▪ Cell viability
RAD18 homolog (S. cerevisiae)	RAD18	PCNA RAD18 GAG-POL	RAD18 N-Ac-Leu-Leu-norleucinal UBE2A	UBE2B UBE2A PCNA	▪ Survival ▪ S phase checkpoint control ▪ Homologous recombination (repair)
Three prime repair exonuclease 1	TREX1	RPA2	ATR (includes EG:545) Cyclin A CDK2	ATR (includes EG:545) NBN MCM7	▪ No Data
Xeroderma pigmentosum, complementation group C	XPC	XPA nucleotide TP53	TP53 DDB2 DDB1	RAD23B GTF2H1 CETN2	▪ DNA damage response ▪ Survival ▪ G2 phase
Twelve Hour Ferrocene Treatment in MCF-7 Cells					
Ankyrin repeat domain 17	ANKRD17	No Data	No Data	NFKBIE	▪ No Data
Ataxia telangiectasia and Rad3 related	ATR	TP53 CHEK1 H2AFX	CDKN2A KAT5 methoxsalen	TREX1 (includes EG:11277) ATM BRCA1	▪ DNA damage response ▪ Survival ▪ Apoptosis
CHK1 checkpoint homolog (S. pombe)	CHEK1	CDC25C CDC25A TP53	ATR (includes EG:545) hydroxyurea ATM	PHKB CDC25A TP53	▪ Proliferation ▪ Cell death ▪ DNA damage response
DNA-damage-inducible	DDIT3	TNFRSF10B	tunicamycin	CEBPB	▪ Apoptosis

Gene Name	Gene Abbreviation	Regulates	Regulated By	Binds	Role in Cell
transcript 3		BAK1 ANKRD1	thapsigargin benzyloxycarbonyl-Leu-Leu-Leu aldehyde	CEBPG ATF3	▪ Cell death ▪ Growth
Flap structure-specific endonuclease 1	FEN1	FEN1 PCNA RAD51	estrogen FEN1 IGF2	ARHGDIA PCNA WRN (includes EG:7486)	▪ Accumulation ▪ Quantity ▪ Colony formation
X-ray repair complementing defective repair in Chinese hamster cells 6 (Ku autoantigen, 70kDa)	XRCC6	TP53 WRN (includes EG:7486) XRCC6	XRCC5 XRCC6 wortmannin	XRCC5 PRKDC WRN (includes EG:7486)	▪ Apoptosis ▪ DNA damage response ▪ Radiosensitivity
Growth arrest and DNA-damage-inducible, gamma	GADD45G	MAP3K4 CCNB1 Jnk	IL2 methyl methanesulfonate PCNA MAP3K4 PLEKHM1 HRAS	PCNA MAP3K4 PLEKHM1	▪ Apoptosis ▪ G2/M phase transition ▪ G1/S phase transition
General transcription factor IIH, polypeptide 1, 62kDa	GTF2H1	RNA polymerase II POLR2A SUB1	ERCC2 TP53 ERCC3	GTF2E1 ERCC3 CDK7	▪ No Data
General transcription factor IIH, polypeptide 2, 44kDa	GTF2H2	POLR2A RNA polymerase II SUB1	ERCC3 ERCC2 ERCC6	ERCC3 ERCC2 GTF2H1	▪ No data
HUS1 checkpoint homolog (S. pombe)	HUS1	amino acids H2AFX CHEK1	camptothecin celecoxib N-(3-(aminomethyl)benzyl)acetamidine.2HCl	RAD9A RAD1 RAD17	▪ DNA damage response
Mitogen-activated protein kinase 12	MAPK12	JUN ATF2 AP-1	TNF lipopolysaccharide EGF	JUN MAPK8IP1 MAP2K4	▪ Apoptosis ▪ Cell death ▪ Survival

Gene Name	Gene Abbreviation	Regulates	Regulated By	Binds	Role in Cell
Menage a trois homolog 1, cyclin H assembly factor (Xenopus laevis)	MNAT1	RNA polymerase II CDK2 RB1	Core retinoic acid Bcr	CDK7 CCNH ERCC3	▪ Proliferation ▪ Apoptosis ▪ G1/S phase transition
N-methylpurine-DNA glycosylase	MPG	3-methyladenine 1,N(6)-ethenoadenine hypoxanthine	ESR1 PPARA KAT5	MACF1 ACAT1 PGRMC1	▪ Survival ▪ Accumulation ▪ Cytotoxic reaction
Proliferating cell nuclear antigen	PCNA	POLD1 LIG1 Pol delta	beta-estradiol E2F1 RB1	CDKN1A FEN1 GADD45A	▪ Proliferation ▪ Cell cycle progression ▪ Homologous recombination (repair)
Apoptosis-inducing factor, mitochondrion-associated, 1	AIFM1	Respiratory Chain Complex I AIFM1 Mitochondrial complex 1	staurosporine BCL2 PARP1	Hsp70 HSPA1B PPIA (includes EG:5478)	▪ Apoptosis ▪ Condensation ▪ Cell death
PMS2 postmeiotic segregation increased 2 (S. cerevisiae)	PMS2	MutL alpha MutS alpha EXO1	MLH1 ATP MBD4	MLH1 BRIP1 EXO1	▪ DNA damage response ▪ Apoptosis ▪ Checkpoint control
RAD17 homolog (S. pombe)	RAD17	TP53 CHEK1	ATM ATR (includes EG:545) hydroxyurea	RAD9A RFC4 RAD1	▪ DNA damage response ▪ S phase checkpoint control ▪ G2/M phase transition
RAD51 homolog (RecA	RAD51	TP53	hydroxyurea	BRCA2	▪ Survival

159

Gene Name	Gene Abbreviation	Regulates	Regulated By	Binds	Role in Cell
homolog, E. coli) (S. cerevisiae)		SupFG1 reporter gene plasmid	ABL1 TP53	RAD51 TP53	▪ Cell death ▪ DNA damage response
RAD9 homolog A (S. pombe)	RAD9A	RAD9A CDKN1A LIG1	hydroxyurea RAD9A ATM	RAD1 HUS1 RAD17	▪ Apoptosis ▪ DNA damage response ▪ Double-stranded DNA break repair
Sema domain, immunoglobulin domain (Ig), transmembrane domain (TM) and short cytoplasmic domain, (semaphorin) 4A	SEMA4A	TBX21	MYC TP53	TIMD2 PLXNB2 PLXND1	▪ Differentiation ▪ Response ▪ Function
Uracil-DNA glycosylase	UNG	uracil BDNF 5-fluorouracil	folic acid EPAS1 Igm	SNRPB RPA2 VPR	▪ Apoptosis ▪ Cell death ▪ Mutation
Xeroderma pigmentosum, complementation group A	XPA	nucleotide Rpa SupFG1 reporter gene	XPC UCN-01 Rpa	ERCC1 RPA2 RPA1	▪ Apoptosis ▪ Response ▪ DNA damage response
Xeroderma pigmentosum, complementation group C	XPC	XPA nucleotide TP53	TP53 DDB2 DDB1	RAD23B GTF2H1 CETN2	▪ DNA damage response ▪ Survival ▪ G2 phase
X-ray repair complementing defective repair in Chinese hamster cells 3	XRCC3	No data	RAD51C RBL2 CXCL12	RAD51C RAD51 MSH5	▪ DNA damage response ▪ Survival
Sterile alpha motif and leucine zipper containing kinase AZK	ZAK	Jnk amino acids MAPK14	Sos FOS MAPK1	ZAK TGFBR1 SFN	▪ Apoptosis ▪ Cell cycle progression ▪ Transformation

*Up-regulation is indicated by values printed in green whereas down-regulation is indicated by red text.

Table A4.2: DNA Damage Array relative expression data for Ferrocene exposures of six and twelve hours in MCF-12A cells as compared to mock-treated controls. Selected aspects of gene association (regulation, binding and cellular function) are summarised from the "Your Favourite Gene" resource (www.sigma-aldrich.com).*

Gene Name	Gene Abbreviation	Regulates	Regulated By	Binds	Role in Cell
Six Hour Ferrocene Treatment in MCF-12A Cells					
Ataxia telangiectasia and Rad3 related	ATR	TP53 CHEK1 H2AFX	CDKN2A KAT5 methoxsalen	TREX1 (includes EG:11277) ATM BRCA1	▪ DNA damage response ▪ Survival ▪ Apoptosis
Cell death-inducing DFFA-like effector a	CIDEA	lipid	PPARG NRIP1 PPARA	PRKAG1 UCP1 CIDEC	▪ DNA damage response ▪ Apoptosis
Fanconi anemia, complementation group G	FANCG	EIF2AK2 FANCA FANCD2	mitomycin C hydrogen peroxide FANCA	FANCA FANCF FANCE	▪ DNA damage response ▪ Cell death ▪ Biogenesis
Flap structure-specific endonuclease 1	FEN1	FEN1 PCNA RAD51	estrogen FEN1 IGF2	ARHGDIA PCNA WRN (includes EG:7486)	▪ Accumulation ▪ Colony formation
Growth arrest and DNA-damage-inducible, alpha	GADD45A	MAP3K4 P38 MAPK MAPK14	TP53 MYC BRCA1	TP53 PCNA CDC2	▪ Apoptosis ▪ G2/M phase transition ▪ Growth
General transcription factor IIH, polypeptide 2, 44kDa	GTF2H2	POLR2A RNA polymerase II SUB1	ERCC3 ERCC2 ERCC6	ERCC3 ERCC2 GTF2H1	▪ No data
XRCC6 binding protein 1	XRCC6BP1	No Data	No Data	CDKN2C	▪ No data
MutL homolog 1, colon cancer, nonpolyposis type 2 (E. coli)	MLH1	PMS2 MLH1	decitabine 5-azacytidine	PMS2 EXO1	▪ DNA damage response

Gene Name	Gene Abbreviation	Regulates	Regulated By	Binds	Role in Cell
		TP53	vorinostat	BRIP1	• Apoptosis • Survival
8-oxoguanine DNA glycosylase	OGG1	8-hydroxyguanine 4,6-diamino-5-N-formamidopyrimidine 2,6-diamino-4-hydroxy-5-formamidopyrimidine	heavy metal OGG1 PPARA	Cbp/p300 HDAC2 HDAC3	• Cell viability • Excision repair • Apoptosis
PMS1 postmeiotic segregation increased 1 (S. cerevisiae)	PMS1	No data	IGF2 Ins DARC	MLH1 CCNT1 RANGAP1	• No Data
Polynucleotide kinase 3'-phosphatase	PNKP	nucleotide	POLB XRCC1 LIG3	XRCC1 LIG3 MCM3	• DNA damage response
RAD17 homolog (S. pombe)	RAD17	TP53 CHEK1	ATM ATR (includes EG:545) hydroxyurea	RAD9A RFC4 RAD1	• DNA damage response • S phase checkpoint control • G2/M phase transition
RAD18 homolog (S. cerevisiae)	RAD18	PCNA RAD18 GAG-POL	RAD18 N-Ac-Leu-Leu-norleucinal UBE2A	UBE2B UBE2A PCNA	• Survival • S phase checkpoint control • Homologous recombination repair
Sema domain, immunoglobulin domain (Ig), transmembrane domain (TM) and short cytoplasmic domain, (semaphorin) 4A	SEMA4A	TBX21	MYC TP53	TIMD2 PLXNB2 PLXND1	• Differentiation
Sestrin 1	SESN1	reactive oxygen species	TP53 cisplatin	MIR298 (includes	• Proliferation • DNA damage

Gene Name	Gene Abbreviation	Regulates	Regulated By	Binds	Role in Cell
			doxorubicin	EG:723832) NFYB	response
SMT3 suppressor of mif two 3 homolog 1 (S. cerevisiae)	SUMO1	GC-GCR dimer TDG NR3C1	SAE1 SENP1 SENP2	UBE2I RANGAP1 TP53	▪ Sumoylation in apoptosis ▪ Proliferation
Three prime repair exonuclease 1	TREX1	RPA2	ATR (includes EG:545) Cyclin A CDK2	ATR (includes EG:545) NBN MCM7	▪ No Data
Xeroderma pigmentosum, complementation group C	XPC	XPA nucleotide TP53	TP53 DDB2 DDB1	RAD23B GTF2H1 CETN2	▪ DNA damage response ▪ Survival ▪ G2 phase
Twelve Hour Ferrocene Treatment in MCF-12A Cells					
APEX nuclease (multifunctional DNA repair enzyme) 1	APEX 1	TP53 AP-1 TDG	MYC TP53 reactive oxygen species	HSPA1B EPAS1 TXN	▪ Survival ▪ Cell death
Ataxia telangiectasia and Rad3 related	ATR	TP53 CHEK1 H2AFX	CDKN2A KAT5 methoxsalen	TREX1 (includes EG:11277) ATM BRCA1	▪ DNA damage response ▪ Survival ▪ Apoptosis
Breast cancer 1, early onset	BRCA 1	CDKN1A BRCA1 TP53	BRCA1 ATM TP53	BARD1 FANCD2 RBBP8	▪ Apoptosis ▪ Proliferation ▪ Survival
Cell death-inducing DFFA-like effector a	CIDEA	lipid	PPARG NRIP1 PPARA	PRKAG1 UCP1 CIDEC	▪ DNA damage response ▪ Apoptosis
G-2 and S-phase expressed 1	GTSE1	GTSE1	TP53	FZR1	▪ No Data

163

Gene Name	Gene Abbreviation	Regulates	Regulated By	Binds	Role in Cell
			GTSE1 Cdh1/APC	CDH1	
Immunoglobulin mu binding protein 2	IGHMBP2	Bzlf1 E1b TFIIA	HGF	BTK TAF7 LSM8	▪ No Data
Inositol hexaphosphate kinase 3	IHPK3	phosphatidylinositol	NR3C1 dexamethasone	No Data	▪ Survival
Nth endonuclease III-like 1 (E. coli)	NTHL1	,6-diamino-5-N-formamidopyrimidine 2,6-diamino-4-hydroxy-5-formamidopyrimidine NTHL1	ERCC5 PPARA retinoic acid	YBX1 MYH7 RBL1	▪ No Data
8-oxoguanine DNA glycosylase	OGG1	8-hydroxyguanine 4,6-diamino-5-N-formamidopyrimidine 2,6-diamino-4-hydroxy-5-formamidopyrimidine	heavy metal OGG1 PPARA	Cbp/p300 HDAC2 HDAC3	▪ Cell viability ▪ Excision repair ▪ Apoptosis
Proliferating cell nuclear antigen	PCNA1	POLD1 LIG1 Pol delta	beta-estradiol E2F1 RB1	CDKN1A FEN1 GADD45A	▪ Proliferation ▪ Cell cycle progression ▪ Homologous recombination
Xeroderma pigmentosum, complementation group A	XPA	nucleotide Rpa SupFG1 reporter gene	XPC UCN-01 Rpa	ERCC1 RPA2 RPA1	▪ Apoptosis ▪ DNA damage response
X-ray repair complementing defective repair in Chinese hamster cells 1	XRCC1	PARP2 OGG1 PNKP	muscle cells ANGPT2 myoblasts	LIG3 APLF POLB	▪ Survival

*Up-regulation is indicated by values printed in green whereas down-regulation is indicated by red text.

Table A4.3: DNA Damage Array relative expression data for Rhodium-ferrocene exposures of six and twelve hours in MCF-7 cells as compared to mock-treated controls. Selected aspects of gene association (regulation, binding and cellular function) are summarised from the "Your Favourite Gene" resource (www.sigma-aldrich.com).*

Gene Name	Gene Abbreviation	Regulates	Regulated By	Binds	Role in Cell
Six Hour Rhodium-ferrocene Treatment in MCF-7 Cells					
Ankyrin repeat domain 17	ANKRD17	No Data	No Data	NFKBIE	▪ No Data
Cell death-inducing DFFA-like effector a	CIDEA	lipid	PPARG NRIP1 PPARA	PRKAG1 UCP1 CIDEC	▪ DNA damage response ▪ apoptosis
Excision repair cross-complementing rodent repair deficiency, complementation group 1 (includes overlapping antisense sequence)	ERCC1	nucleotide pyrimidine dimer ERCC1	cisplatin HRAS EGF	XPA ERCC4 Rpa	▪ DNA damage response ▪ Development
X-ray repair complementing defective repair in Chinese hamster cells 6 (Ku autoantigen, 70kDa)	XRCC6	TP53 WRN (includes EG:7486) XRCC6	XRCC5 XRCC6 wortmannin	XRCC5 PRKDC WRN (includes EG:7486)	▪ Apoptosis ▪ DNA damage response ▪ Radiosensitivity
Growth arrest and DNA-damage-inducible, gamma	GADD45G	MAP3K4 CCNB1 Jnk	IL2 methyl methanesulfonate PCNA MAP3K4 PLEKHM1 HRAS	PCNA MAP3K4 PLEKHM1	▪ Apoptosis ▪ G2/M phase transition ▪ G1/S phase transition
Inositol hexaphosphate kinase 3	IHPK3	phosphatidylinositol	NR3C1 dexamethasone	No Data	▪ Survival
Nedd4 binding protein 2	N4BP2	ATP plasmid	N4BP2 NEDD4	EP300 Nedd4 NEDD4	▪ No Data
8-oxoguanine DNA glycosylase	OGG1	8-hydroxyguanine 4,6-diamino-5-N-formamidopyrimidine	heavy metal OGG1 PPARA	Cbp/p300 HDAC2 HDAC3	▪ Cell viability ▪ Excision repair ▪ Apoptosis

Gene Name	Gene Abbreviation	Regulates	Regulated By	Binds	Role in Cell
		2,6-diamino-4-hydroxy-5-formamidopyrimidine			
Proliferating cell nuclear antigen	PCNA	POLD1￼LIG1￼Pol delta	beta-estradiol￼E2F1￼RB1	CDKN1A￼FEN1￼GADD45A	▪ Proliferation￼▪ Cell cycle progression￼▪ Homologous recombination repair
PMS2 postmeiotic segregation increased 2 (S. cerevisiae)	PMS2	MutL alpha￼MutS alpha￼EXO1	MLH1￼ATP￼MBD4	MLH1￼BRIP1￼EXO1	▪ DNA damage response￼▪ Apoptosis￼▪ Checkpoint control
RAD1 homolog (S. pombe)	RAD1	LIG1	RPA2￼Collagen￼Caco2 cells	RAD9A￼HUS1￼RAD17	▪ DNA damage response￼▪ cell viability
Retinoblastoma binding protein 8	RBPP8	RBBP8￼CCND1	E2F6￼RBBP8￼ATM	BRCA1￼RBL1￼CTBP1	▪ G1/S phase transition￼▪ G2/M phase
Three prime repair exonuclease 1	TREX1	RPA2	ATR (includes EG:545)￼Cyclin A￼CDK2	ATR (includes EG:545)￼NBN￼MCM7	▪ No Data
Xeroderma pigmentosum, complementation group C	XPC	XPA￼nucleotide￼TP53	TP53￼DDB2￼DDB1	RAD23B￼GTF2H1￼CETN2	▪ DNA damage response￼▪ Survival￼▪ G2 phase
Twelve Hour Rhodium-ferrocene Treatment in MCF-7 Cells					
Ankyrin repeat domain 17	ANKRD17	No Data	No Data	NFKBIE	▪ No Data

166

Gene Name	Gene Abbreviation	Regulates	Regulated By	Binds	Role in Cell
BTG family, member 2	BTG2	CCND1 BTG1 HOXB9	TP53 retinoic acid cisplatin	CNOT7 PRMT1 HOXC8	▪ Proliferation ▪ Differentiation ▪ DNA damage response
DNA-damage-inducible transcript 3	DDIT3	TNFRSF10B BAK1 ANKRD1	tunicamycin thapsigargin benzyloxycarbonyl-Leu-Leu-Leu aldehyde	CEBPB CEBPG ATF3	▪ Apoptosis ▪ cell death growth
Excision repair cross-complementing rodent repair deficiency, complementation group 1 (includes overlapping antisense sequence)	ERCC1	nucleotide pyrimidine dimer ERCC1	cisplatin HRAS EGF	XPA ERCC4 Rpa	▪ DNA damage response ▪ Development
Flap structure-specific endonuclease 1	FEN1	FEN1 PCNA RAD51	estrogen FEN1 IGF2	ARHGDIA PCNA WRN (includes EG:7486)	▪ Accumulation ▪ Colony
Growth arrest and DNA-damage-inducible, gamma	GADD45G	MAP3K4 CCNB1 Jnk	IL2 methyl methanesulfonate PCNA MAP3K4 PLEKHM1 HRAS	PCNA MAP3K4 PLEKHM1	▪ Apoptosis ▪ G2/M phase transition ▪ G1/S phase transition
Glycosylphosphatidylinositol anchored molecule like protein	GML	No Data Available	CFTR	No Data Available	▪ DNA damage response ▪ Proliferation ▪ Sensitization
G-2 and S-phase expressed 1	GTSE1	GTSE1	TP53 GTSE1 Cdh1/APC	FZR1 CDH1	▪ No Data
HUS1 checkpoint homolog (S.	HUS1	amino acids	camptothecin	RAD9A	▪ DNA damage

Gene Name	Gene Abbreviation	Regulates	Regulated By	Binds	Role in Cell
pombe)		H2AFX CHEK1	celecoxib N-(3-(aminomethyl)benzyl)acetamidine.2HCl	RAD1 RAD17	response
Inositol hexaphosphate kinase 3	IHPK3	phosphatidylinositol	NR3C1 dexamethasone	No Data Available	▪ Survival
XRCC6 binding protein 1	XRCC6BP1	No Data	No Data	CDKN2C	▪ No Data
Mitogen-activated protein kinase kinase 6	MAP2K6	P38 MAPK MAPK14 Erk1/2	Map3k LEF MAP3K7	MAPK14 MAP3K5 (includes EG:4217) Mapk	▪ Apoptosis ▪ Activation in transformation
Mitogen-activated protein kinase 12	MAPK12	JUN ATF2 AP-1	TNF lipopolysaccharide EGF	JUN MAPK8IP1 MAP2K4	▪ Apoptosis ▪ Cell death ▪ Survival
Menage a trois homolog 1, cyclin H assembly factor (Xenopus laevis)	MNAT1	RNA polymerase II CDK2 RB1	Core retinoic acid Bcr	CDK7 CCNH ERCC3	▪ Proliferation ▪ Apoptosis ▪ G1/S phase transition
Proliferating cell nuclear antigen	PCNA	POLD1 LIG1 Pol delta	beta-estradiol E2F1 RB1	CDKN1A FEN1 GADD45A	▪ Proliferation ▪ Cell cycle progression ▪ Homologous recombination repair
Protein kinase, DNA-activated, catalytic polypeptide	PRKDC	TP53 MDM2 Akt	wortmannin XRCC5 silibinin	XRCC5 XRCC6 Ku	▪ Apoptosis ▪ Survival ▪ Differentiation
Sema domain, immunoglobulin domain (Ig), transmembrane domain (TM) and short cytoplasmic domain	SEMA4A	reactive oxygen species	TP53 cisplatin doxorubicin	MIR298 (includes EG:723832) NFYB	▪ Proliferation ▪ DNA damage response

Gene Name	Gene Abbreviation	Regulates	Regulated By	Binds	Role in Cell
Sestrin 1	SESN1	reactive oxygen species	TP53 cisplatin doxorubicin	MIR298 (includes EG:723832) NFYB	▪ Proliferation ▪ DNA damage response
Structural maintenance of chromosomes 1A	SMC1A	DMC1	ATM NBN Mre11	SMC3 STAG1 RAD21	▪ DNA damage response ▪ Biogenesis ▪ Cohesion
Tumor protein p53	TP73	CDKN1A MDM2 BAX	TP73 E2F1 cisplatin	TP53 TP73 MDM2	▪ Apoptosis ▪ Growth ▪ Cell death
Three prime repair exonuclease 1	TREX1	RPA2	ATR (includes EG:545) Cyclin A CDK2	ATR (includes EG:545) NBN MCM7	▪ No Data
Uracil-DNA glycosylase	UNG	uracil BDNF 5-fluorouracil	folic acid EPAS1 Igm	SNRPB RPA2 VPR	▪ Apoptosis ▪ Cell death ▪ Mutation
Xeroderma pigmentosum, complementation group C	XPC	XPA nucleotide TP53	TP53 DDB2 DDB1	RAD23B GTF2H1 CETN2	▪ DNA damage response ▪ Survival ▪ G2 phase
X-ray repair complementing defective repair in Chinese hamster cells 3	XRCC3	No data	RAD51C RBL2 CXCL12	RAD51C RAD51 MSH5	▪ DNA damage response ▪ Survival
Sterile alpha motif and leucine zipper containing kinase AZK	ZAK	Jnk amino acids MAPK14	Sos FOS MAPK1	ZAK TGFBR1 SFN	▪ Apoptosis ▪ Cell cycle progression

*Up-regulation is indicated by values printed in green whereas down-regulation is indicated by red text.

Table A4.4: DNA Damage Array (SABiosciences) relative expression data for Rhodium-ferrocene exposures of six and twelve hours in MCF-12A cells as compared to mock-treated controls. Selected aspects of gene association (regulation, binding and cellular function) are summarised from the "Your Favourite Gene" resource (www.sigma-aldrich.com).*

Gene Name	Gene Abbreviation	Regulates	Regulated By	Binds	Role in Cell
Six Hour Rhodium-ferrocene Treatment in MCF-12A Cells					
Ataxia telangiectasia and Rad3 related	ATR	TP53 CHEK1 H2AFX	CDKN2A KAT5 methoxsalen	TREX1 (includes EG:11277) ATM BRCA1	▪ DNA damage response ▪ Survival ▪ Apoptosis
Alpha thalassemia/mental retardation syndrome X-linked (RAD54 homolog, S. cerevisiae)	ATRX	CBX5 ATRX	Tax ADAM10 Ebna2	RAD51 V ANTIGEN MSH4	▪ Apoptosis ▪ Survival
BTG family, member 2	BTG2	CCND1 BTG1 HOXB9	TP53 retinoic acid cisplatin	CNOT7 PRMT1 HOXC8	▪ Proliferation ▪ Differentiation ▪ DNA damage response
Cell death-inducing DFFA-like effector a	CIDEA	lipid	PPARG NRIP1 PPARA	PRKAG1 UCP1 CIDEC	▪ DNA damage response ▪ Apoptosis
Fanconi anemia, complementation group G	FANCG	EIF2AK2 FANCA FANCD2	mitomycin C hydrogen peroxide FANCA	FANCA FANCF FANCE	▪ DNA damage response ▪ Cell death ▪ Biogenesis
X-ray repair complementing defective repair in Chinese hamster cells 6 (Ku autoantigen, 70kDa)	XRCC6	TP53 WRN (includes EG:7486) XRCC6	XRCC5 XRCC6 wortmannin	XRCC5 PRKDC WRN (includes EG:7486)	▪ Apoptosis ▪ DNA damage response ▪ Radiosensitivity
Growth arrest and DNA-damage-inducible, gamma	GADD45G	MAP3K4 CCNB1 Jnk	IL2 methyl methanesulfonate	PCNA MAP3K4 PLEKHM1	▪ Apoptosis ▪ G2/M phase transition

Gene Name	Gene Abbreviation	Regulates	Regulated By	Binds	Role in Cell
			PCNA MAP3K4 PLEKHM1 HRAS		▪ G1/S phase transition
Immunoglobulin mu binding protein 2	IGHMBP2	Bzlf1 E1b TFIIA	HGF	BTK TAF7 LSM8	▪ No Data
N-methylpurine-DNA glycosylase	MPG	3-methyladenine 1,N(6)-ethenoadenine hypoxanthine	ESR1 PPARA KAT5	MACF1 ACAT1 PGRMC1	▪ Survival ▪ Accumulation ▪ Cytotoxic reaction
Nibrin	NBN	CHEK2 SMC1A ATM	ATM hydroxyurea ATR (includes EG:545)	MRE11A RAD50 ATM	▪ proliferation ▪ Survival ▪ DNA damage response
8-oxoguanine DNA glycosylase	OGG1	8-hydroxyguanine 4,6-diamino-5-N-formamidopyrimidine 2,6-diamino-4-hydroxy-5-formamidopyrimidine	heavy metal OGG1 PPARA	Cbp/p300 HDAC2 HDAC3	▪ Cell viability ▪ Excision repair ▪ Apoptosis
PMS1 postmeiotic segregation increased 1 (S. cerevisiae)	PMS1	No Data Available	IGF2 Ins DARC	MLH1 CCNT1 RANGAP1	▪ No Data
Protein kinase, DNA-activated, catalytic polypeptide	PRKDC	TP53 MDM2 Akt	wortmannin XRCC5 silibinin	XRCC5 XRCC6 Ku	▪ Apoptosis ▪ Survival ▪ Differentiation
RAD18 homolog (S. cerevisiae)	RAD18	PCNA RAD18 GAG-POL	RAD18 N-Ac-Leu-Leu-norleucinal UBE2A	UBE2B UBE2A PCNA	▪ Survival ▪ S phase checkpoint control ▪ Homologous recombination (repair)

Gene Name	Gene Abbreviation	Regulates	Regulated By	Binds	Role in Cell
RAD50 homolog (S. cerevisiae)	RAD50	CHEK2 TP53 ATM	NBN hepatitis B virus Lmp2a	NBN MRE11A BRCA1	▪ No Data
RAD9 homolog A (S. pombe)	RAD9A	RAD9A CDKN1A LIG1	hydroxyurea RAD9A ATM	RAD1 HUS1 RAD17	▪ Apoptosis ▪ DNA damage response ▪ Double-stranded DNA break repair
SMT3 suppressor of mif two 3 homolog 1 (S. cerevisiae)	SUMO1	GC-GCR dimer TDG NR3C1	SAE1 SENP1 SENP2	UBE2I RANGAP1 TP53	▪ Sumoylation in apoptosis ▪ Proliferation
Twelve Hour Rhodium-ferrocene Treatment in MCF-12A Cells					
Ataxia telangiectasia mutated	ATM	TP53 CHEK2 NBN	ATM NBN NBS1-Rad50-MRE11	TP53 BRCA1 NBN	▪ Apoptosis ▪ DNA damage response ▪ Survival
Breast cancer 1, early onset	BRCA1	CDKN1A BRCA1 TP53	BRCA1 ATM TP53	BARD1 FANCD2 RBBP8	▪ Apoptosis ▪ Proliferation ▪ Survival
Cyclin-dependent kinase 7	CDK7	RB1 RNA polymerase II CDK2	CDKN1A CDC25C CDKN2A	CCNH MNAT1 GTF2H1	▪ Proliferation ▪ Cell cycle progression ▪ G1/S phase transition
Cell death-inducing DFFA-like effector a	CIDEA	lipid	PPARG NRIP1 PPARA	PRKAG1 UCP1 CIDEC	▪ DNA damage response ▪ Apoptosis
Cryptochrome 1 (photolyase-like)	CRY1	PER2 PER1 DBP	PER1 CRY2 Ins	CLOCK ARNTL PER2	▪ No Data
X-ray repair complementing defective	XRCC6	TP53	XRCC5	XRCC5	▪ Apoptosis

Gene Name	Gene Abbreviation	Regulates	Regulated By	Binds	Role in Cell
		WRN (includes EG:7486) XRCC6	XRCC6 wortmannin	PRKDC WRN (includes EG:7486)	▪ DNA damage response ▪ Radiosensitivity
Immunoglobulin mu binding protein 2	IGHMBP2	Bzlf1 E1b TFIIA	HGF	BTK TAF7 LSM8	▪ No Data
Inositol hexaphosphate kinase 3	IHPK3	phosphatidylinositol	NR3C1 dexamethasone	No Data Available	▪ Survival
Nth endonuclease III-like 1 (E. coli)	NTHL1	,6-diamino-5-N-formamidopyrimidine 2,6-diamino-4-hydroxy-5-formamidopyrimidine NTHL1	ERCC5 PPARA retinoic acid	YBX1 MYH7 RBL1	▪ No Data
Proliferating cell nuclear antigen	PCNA	POLD1 LIG1 Pol delta	beta-estradiol E2F1 RB1	CDKN1A FEN1 GADD45A	▪ Proliferation ▪ Cell cycle progression ▪ Homologous recombination repair
Protein kinase, DNA-activated, catalytic polypeptide	PRKDC	TP53 MDM2 Akt	wortmannin XRCC5 silibinin	XRCC5 XRCC6 Ku	▪ Apoptosis ▪ Survival ▪ Differentiation
Three prime repair exonuclease 1	TREX1	RPA2	ATR (includes EG:545) Cyclin A CDK2	ATR (includes EG:545) NBN MCM7	▪ No Data

*Up-regulation is indicated by values printed in green whereas down-regulation is indicated by red text.

SUMMARY

Organometallic chemotherapeutic agents, many of which target DNA, have been shown to be effective in the treatment of cancer. With that said though, these compounds have a number of side affects such as nephrotoxicity. Two novel compounds, Ferrocene [ferrocenoyltrichloroacetone] and Rhodium-ferrocene [(1.5 cyclooctadiene)(1-ferrocenyl-4,4,4-trichloro-1,3-butanedionate], synthesised by the research group of J Swarts (University of the Free State) were evaluated to determine their mechanism of action and their potential use as novel therapeutic agents.

It is hypothesized, by merit of their chemical structures, that these compounds' anti-cancer activity is due to their interaction with DNA. Both drugs were evaluated from a cellular to a molecular level, *in vitro*, to validate this hypothesis. Linearised DNA was exposed to both drugs and digested with a variety of restriction enzymes. It was found that the compounds bind to the PstI restriction site; thereby inhibiting the enzyme's restriction activity. From this point it was necessary to show that the compounds are able to interact with DNA in a cellular system.

By exposing a transformed breast epithelial cell line (MCF-12A) and a cancerous breast epithelial cell line (MCF-7) to the compounds, for various times, followed by flow cytometric analyses, it was found that both affect progression through the cell cycle. Cells accumulated at various phases of the cell cycle, as a result of checkpoint gene activation. Further flow cytometric analyses showed that both drugs induce necrosis in MCF-7 cells. The "normal" cell line however did not show this response as it is believed that cell cycle arrest and repair mechanisms were initiated, which would delay cell death.

Gene expression analyses were performed by reverse transcriptase real-time PCR in which panels of cell cycle related genes as well as DNA damage associated genes were probed in two separate array formats. These studies revealed that a number of DNA damage and

repair genes are activated; specifically those associated with excision repair and free-radical induced DNA damage. Members of the *RAD* family as well as the genes *GADD45A, XPC* and *OGG1* were found to be upregulated as a result of Ferrocene treatment. This could be expected as it was shown that ferrocene binds to DNA, and it logically then follows that this would lead to excision repair being attempted by the cell. Similar gene expression patterns were found following Rhodium-ferrocene treatment with the up-regulation of genes such as *OGG1*, *ATM* and *GADD45G*, albeit to a lesser extent. It is hypothesised that the larger molecule may not interact as effectively with DNA, due to steric hinderance. Arrest mechanisms, for both drugs, were more pronounced in the "normal" cell line and it is believed that this is due to the fact that many of these genes have been inactivated in the cancerous cell line.

We have shown, on multiple levels, that both compounds' therapeutic action is as a result of their interaction with the cell's DNA. This interaction leads to cell death in both the transformed and the cancerous cell line. In order to clarify these mechanisms it is suggested that proteomic and metabolomic studies should be performed.

Keywords: Ferrocene, Rhodium-ferrocene, gene expression, *in vitro*, DNA damage, flow cytometry, real-time PCR.

UNIVERSITEIT VAN PRETORIA
UNIVERSITY OF PRETORIA
YUNIBESITHI YA PRETORIA

Faculty of Health Sciences Research Ethics Committee

6/11/2012
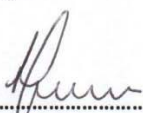
Number	:	**S194/2012**
Title	:	Identification of key mechanisms in the cytotoxic effect of two novel anti-cancer compounds on breast cancer cells
Investigator	:	Timothy Paul Wood, Department of Genetics Human, Genetics Section, University of Pretoria (SUPERVISOR: Prof E (Lizette) Jansen van Rensburg)
Sponsor	:	None
Study Degree:		**None**

> **This Student Protocol was reviewed by the Faculty of Health Sciences, Student Research Ethics Committee, University of Pretoria on 6/11/2012 and found to be acceptable. The approval is valid for a period of 3 years.**

Prof M J Bester	BSc (Chemistry and Biochemistry); BSc (Hons)(Biochemistry); MSc (Biochemistry); PhD (Medical Biochemistry)
Prof R Delport	(female)BA et Scien, B Curationis (Hons) (Intensive care Nursing), M Sc (Physiology), PhD (Medicine), M Ed Computer Assisted Education
Dr NK Likibi	MBB HM – (Representing Gauteng Department of Health) MPH
Dr MP Mathebula	Deputy CEO: Steve Biko Academic Hospital
Prof A Nienaber	(Female) BA (Hons) (Wits); LLB (Pretoria); LLM (Pretoria); LLD (Pretoria); PhD; Diploma in Datametrics (UNISA)
Prof L M Ntlhe	MBChB(Natal); FCS(SA)
Mrs M C Nzeku	(Female) BSc(NUL); MSc Biochem(UCL,UK)
Snr Sr J. Phatoli	(Female) BCur (Et.Al); BTech Oncology
Dr R Reynders	MBChB (Pret), FCPaed (CMSA) MRCPCH (Lon) Cert Med. Onc (CMSA)
Dr T Rossouw	(Female) MBChB.(cum laude); M.Phil (Applied Ethics) (cum laude), MPH (Biostatistics and Epidemiology (cum laude), D.Phil
Mr Y Sikweyiya	MPH (Umea University Umea, Sweden); Master Level Fellowship (Research Ethics) (Pretoria and UKZN); Post Grad. Diploma in Health Promotion (Unitra); BSc in Health Promotion (Unitra)
Dr L Schoeman	(Female) BPharm (NWU); BAHons (Psychology)(UP); PhD (UKZN); International Diploma in Research Ethics (UCT)
Dr R Sommers	**Vice-Chair (Female)** - MBChB; MMed (Int); MPharMed.
Prof T J P Swart	BChD, MSc (Odont), MChD (Oral Path), PGCHE
Prof C W van Staden	**Chairperson** - MBChB; MMed (Psych); MD; FCPsych; FTCL; UPLM; Dept of Psychiatry

Student Ethics Sub-Committee

Prof R S K Apatu	MBChB (Legon,UG); PhD (Cantab); PGDip International Research Ethics (UCT)
Mrs N Briers	(female) BSc (Stell); BSc Hons (Pretoria); MSc (Pretoria); DHETP (Pretoria)
Prof M M Ehlers	(female) BSc (Agric) Microbiology (Pret); BSc (Agric) Hons Microbiology (Pret); MSc (Agric) Microbiology (Pret); PhD Microbiology (Pret); Post Doctoral Fellow (Pret)
Dr R Leech	(female) B.Art et Scien; BA Cur; BA (Hons); M (ECI); PhD Nursing Science
Mr S B Masombuka	BA (Communication Science) UNISA; Certificate in Health Research Ethics Course (B compliant cc)
Dr S A S Olorunju	BSc (Hons). Stats (Ahmadu Bello University –Nigeria); MSc (Applied Statistics (UKC United Kingdom); PhD (Ahmadu Bello University – Nigeria)
Dr L Schoeman	**CHAIRPERSON:** (female) BPharm (North West); BAHons (Psychology)(Pretoria); PhD (KwaZulu-Natal); International Diploma in Research Ethics (UCT)
Dr R Sommers	**Vice-Chair** (Female) MBChB; M.Med (Int); MPhar.Med
Prof L Sykes	(female) BSc, BDS, MDent (Pros)

....
DR L SCHOEMAN; BPharm, BA Hons (Psy), PhD;
Dip. International Research Ethics
CHAIRPERSON of the Faculty of Health Sciences
Student Research Ethics Committee, University of Pretoria

....
DR R SOMMERS; MBChB; M.Med (Int); MPhar.Med.
VICE-CHAIR of the Faculty of Health Sciences Research
Ethics Committee, University of Pretoria

☎ 012 354 1677   📠 0866516047   ✉ deepeka.behari@up.ac.za   🖥 http://www.healthethics-up.co.za
✉ Private Bag X323, Arcadia, 0007 - 31 Bophelo Road, HW Snyman South Building, Level 2, Room 2.33, Gezina, Pretoria